THE PREPARATION AND ACTIVITY OF NICKEL-MOLYBDENUM COAL HYDROGENATION CATALYSTS

by

RICARDO BADILLA-OHLBAUM

Department of Chemical Engineering and Chemical Technology

Imperial College, London

A Thesis submitted for the Degree of Doctor of Philosophy to the University of London and for the Diploma of Imperial College

August, 1979

THE PREPARATION AND ACTIVITY OF NICKEL-MOLYBDENUM COAL HYDROGENATION CATALYSTS

Ricardo Badilla-Ohlbaum

ABSTRACT

The mode of action and the influence of the fundamental physical properties (pore size distribution, particle size) on the activity of Ni-Mo/γ-Al_2O_3 catalysts have been studied by hydroprocessing a model feedstock containing compounds typical of those occurring in coal-derived liquids at conditions close to that of industrial operation. Sulphur was removed without the need for saturation of the S-containing ring, whereas for both HDN and HDO, at least one ring appears to require saturation before scission of the C-N or C-O bonds. Hydrocracking of phenanthrene proceeds through a multistep mechanism involving hydrogenation, isomerization, cracking and re-hydrogenation. With increasing catalyst acidity, the rate of all reactions studied increased, as did the degree of hydrocracking relative to hydrogenation. Coke formation on the catalyst also increased markedly with acidity. The particle size and pore size distribution of the catalyst is critical for the performance of the catalyst, since mass transfer limitation are important in hydrotreating coal-derived liquids.

Equilibrium adsorption isotherms for the impregnation of γ-Al_2O_3 by Ni and Mo have been determined. ESCA and u.v. reflectance spectroscopy show that the dispersion and surface structures of both Ni and Mo are strongly dependent on the impregnation and calcination conditions. Measurements of thiophene HDS at atmospheric pressure show that the activity of the catalyst correlates well with the formation of Ni Al_2O_4 spinel and with the presence of Mo in octahedral sites. This pattern of activity was found to be maintained at high pressure for HDN, HDO and hydrogenation/hydrocracking reactions.

The conversion of the oxidic state of the catalysts into the active sulphide form has been studied by gravimetric analysis and ESCA characterization of the oxidic and sulphided surfaces. It was found from both sets of measurements that in catalysts of high activity, Ni and Mo are completely sulphided, whereas this is not the case when the catalyst activity is relatively low. There is a good correlation between the extent of sulphidation and the degree of dispersion of Mo and Ni in the oxidic state which may be related directly to the impregnation conditions. A model for the formation of the active state of the catalyst in relation to the preparation conditions is presented.

to Maria Angelica, who made it possible

to Adela and Sergio, who prepared the way

ACKNOWLEDGMENTS

My sincere thanks are due to Dr. D. Chadwick for his interest, enthusiasm and guidance during the latter and most important part of this research project. I would also like to thank Dr. K. C. Pratt for his supervision during the initial stage of this work. My special thanks are also due to Professor D. L. Trimm whose friendship and advice helped me throughout this period of work.

I wish also to thank Professor D. A. Dowden, Dr. L. Kershenbaum and Dr. G. S. Parry for their valuable contributions, my colleagues for many hours of friendly discussions and the technical staff of the Department for their ready assistance. My thanks also to Miss Sara Dodds for typing this manuscript.

I would also like to express my gratitude to the National Coal Board for a substantial grant towards equipment and materials employed during this research and for the award of a generous scholarship covering the entire period of study. In particular, I am indebted to Mr. G. O. Davies, Dr. D. Gavin and Mr. M. Jones of the NCB-CRE for their valuable advice and supervision of the catalyst tests and mass spectrometric analyses performed at Stoke-Orchard.

Finally, I am most grateful to my wife, Maria Angelica, for her encouragement and support during this important period of our lives.

CONTENTS

CHAPTER ONE: INTRODUCTION

1.1 COAL LIQUEFACTION

1.1.1 General Aspects

One of the major challenges of our times is the solution of the energy problem. The continuing decline of oil and natural gas reserves in the world and the increasing demands for larger royalties by the oil producing nations have focussed attention during recent years on the finite limits to the world's supply of oil and natural gas. Recent studies (Ezra 1978) have indicated that by the year 2000, compared with 1975, the world energy demand would double, that perhaps only a 5% increase in production by non-conventional methods will be obtained, and that nuclear energy is likely to increase only to 10 - 15% of the whole. Oil consumption cannot increase at the rate it did between 1950 and 1975, when total demand trebled; on the contrary, oil production is more likely to reach a peak between the 1980s and 1990s (Day 1972) and that of natural gas soon afterwards. Since coal and oil together now contribute more than 75% of the world energy supply, there is a considerable potential gap to be filled by coal or additional alternative sources of energy. Coal must become a major source for liquid and gaseous fuels in the future.

The feasibility of the catalytic conversion of coal into liquid and gaseous fuels was demonstrated during World War II when several plants, based on different technologies, operated in Germany, Great Britain, Czechoslovakia, Spain and U.S.S.R. (Donath 1963, Wu and Storch 1968). However, there is a need for a significant improvement in these processes to make coal conversion an economically attractive venture and to permit coal-derived fuels to play an important part in replacing or supplementing our critical oil and gas supplies (Davis 1976).

The conversion of coal to synthetic fuels involves a number of catalytic processes and reactions, the most important of which are summarised in Table 1.1. This list includes many catalytic

TABLE 1.1

CATALYTIC REACTIONS IN COAL CONVERSION

Process	General Reactions	Specific Reaction/Products
Direct liquefaction	Hydrogenation Cracking Hydroprocessing	Aromatic liquids Hydrodesulphurization (HDS) Hydrodeoxygenation (HDN) Hydrodemetallation (HDM)
CO/H_2	Fischer Tropsch	SNG Hydrocarbon liquids Alcohols Chemicals
Water gas shift		Hydrogen
Direct gasification	Hydrogasification	Methane Hydrocarbon liquids
Liquids refining and upgrading	Cracking Reforming Hydroforming	Hydrogenation Dehydrogenation Dehydrocyclization Isomerization Hydrogenolysis Hydrodesulphurization (HDS) Hydrodeoxygenation (HDO) Hydrodenitrogenation (HDN)

reactions used in the refining of petroleum and, therefore, the coal conversion industry is most likely to utilise a significant fraction of presently known catalytic materials. Because of the complex nature of coal, the technical challenges for the development of efficient processes are more difficult than those encountered in the petroleum industry. Factors such as control of selectivity and activity, minimising catalyst poisoning, sintering and mechanical degradation and the development of efficient regeneration procedures and of reactor design for optimum heat

and mass transfer (Consumano et al 1978) are more difficult in coal processing.

Comparison of typical analysis of a crude oil (British Petroleum 1972) and coals (Consumano et al 1978), Table 1.2, shows

TABLE 1.2

ANALYSIS OF OIL AND COAL /%w

	C	H	O	S	N	Ash	Atomic H/C ratio
Bituminous	73	5	9	3	1.5	8.5	0.82
Subbituminous	71	5	16	0.5	1.5	6.0	0.85
Lignite	64	4.6	18	0.5	1.5	11.4	0.86
Crude oil	85.4	12.6	-	2.0	-	10^{-2}	1.7

that coal conversion involves increasing the hydrogen content, removing (inorganic) ash and removing heteroatoms which are chemically bound in the coal. In principle, all of the conventional petroleum fuels are potentially available from coal liquids. However, there are important differences in the chemical composition among these fuels (Consumano et al 1978), and therefore different processes may be needed to produce them (Table 1.1). Motor gasolines are characterised by a blend of paraffins, naphthenes and aromatics, with a substantial fraction of branched paraffins, benzene, toluenes and xylenes (BTX), which are the typical high octane components. Jet fuel is a highly paraffinic kerosene fraction with an aromatic content limited to less than about 10%v (Solash et al 1978), while diesel fuels have long paraffinic molecules (n-hexadecane). Gas turbine fuels demand a minimum of about 11%w of hydrogen and as in the case of heating oils and residual oils, less than 1% sulphur or nitrogen (to minimise NO_x formation during combustion) and metals.

Although several processes for coal conversion have been developed over the years (White and Neuworth 1976, Spitz 1977), the most direct route involves the hydrogenation of coal. In principle, there are only two approaches to liquefaction: degradation or synthesis. The first means the partial breaking down of the complex coal structure into simpler molecules comparable with crude oils and even premium distillate fractions of petroleum. Unlike degradative processes, which preserve as much as possible of the chemical structures present in coal, the synthesis route involves complete disruption of the whole structure by gasification to form synthesis gas, which can be converted to liquid fuels and a wide range or chemicals, including methanol, by catalytic processes of the Fischer-Tropsch type. The products of synthesis are almost entirely aliphatic, whereas those of degradative processes are predominantly aromatic. Therefore, future coal refineries would have combined processes based in these two technologies to produce a broad spectrum of fuels and petrochemical products (O'Hara et al 1978, Neben 1978).

1.1.2 Direct Liquefaction Processes

There are many variants of the degradative approach, most of which involve some degree of hydrogenation to effect the reduction in molecular complexity. All involve pyrolysis (decomposition caused by heating) to some extent, but it is possible to distinguish between pyrolysis and hydrogenation processes (Gibson 1978). Some variants incorporate the use of solvents which can sometimes play an important role in breaking down coal structures (Fisher et al 1978).

1.1.2.1 Pyrolysis Processes

Pure pyrolysis processes is synonymous with carbonisation. The traditional processes of the manufacture of cokes and coal gas yields coal tars and benzole as by-products that can be converted to petroleum replacements, but their scale of production is limited. Of the new processes currently under development the best known are COED (FMC Corporation 1973) and the Occidental Flash Pyrolysis process (White and Neuworth 1976). In the first process, pulverised and dried coal is heated to successively higher temperatures in a series of four dense fluidised-bed reactors operating at 580, 730, 810 and 1080 K to prevent agglomeration of the coal. In the Occidental process, the pyrolysis is carried out rapidly at temperatures not less than 1050 K in a single fluidised-bed reactor. In general, pyrolysis liquid yields are much higher in the latter process: about 38%w compared with closer to 23%w in the COED process and about 9%w in the conventional carbonisation processes.

The hydrocarbonisation, i.e. pyrolysis in the presence of hydrogen, is another possibility. In the COALCON process (Consumano et al 1978) the pyrolysis of coal is carried out at about 820 K and 3.7 MPa, producing liquid, gaseous and solid products, and is similar to the Pyrolysis process currently under development by the National Coal Board (U.K.) (Fishlock 1978). The gas is separated from the liquid to produce synthetic natural gas (SNG) and liquified petroleum gas (LPG). The liquid is segregated into light and heavy fractions with characteristics similar to those of a light to heavy petroleum naphtha and to a light to a medium oil, respectively. The solid char is used for fuel and for hydrogen generation. The overall yields of the COALCON process are about 44%w for SNG, 7.3%w for LPG, 14.3%w for light and 33.7%w for heavy oil fractions.

1.1.2.2 Solvent Extraction Processes

In these processes, the coal structure is broken down by the presence of a suitable solvent which is capable of dissolving and extracting most of the components of coal. Degrading solvents, such as anthracene in the presence of hydrogen, extract large amounts of the coal (up to more than 90%w) at temperatures of about 673 K (Davies et al 1977); reacting solvents, such as tetraline, dissolve the coal by reacting with it (Doyle 1975). Solvent extraction may be carried out with or without the presence of hydrogen and/or catalysts, and it forms the basis of most of the coal conversion processes currently under development. Inorganic constituents normally found in coals (Fe, Mg, etc.) have important effects on conversion yields (Jackson et al 1979). In addition, it is possible to use compressed gases in the supercritical state as solvent (Davies 1978), such as toluene (Tugrul and Olcay 1978), in which case a yield of liquid products of about 25%w is achieved at 663 K and about 47.5% in the presence of hydrogen (Gibson 1978).

Most of the solvent extraction processes under development use the coal-derived liquors as degrading solvents, although they do not conform entirely to the definition, since they are not always recovered unchanged from the coal solution. Moreover, these solvents also have the reactive capability due to the presence of naphthenes which can transfer hydrogen to the coal. Reactive types of solvents produce extracts which are generally of lower molecular weight than those produced by degrading solvents (Schiller and Knudson 1978). The different processes can be divided into two general categories: a single stage process of extraction with catalytic hydrogenation such as the H-COAL (White and Neuworth 1976) and the Synthoil process (Yavorsky et al 1975), and the two stage

processes of solvent extraction followed by a separate catalytic hydrogenation such as the National Coal Board (U.K.) (Davies 1978) and the Exxon EDS process (Brunson 1979).

In the H-COAL process, the reaction is carried out in a highly ebullient slurry reactor into which a slurry of hydrogen, coal, coal-liquids and catalyst (Co-Mo) at 640 K and 20.2 M Pa is fed. In the Synthoil process, a highly turbulent fixed-bed reactor is employed at similar conditions. In the SRC process, coal is dissolved in an aromatic (anthracene) oil at 700 K under a pressure of hydrogen of 6.89 MPa, without any catalyst in the reactor.

An outline of the NCB process is shown in Figure 1.1 (Davies et al 1977, Davies 1978). In this process, coal is dissolved in an anthracene oil, which is a product of the process, and digested in a reactor at about 673 K. The liquid products, which contain up to 95%w of the coal are separated from the unreacted coal and ash in a filtration stage; the solvent is partially recovered in a fractionation stage and the resulting product, containing an approximate coal-liquors to solvent ratio of 1:1 is catalytically hydrotreated to obtain several products. Some of the heavy and middle oil fractions of the hydrogenated products are recycled to maintain the solvent balance.

1.1.3 Coal-Derived Liquors

A wide range of gaseous and liquid products are obtained in the coal-conversion processes. The term "syncrude" (synthetic crude) has been employed to describe the heavier fractions (boiling point above 450 K) of coal-derived liquors, which constitute a substantial portion of the products of most of the coal conversion processes under development and are the most difficult to upgrade into useful chemicals and fuels. Although syncrude chemical compositions may

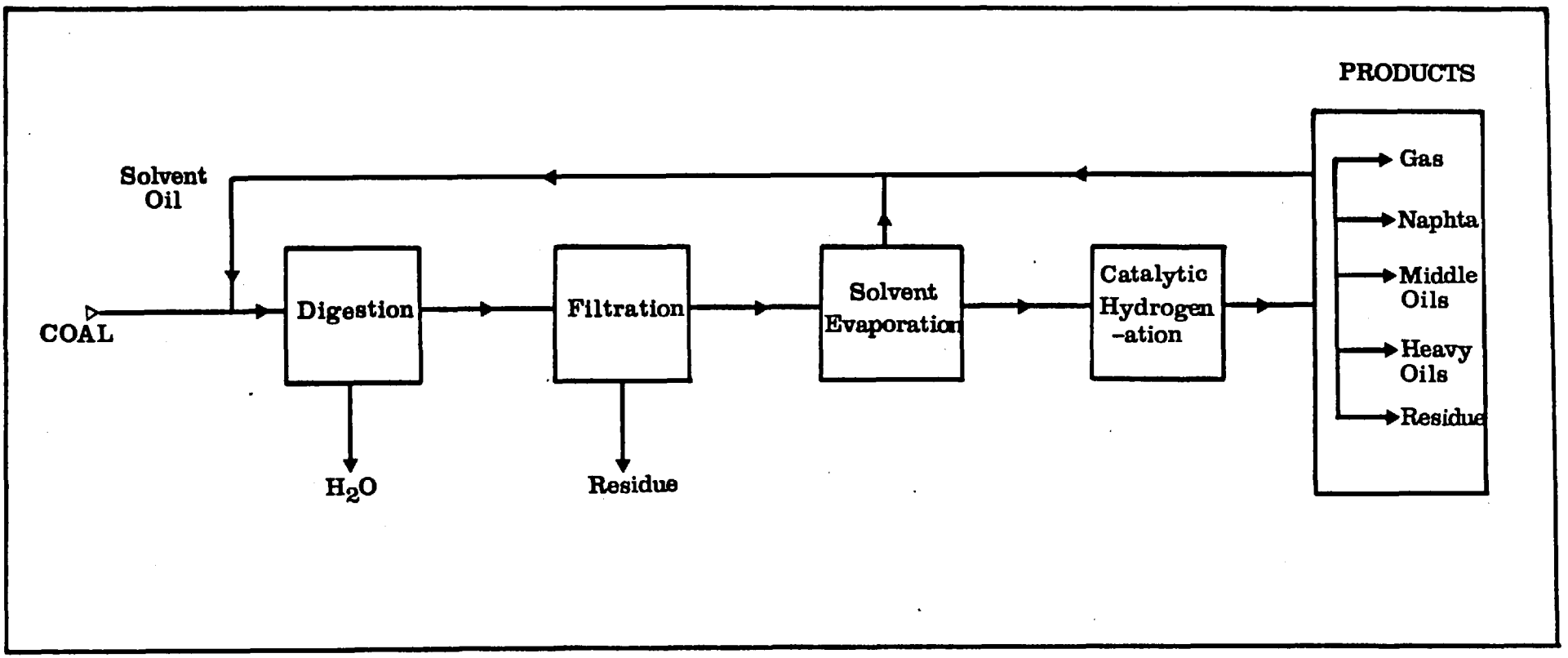

FIGURE 1.1: NCB-CRE COAL LIQUEFACTION PROCESS

TABLE 1.3

COMPARISON OF DISTILLATES (w%) OF SIMILAR BOILING RANGES FRACTIONS FOR SYNCRUDES

PROCESS	SYNTHOIL			COED			
Coal type	West Virginia			West Kentucky		Utah	
Boiling range	>480 K	480-635 K	635-804 K	477-653 K	653 K+	477-653 K	653 K+
Saturated	30.3	16.0	9.7	25.0	23.8	27.8	25.8
Monoaromatics	27.6	27.3	4.7	42.0	25.1	25.1	14.4
Diaromatics	3.2	21.6	22.6	13.0	24.3	17.5	18.4
Polynuclear aromatics		7.9	41.1	5.4	20.0	7.1	25.1
Heteroatomics	35.3	22.2	15.6	4.4	4.5	15.2	7.4
Distillate (%w) of Syncrude		42.6	27.3	54.2	24.2	45.4	40.3

vary with the nature of the coal employed and from one process to another, they are similar with respect to various molecular constituents. Table 1.3 shows a comparison of similar boiling ranges fractions of three syncrudes produced by the Synthoil and the COED coal conversion processes (Consumano et al 1978). The high aromaticity of these products is readily seen and presents a major problem in their hydroprocessing to lighter derivatives, as these structures are major precursors of coke deposition on hydroprocessing catalyst surfaces (Ocampo et al 1978). A specially severe problem is the presence of large amounts of heteroatomic molecules containing S,O,N and metals which have to be hydrotreated before further catalytic processing can take place without the danger of poisoning the catalysts employed in conventional petroleum refining. Therefore, the first stage in upgrading coal-derived liquors must be the removal of heteroatoms and the hydrocracking of the multi-ring structures present in the coal-derived oils.

1.2. HYDROPROCESSING OF COAL-DERIVED LIQUORS

1.2.1 Hydrodesulphurization (HDS)

Coal-derived liquors contain substantial amounts of sulphur compounds which are similar to those present in petroleum crudes and include thiophenes, benzothiophenes and naphthobenzo-thiophenes (Akhtar et al 1974, Givens and Venuto 1970). At high partial pressures of hydrogen, the rate of HDS is approximately first order with respect to the sulphur compound (Schuit and Gates 1973 , Hualla et al 1978) and usually decreases with increasing molecular weight of the sulphur compound (Weisser and Landa 1973); at the temperature ranges most often used in technical HDS (573 - 773 K), conversion of

the majority of these compounds to hydrocarbons is almost complete (George 1975), dibenzothiophene being one of the most difficult sulphur compounds to hydrogenate (Frye and Mosby 1967).

Most of the mechanistic and kinetic work in the area of HDS has employed thiophene, the simplest model for heterocyclic sulphur compounds present in petroleum and coal-derived liquors (Schuman and Shalit 1970), and there are numerous studies in the literature concerning this reaction. It has been concluded (Massoth 1977) that the rate-determining step for thiophene hydrogenolysis over Co(Ni)-Mo(W)/alumina catalysts under atmospheric pressure is the surface reaction involving two sites, one upon which thiophene and H_2S competitively chemisorb and one upon which H_2 adsorbs. n-Butene and n-butane are the main products. Hydrogenation of polycyclic sulphur compounds is much slower than that of thiophene (Givens and Venuto 1970). Hualla et al (1978) studied the hydrogenolysis of dibenzothiophene over a presulphided Co-Mo/γ-Al_2O_3 catalyst at 573 K and 10.3 MPa and concluded that the main product was diphenyl and H_2S, whereas Rollman (1977) over the same catalyst but at 673 K and in the presence of oxygen and nitrogen containing heterocyclic compounds, reported cyclohexyl benzene as the main product.

1.2.2 Hydrodenitrogenation (HDN)

Hydrogenolysis of nitrogen containing heterocyclic compounds over sulphide catalysts is, in general, more difficult compared to HDO and HDS. Because of the basic character of the molecules, they can irreversibly adsorb on the acid sites of the surface of the catalysts such as those commonly employed in conventional petroleum refining. The production of fuels from coal-derived liquors provides a second motivating factor for nitrogen removal,

that is, the need to minimise NO_x formation during combustion.

In general, HDN has not received nearly as much attention as HDS, because sulphur, a severe catalyst poison and a serious atmospheric pollutant, has historically been the primary concern in processing petroleum feedstocks. Most of the mechanistic and kinetic work has been on pyridine (Sonnemans and Mars 1974) and the reactivity of nitrogen containing heterocyclic compounds is found to decrease slowly up to four-ring compounds and then increase with increasing numbers of rings (Aboul-Gheit and Abdou 1973). HDN involves first order hydrogenation of aromatic rings followed by scission of C-N bonds (Rollman 1977, Satterfield et al 1978), in contrast with HDS. Sulphur compounds significantly enhance the rate of HDN at temperatures above 598 K, whereas nitrogen-containing molecules reduce the rate of HDS less markedly (Satterfield et al 1975).

1.2.3. Hydrodeoxygenation (HDO)

Phenolic oxygen is the primary heteroatom present in coal-derived liquors (Palmer and Vahrman 1972), fused ring furans and carboxylic acids also being present (Weisser and Landa 1973). The deactivating influence of these compounds has been reported for the case of Co(Ni)-Mo(w) catalysts (Donath 1956) and considerable information exists on the hydrogenolysis of alcohols and phenols, but very little on oxygen removal from heterocyclics (Rollman 1977). In general, HDO is the least important of all heteroatom removal reactions, but due to the high oxygen content of coals it constitutes a major source of hydrogen consumption in the hydrorefining process.

As in the case of HDN, hydrodeoxygenation of benzofuran involves

first order hydrogenation of the heteroatomic ring to form a phenotic intermediate, followed by scission of the C-O bonds, which requires the saturation of the aromatic ring (Landa and Monkova 1966).

1.2.4 Hydrogenation and Cracking of Polynuclear Aromatics

As indicated earlier, it is essential to hydrocrack the multi-ring aromatics present in coal-derived liquors selectively prior to the final upgrading stages, as they lead to catalyst deactivation in conventional petroleum processes, and hydrocracking produces lighter hydrocarbon fractions which are easier to convert into fuels and petrochemicals. Unfortunately, only a limited amount of work has been done concerning detailed kinetic studies of the catalytic conversion of multi-ring aromatics, primarily because of the experimental difficulties connected with rapid catalyst deactivation and the complexity of the products of the reaction. The hydrocracking of polynuclear aromatics proceeds through a multistep mechanism involving hydrogenation, isomerisation, cracking and rehydrogenation (Qader and Hill 1972, Wu and Haynes 1975), leading to a complex mixture of hydroderivatives of the initial substance saturated to different degrees, bicyclic and monocyclic aromatic molecules and naphthalenes; distribution of these species depends largely on the conditions used (Qader and McOmber 1975).

In hydrocracking of naphthalene (Qader 1973), the first step is hydrogenation to tetrahydronaphthalene (tetralin), followed by isomerisation to methylindan, which is then dealkylated to indan. Alkylated benzenes form from indan and or tetralin by C-C bond scission. The first reaction in the hydrocracking of anthracene over a Ni-W/Al_2O_3 catalyst at 748 K and 20.6 MPa (Qader 1973) is the

stepwise hydrogenation to di-, tetra- and octahydroanthracenes. The cyclohexane rings of tetra- and octahydroanthracenes are then isomerised to five member rings which subsequently crack to naphthalenes. The latter are then converted to benzenes via hydrogenation, isomerisation and cracking of one of the rings. The selective saturation and cracking of the central ring is desirable for minimum hydrogen consumption and a maximised yield of alkylbenzenes is not significant under the conditions of the test. Under similar conditions, phenanthrene reacts more slowly than anthracene (Qader and McOmber 1975), and being thermodynamically more stable (Aczel 1972) it is usually present in greater abundance in coal-derived liquors (Sternberg et al 1976). The reaction paths for phenanthrene are similar to those of anthracene (Wu and Haynes 1975) and cracking reactions become significant at temperatures above 693 K over Co-Mo catalysts (Huang et al 1977). According to Wu and Haynes (1975) centre-ring cracking of phenanthrene is indicated on a Cr_2O_3-Al_2O_3 catalyst at temperatures above 710 K by the presence of significant amounts of diphenyl and 2-ethyldiphenyl among the products. Therefore, the use of controlled acidity in the presence of transition metal cations such as chromium may be an approach to enhance the selectivity of desired central-ring cracking reaction pathway.

1.3 COAL CONVERSION CATALYSTS

One of the significant advances in heterogeneous catalysis is the development of multicomponent catalysts for the control of catalytic properties (Anderson 1975). Bimetallic systems have been the interest to catalytic scientists for some time and much of the work in this area concerns the relationship between catalytic activity and the electronic and geometric structures of these catalysts (Thomas

and Thomas 1967, Dowden 1972). Moreover, the application of these scientific ideas has led to the establishment of general guide lines for catalyst design (Dowden 1967, Dowden et al 1968, Trimm 1973, Trimm 1978). Table 1.4 shows the mass reactions occurring in the hydrotreating of coal-derived liquors and examples of metal catalysts to promote these reactions (Consumano et al 1978).

TABLE 1.4

Examples of metal-catalysed reactions in coal conversion processes

Reaction	Typical metal catalysts	High-activity metals
Hydrogenation of aromatics	Group VIII, Mo, W, Re	Pt, Rh, Pd
Dehydrogenation	Group VIII	Pt, Pd
Dehydrocyclization	Pt, Pd, Ir, Rh, Ru	Pt, Ir
Hydrogenolysis		
C-C bonds	Group VIII, Re, W, Mo	Ru, Ir, Ni
C-N bonds	Group VIII, Re, W, Mo, Cu	Ni, Pt, Pd
C-O bonds	Group VIII, Re, W, Mo, Cu, Ag	Pt. Pd
C-S bonds	Group VIII, Re, W, Mo, Cu, Ag	Pt, Pd, Rh
Isomerisation		
Double bond shift	Group VIII	Pd, Pt
Skeletal	Pt, Ir, Pd, Au	Pt

However, metallic catalysts in general are not expected to survive as metals in a coal conversion environment at sulphur levels exceeding 1% and temperatures over 550 K. Under these conditions all metals can form bulk sulphides (Boudart et al 1975), and therefore

the true catalyst would be a mixed sulphide and not a bimetallic system. Of these, the most widely employed in modern coal conversion processes are mixtures of sulphides from the Group VIA (Mo or W) and the Group VIII (Ni or Co). As in the case of oxide catalysts, they are intermediate between metallic catalyst and insulators due to their semiconductive properties, which give them their polyfunctional catalytic character. Besides oxidation-reduction promotion capabilities, they have the properties of acid catalysts and can promote cracking, isomerisation, hydrogenolysis and dehydration reactions (Weisser and Landa 1973).

Although sulphide catalysts have been applied in industrial catalytic hydrotreatment of heavy feedstocks already for about 45 years, fundamental questions concerning their structure and the nature of the active sites remain unanswered, in spite of the development of powerful techniques for surface characterisation. The reason for this lies mainly with the problem of satisfactory characterisation of the catalyst surface and how the surface is modified during reaction. For example, sulphide catalysts of the Ni(Co)-Mo(W) type generally operate at high temperature (over 550 K) and high pressure (over 500 kPa) and in the presence of H_2S, but most of the studies have been carried out on the supported oxides which constitute the precursors of the working catalyst. In addition, the problems arising from the complex nature of the catalyst preparation process (Berrebi and Bernusset 1976) have been frequently overlooked leaving most of the results open to question.

The most widely investigated system has been Co-Mo, though there is recent evidence to suggest that the Ni-Mo catalysts are superior for the hydrotreating of coal derived liquors (Hillebrand et al 1977, Kang and Gendler 1978). These catalysts are usually

supported on carriers which, in practically all cases, have a significant influence on the overall catalyst efficiency. They are only rarely used in the unsupported form (Gardes et al 1976). The activity of the catalyst for all the hydrotreating reactions depends largely on the fundamental physical properties such as surface area, pore size distribution and pore volume, since mass transfer resistances are important in hydrotreating coal-derived liquors. Optimisation of these properties is essential in order to achieve a good catalyst performance in industrial operation (Chiou and Olson 1978).

Catalysts having a Co(Ni)/(Co(Ni)+Mo(W)) in the range from 0 - 1 (molar ratio) have been described. The optimum rate for maximum activity is given by some authors as 0.3 (Zabala et al 1975) and by others as 0.5 (Weisser and Landa 1973). The active component loading (MoO_3) in the catalyst varies from 2 - 20%w, the most used value being around 12 - 15%w and the promoter (Ni or Co) around 3%w (Mitchell 1967).

1.4 THE PREPARATION OF Ni-Mo/γ-Al_2O_3 CATALYSTS

For many years catalyst preparation has been regarded as an art and due to the proprietary nature of the processes, most of the available detailed information is contained in the patent literature (Weisser and Landa 1973). In the preparation of a catalyst, one is confronted with the difficult task of understanding and controlling in a reproducible manner many different steps, such as impregnation, drying, calcination, activation, etc., and in each step variables such as time, temperature, concentration, atmosphere, etc. (Delmon and Hualla 1978). Naturally, the goal in such preparations is to maximise the activity and life of the catalyst. Many new techniques

have been developed for catalyst characterisation, and these have played an important role in understanding the effect of the preparative variables on catalytic properties.

The following description deals with the preparation and surface characteristics of the Ni(Co)-Mo(W)/γ-$A\ell_2O_3$ catalyst. The most widely investigated catalyst has been Co-Mo, but most of the findings apply equally to the Ni-Mo system.

1.4.1 Impregnation

The first stage in the preparation of a supported catalyst such as the Ni(Co)-Mo(W)/γ-$A\ell_2O_3$ is the dispersion of the metals on the surface of the support. The choice of the proper procedure for maximising dispersion of the metals on the support depends upon the chemistry involved and its compatability with the surface properties of the support. The most common technique is the impregnation of the support with an aqueous solution containing salts of the catalytic metals, and both the distribution (i.e. the concentration profile of the active metals throughout the catalyst pellet) and the dispersion of the active components on the surface of the support are largely determined by the impregnation and drying conditions (Anderson 1975, Delmon and Hualla 1978). If the extent of cationic and anionic adsorption of the metal species from solution to the surface of the support is negligible compared to their total concentration on the support, the distribution depends primarily on the drying conditions (Fenelov *et al* 1978).

The most commonly employed method in impregnation from solutions is the impregnation to drying (pore filling), that is, using only enough solution to fill the pore volume of the support (de Beer *et al* 1976, Laine 1977, Gajardo 1978, Ianibello and Mitchell 1978) and removing the moisture excess by evaporation. Whenever there is a

strong adsorption of the catalytic metal ion on the carrier, it can be impregnated using an excess amount of solution, and in this case, a change on the metal distribution on drying is unlikely (Ianibello and Trifiro 1975, van den Berg and Rijnten 1978, Brunell 1978). In the latter method, the amount of solution can be much larger than the pore volume of the support and, therefore, the variables of the impregnation process can be better controlled than in the dry impregnation method.

In the studies of the preparation of the Co-Mo/γ-Al_2O_3 catalysts it has been usual to carry out impregnation under essentially neutral conditions allowing the pH to vary freely as adsorption on the support material proceeds (Laine 1977, Yamagata et al 1977, Gajardo 1978, Ianibello and Mitchell 1978). Indeed, the pH has sometimes been used as a guide to the completion of adsorption processes (Ianibello and Mitchell 1978). However, it is well known that the surface chemistry of alumina is dependent on the pH of its environment (Amphett 1974, Anderson 1975) via the following equilibria involving surface hydroxyl groups:

$$Al(OH)_2^+ + OH^- \rightleftarrows Al(OH)_3 \rightleftarrows AlO(OH)_2^- + H^+$$

The above equilibria imply that the alumina surface may be made to carry a net positive or a net negative charge by appropriate adjustment of the pH of the solution (Amphett 1974). For γ-alumina, the pH required to give zero net surface charge lies in the range of 7 - 8 (Anderson 1975, Brunell 1978). In principle, the adsorption of anions by γ-alumina should be favoured in acid conditions and the adsorption of cations favoured in basic conditions. Therefore, in catalysts impregnated under neutral conditions, Mo is deposited on the surface mainly by crystallisation on the surface and not by adsorption. Accurate control over pH is made difficult by

the tendency of γ-alumina to buffer the pH at a constant value (Pourbaix 1966, Perrin and Dempsey 1974).

The nature of the Mo ions present in a solution is strongly pH dependent (Cotton and Wilkinson 1972). In a basic environment the predominant species is MoO_4^{2-} and at pH < 6 the molybdate ions condense to form polymolybdates (Pourbaix 1966). These considerations indicate that control of the pH of the impregnation would allow some control over surface species present in the final catalyst, and this will be shown in Chapter 5.

Other techniques ensuring high dispersion are the homogeneous co-precipitation of the support and the active metals (Geus 1970), the aerogel procedure (Gardes et al 1976), the gas-phase adsorption of $MoO_2(OH)_2$ on the support (Fransen et al 1976), and of organic transition metal complexes (Anderson and Mainwaring 1974).

In addition to the method of impregnation, it is possible to prepare catalysts by co-impregnation or successive impregnation. For Co-Mo catalysts it is found that impregnation first with Mo then with Co produces a favourable effect on HDS activity (de Beer and Schuit 1976) while for Ni-Mo catalyst, the reverse cycle produces a more active catalyst (Mone and Moscou 1975, Laine 1977, Ochoa et al 1978).

1.4.2 Calcination

The calcination of the deposited precursors of the active compounds brings about several transformations and solid state reactions. The main purpose of this process is the decomposition of the dried precursors to form the oxidic precursors of Ni(Co) and Mo(W) of the active catalyst in which solid state transformation of the support structure (Tanabe 1970), reactions between the oxides and the

support, and sintering of the various phases existing on the surface (Delmon and Hualla 1978) are also occurring.

As in the case of the impregnation, the calcination conditions largely determine the degree of dispersion and the nature of the oxidic phases present at the surface. Several situations may exist on the catalyst, and these have been summarised by Delmon and Hualla (1978) and shown in Figure 1.2.

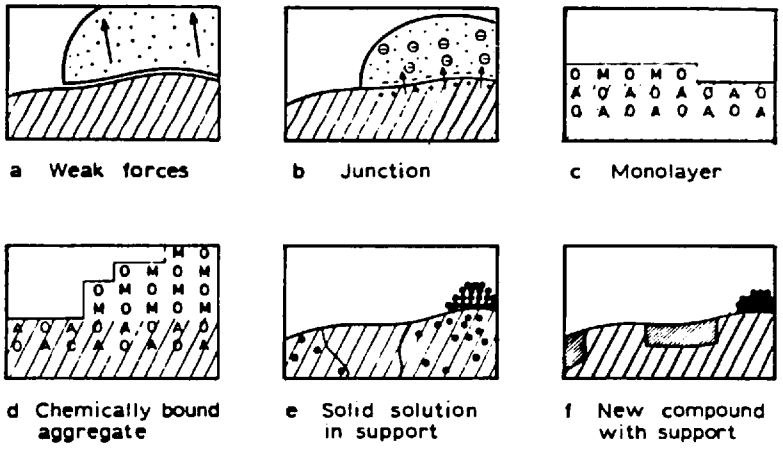

FIGURE 1.2

Active Oxide-Support Interactions

When the interaction is due to weak forces (van der Waals), the role of support is only to disperse the catalyst (Figure 1.2a). Graphite (Stevens and Edmonds 1978) and silica (Gajardo 1978) are typical support in which this type of interaction is dominant. In the case of semi-conducting or conducting substances deposited on a semi-conducting support, a junction (Figure 1.2b) may be formed between the support and the oxides, even if no chemical bonds (in the conventional sense) are formed. Electron transfer across the boundary would change the electron density of the deposited materials thus affecting their catalytic activity. If most of the atoms of the supported substance are exposed on the surface a monolayer is formed

and the active substances may chemically combine with the carrier (Figure 1.2c). Much evidence has been presented for this situation (Schuit and Gates 1973, Ianibello and Trifiro 1975, Hall and Lo Jacomo 1977) for the Mo-$\gamma/A\ell_2O_3$ system. When the active phase loading exceeds the amount which corresponds to a monolayer, it is likely that the excess oxides will form aggregates (Figure 1.2d) and present characteristics similar to bulk oxides since the interaction with the support will exert relatively less and less influence when the ratio active phase volume/contact area decreases. At high temperatures of calcination the oxide and the support (if their structures are compatible), can dissolve in each other to different extents (Figure 1.2c), ranging from ionic exchange confined to the interface to a multilayer solid solution and even to a homogeneous solution, as in the case of Cr_2O_3-$A\ell_2O_3$. Finally, there may be the formation of new compounds such as surface spinels and/or pseudo-aluminates (Figure 1.2f), and this is well documented for the case of Ni (Lo Jacomo et al 1971) and for high loadings of MoO_3 on $A\ell_2O_3$ (over 20%w) in which case $A\ell_2(MoO_4)_3$ can be observed (Giordano et al 1975).

It is obvious from the above description that each of these situations may exist in a Ni(Co)-Mo(W) supported catalyst. Moreover, many of them may coexist and the predominance of one over another will largely depend on the conditions of the impregnation and calcination of the catalyst. There is very little information in the literature about the influence of the calcination conditions (temperature, atmosphere) on the catalytic activity of Ni(Co)-Mo(W)/ γ-$A\ell_2O_3$ catalysts. Nickel containing catalysts are known to be sensitive to high calcination temperatures, and catalysts calcined at about 773 K in air are twice as active as catalysts calcined at 923 K (Mone and Moscou 1975, Laine 1977).

1.4.3 Activation

Conversion of the Ni(Co) and Mo(W) oxidic phases present on the catalyst surface to sulphur compounds occurs while the catalyst is in use, or during pre-sulphiding, and this step constitutes the activation of the catalyst. It is uncertain whether the sulphiding is complete (Weisser and Landa 1973, Gajardo 1978) but the formation of MoS_2 and sulphides of Ni(Co) is considered to be the most likely process (van der Aalst and de Beer 1977).

Most of the work in surface characterisation of sulphide catalysts has been carried out for the Co-Mo/γ-$A\ell_2O_3$ and in spite of the enormous effort in the subject, the problem of the determination of the nature of the active sites remains unsolved, and there are discrepancies in the conceptions of the structure of these catalysts. This can be explained by the fact that different catalyst preparation methods have been used among the various authors and that the various physico-chemical methods for surface characterisation employed only give partial information about the nature of the catalyst. In addition, there is little information in the literature on the relationship between surface structure and catalyst activity measured under relevant industrial conditions.

Three main models of the Co-Mo system have been described: the monolayer (Lipsh and Schuit 1969), the pseudo-intercalation (Voorhoeve and Stuiver 1971, Farragher and Cossee 1973) and the synergy (Hagenbach et al 1971). The monolayer model pictures the existence of an epitaxial Mo(VI) monolayer on the alumina surface with Co(II) being located in the alumina superficial layer beneath the Mo(VI) monolayer, and that a certain portion of the promoter cations penetrates some distance into the support, Co(II) preferring tetrahedral sites and Ni(II) octahedral sites as in their spinels

(Lo Jacomo et al 1973). Depending on the amount of the promoter oxide introduced (Ni or Co), a certain amount remains also at the surface as NiO or Co_3O_4 (Gajardo 1978). The γ-Al_2O_3 exhibits on the surface mainly the plane (110) and (100). The plane (110) exposes a layer combining anions and aluminium in octahedral and tetrahedral sites or a layer containing anions and aluminum in octahedral sites while the plane (100) exposes anionic sites and cationic octahedral sites (Lo Jacomo et al 1971). According to this model, the tetrahedral sites would be occupied by Co(II), the octahedral sites by Mo(VI) in the fully oxidic system. After reduction and sulphiding, only the oxygen anions situated in the outermost layer (i.e. not taking part in the epitaxial layer) can be replaced by sulphur to such an extent that the maximum S/Mo ratio is 1.0, resulting in the formation of Mo(V) and Mo(IV) sites. UV-reflectance spectroscopy measurements (Ashley and Mitchell 1968, 1969, Stork et al 1974, Hall and Lo Jacomo 1976) have placed some doubt on the assignment of octahedral Mo(VI) ions in the monolayer since there is evidence that MoO_3 on γ-Al_2O_3 is more comparable to $Al_2(MoO_4)_3$ where Mo is surrounded tetrahedrically. In graphite supported Co-Mo catalyst (Stevens and Edmonds 1978) and in silica supported catalyst (Gajardo 1978) the role of the promoter must be different from the one suggested by the monolayer model since the promoter does not incorporate in the surface of the support.

The pseudo-intercalation model is based on the layer structures of disulphides such as MoS_2 and WS_2, where the cations occur in trigonal prismatic surroundings, the cationic sites between successive S-layers being alternatively completely empty or all filled. The trigonal prismatic array splits the cation d-orbitals into a lower singlet and two doublets (Huisman et al 1971). If the lower

singlet contains only one electron it can adopt another electron from a transition metal intercalated into the empty layer positions under transfer of electrons to the original suphide cations. Bulk intercalation is not possible in MoS_2 or WS_2 because the lower singlet is already filled. But Ni(Co) intercalation may still occur at the layer edges between the $MoS_2(WS_2)$ layers in octahedral holes situated adjacent to Mo(W) ions. This leads to the formation of single and dual sites of exposed Mo(III)(W(III)) ions seated above a square planar array of sulphur ions at the edges of the layers. According to this model, the carrier acts only as a diluent and the Ni(Co)/Mo(W) ratio for optimal promotion is strongly dependent with the $MoS_2(WS_2)$ crystal size.

The synergetic model is based on the fact that mixtures of MoS_2 and Co_9S_8 demonstrate a considerable synergetic effect, i.e. Co_9S_8 is not very active but added to MoS_2 it enhances the activity of MoS_2 for thiophene hydrodesulphurisation, cyclohexane hydrogenation and cyclohexane isomerisation (Canesson et al 1976). No explanation except the presumption of electron transfer between adjoining phases, together with extra transfer caused by excess sulphur increasing the catalytic activity of MoS_2 (and/or Co_9S_8) is given for the synergetic effect. Stevens and Edmonds (1978) showed that an exchange of ligands between cobalt and molybdenum sulphides occurs in a Co-Mo/graphite catalyst in which MoS_2 was present in a high proportion of basal plane, and Gajardo (1978) showed that Co oxides are fully sulphided to Co_9S_8 only when MoS_2 is also present at the surface. Also, the presence of Co facilitates the growth of MoS_2 crystals, resulting in less amorphous sulphide phases (Hagenbach et al 1973, van der Aalst and de Beer 1977). Therefore, there is clear evidence for the interaction of Co(Ni) and Mo(W) sulphides on the surface of the catalyst, and both the synergetic and the intercalation models

could explain this interaction, but there is still not enough information to discriminate between these models.

In general, the activation process of the catalyst consists of several steps: diffusion of the activation agent into the surface of the catalyst, adsorption, nucleation and the reaction (interface progress). Many parameters are necessary to describe the activation conditions such as the composition of the activation gas (including the nature, impurities, presence of gaseous products of the reaction, etc.), temperature and time sequence of various conditions. If activation is carried out on unsupported MoO_3 by first reducing the catalyst with H_2 and then introducing H_2S (Zabala et al 1974), sulphidation does not go to completion and stops at an approximately equimolecular mixture of MoS_2 and MoO_2. On Co-Mo/γ-Al_2O_3 catalysts, the extent of sulphidation (S/Mo+Co) depends mainly on the temperature of the activation increasing with temperature (Massoth 1975), and higher degress of sulphiding are achieved when activation is carried out employing a mixture of H_2S in H_2 (about 10%v) (de Beer et al 1976). Higher activities for thiophene hydrodesulphurisation are observed when the activation is carried out between 573 - 623 K (Laine 1977).

1.5 AIMS

The main aims of this work were the study of the factors affecting the activity of Ni-Mo/γ-Al_2O_3 coal-conversion catalysts and the development of a preparation procedure to ensure good performance under industrial operation conditions. As indicated in the previous Sections, the main factors which affect the activity of the catalyst are the physico-chemical characteristics of the surface and the fundamental physical properties of the catalyst, such

as surface area and pore size distribution, since mass transfer resistances are important in hydrotreating coal-derived liquids. The former are determined essentially by the preparation procedure, while the latter are given by the characteristics of the support.

In the development of the catalyst, fundamental problems have to be solved, such as:

i) mode of action of the catalyst

ii) influence of the physical properties of the catalyst on the activity

iii) influence of the preparation procedure on the activity of the catalyst and on the physico-chemical characteristics of the surface

iv) relationship between surface structure and catalytic activity

and these were the main concerns of the present research. Under section (i), the purpose was to investigate the reactions occurring in hydroprocessing of coal-derived liquids employing a model feedstock containing compounds typical of those present in coal-derived oils at conditions close to those of industrial operation. Under section(ii), the purpose was to study the influence of the support characteristics on the activity of the catalyst and on the performance of trickle-bed reactors, which are commonly employed in industrial operation. Under (iii) and (iv), the purpose was to establish the relationship between (a) the preparation procedure and the activity and (b) the surface structure and the activity. Catalyst surfaces were characterised by gravimetric and spectroscopic methods (ESCA and u.v. reflectance spectroscopy), and the activity was measured both for HDS at atmospheric pressure (employing thiophene) and for HDS, HDO, HDN and hydrocracking/hydrogenation at high pressure (employing a model feedstock).

A secondary aim of the research was a catalyst development study in order to establish a "best" preparation procedure. Therefore this objective was borne in mind throughout when evaluating results and led to the step by step improvement of the method of preparation starting from the impregnation of Ni and Mo on the support from solutions containing the ions.

In order to achieve these objectives, a wide selection of catalysts was prepared employing different impregnation conditions (which also showed different surface characteristics) and subjected to standardised calcination and activation conditions and tested to evaluate their initial activities. In the calcination studies, the "best" procedure of impregnation was adopted, and a wide variety of catalysts was prepared employing different calcination conditions, and subject to standardised activation and testing conditions in order to evaluate their initial activity.

Finally, from a study of the sulphided state of the catalyst surfaces, a contribution has been made to the understanding of the nature of the active surface and the relationship between the method of preparation and the activity of Ni-Mo/γ-Al_2O_3 catalysts.

CHAPTER TWO: EXPERIMENTAL

2.1 INTRODUCTION

The experiments performed during the present research consisted of preparation of catalysts, catalyst testing and physico-chemical characterization of catalysts. The catalysts were prepared by impregnating the support with the active components from solutions containing Ni and Mo ions and subsequent drying, calcination and sulphiding. Two reaction systems were employed for catalyst testing: an atmospheric pressure reaction system to determine their HDS initial activity employing thiophene, and a high pressure reaction system employing a model feedstock simulating a coal-derived liquor. In the latter system, it was possible to evaluate the HDS, HDN, HDO and hydrogenation/hydrocracking capabilities of the catalysts under conditions close to industrial processing.

A study of the hydroprocessing of the model feedstock was carried out to determine the reaction mechanisms of the various components and care was taken to select the appropriate conditions in both reaction systems to ensure no significant mass transfer limitations in the reactor.

Physico-chemical characterization of the catalysts were carried out by: (a) gravimetric methods to determine surfaces areas, pore site distributions, surface acidities and the kinetics of calcination and sulphidation, and (b) spectroscopic methods of surface characterization, ESCA and u.v. reflectance spectroscopy, in which the surface chemical compositions and surface structures were established. Bulk chemical analysis (for Ni and Mo) of samples and catalysts was carried out by X-ray fluorence spectroscopy by Analytical Services, Imperial College.

The apparatus and procedures are described in the following sections.

2.2 HIGH PRESSURE REACTION SYSTEM

2.2.1 Description

The experimental trickle-bed reaction system employed for high pressure catalyst activity measurements is shown in Figure 2.1, the details of the construction are given in Table 2.1. Hydrogen and the feed oil were combined before entering the preheater of the trickle-bed reactor. The liquid feed, from a 3 ℓ capacity, 316 ss, storage tank kept under 180 kPa of nitrogen to avoid oxidation and evaporation, was passed through a micro-filter and pumped by a metering pump. A system of dumpers (resistive and capacitive) was employed to avoid fluctuations in the liquid flow to the reactor. Hydrogen was used directly from the cylinders.

The trickle-bed reactor was made of a 17 cm length of a 1.27 cm ($\frac{1}{2}$ in.) O.D. 316 ss tubing with a 0.16 ($\frac{1}{16}$ in.) O.D. centrally located thermocouple tubing. The catalyst was supported in the reactor by means of two 316 ss sintered discs placed at each end of the reactor tube. For some experiments, the reactor tube consisted of a 10 cm length of a 0.95 cm ($\frac{3}{8}$ in.) O.D. 316 ss tubing. The preheater consisted of a 50 cm length of a 0.32 cm ($\frac{1}{8}$ in.) O.D. 316 ss, coiled around the reactor, as shown in Figure 2.2. All connections were made of Gyrolok tube fittings. The reactor was placed inside an electric furnace, the temperature of which was controlled by a PID temperature controller within a range of ± 3 K.

The products from the reactor were passed through an air cooler, a water-cooled heat exchanger and liquid products were separated from gases in the 500 cm^3 capacity high pressure accumulator, the gases being discharged through a back pressure valve, which also

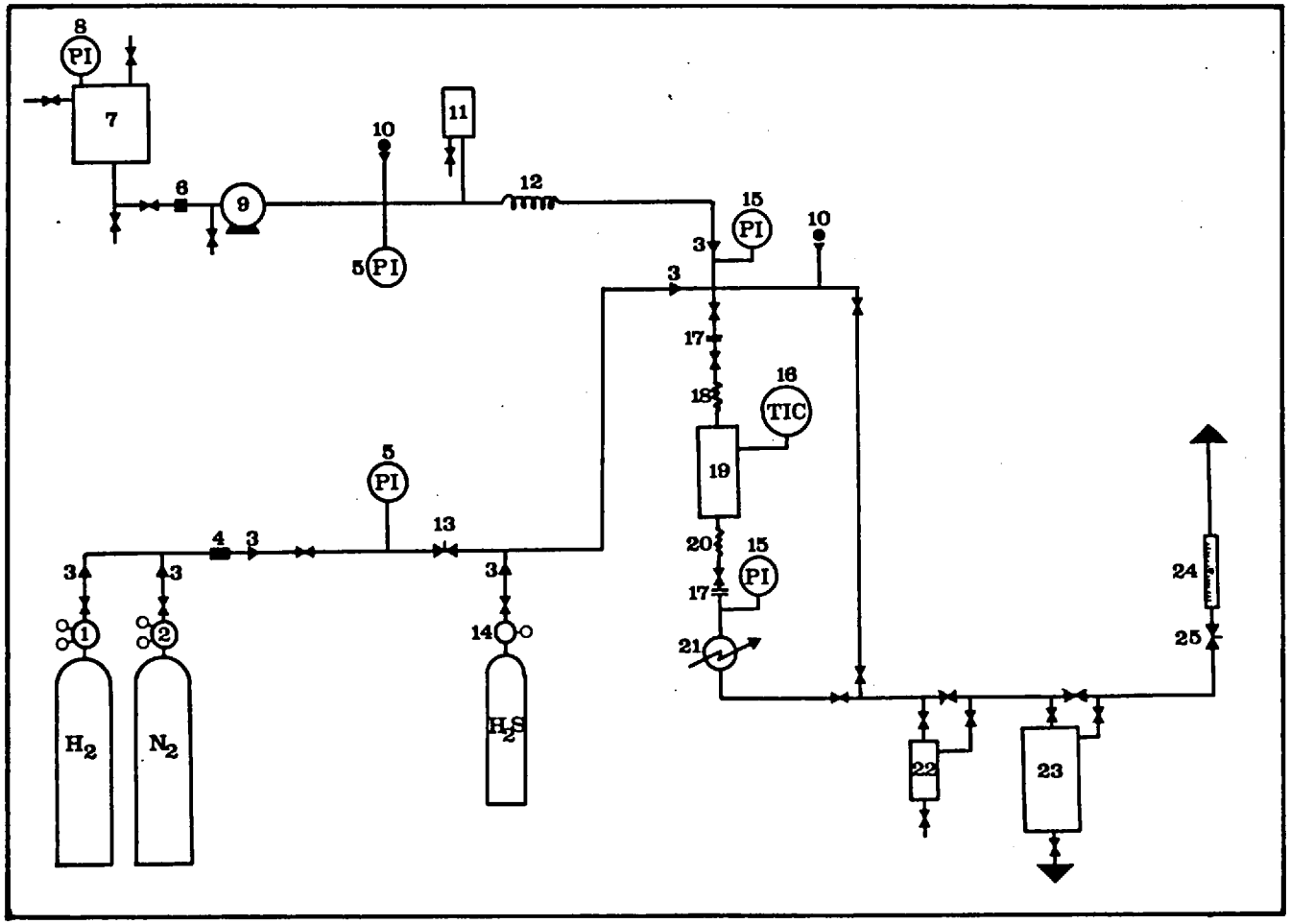

FIGURE 2.1 HIGH PRESSURE REACTION SYSTEM

TABLE 2.1

REACTION SYSTEM COMPONENTS

Key to Figure 3.1

1. Hydrogen pressure regulator, Pressure Control Ltd., 0-2,000 psig
2. Nitrogen pressure regulator, Pressure Control Ltd., 0-2,000 psig
3. Check valve, Hoke Ball Check Valve, 6133G25.
4. Filter, Hoke Micron In-line Filler, 6312F25.
5. Gauge, U.S. Gauge, 0-4,000 psig, 2½" diamter, 316 ss.
6. Filter, Hoke Micron Removable, 6321G4Y.
7. Liquid feed tank, 3 ℓ capacity, welded 316 ss.
8. Gauge, Gallenkamp, 0-15 psig.
9. Metering pump, Dosapro Milton Roy, Mod 19633, 0-300 cc hr^{-1} 3600 psig.
10. Relief valve, Hale-Hamilton RS12, 2500-3600 psig.
11. Damper (capacitance), Water Dumper Accumulator, 100 cm^3.
12. Damper (resistive), 3 m long, 1/16" O.D. 316 ss tubing.
13. Flow valve, Hoke Milli-Mite Forged Metering Valve, 1315G2Y.
14. Hydrogen sulphide pressure regulator, 0-100 psig, Matheson, Mod 11.
15. Gauge, Budenberg, 0-4,000 psig, 6" diameter.
16. Temperature controller, Eurotherm, Mod 020-088-03-023-12-05.
17. Bulkhead connnector, Hoke, 2BCM2-316.
18. Preheater, 50 cm long, ⅛" O.D., 316 ss tubing.
19. Reactor, 16 cm long, ½" O.D., 316 ss tubing.
20. Air cooler, 30 cm long, ⅛" O.D., 316 ss tubing.
21. Water cooler, 15 cm long, jacket ¼" O.D., tube ⅛" O.D., 316 ss tubing.
22. High pressure sampler, 4 cm^3 capacity.
23. High pressure accumulator, Hoke 6HDY500, 500 cm^3 capacity.
24. Float meter, GEC Elliot Process Instruments, Mod 1100, tube D2.
25. Back pressure valve, Hoke Micro-Mite Forged Metering Valve, 1656G2Y.

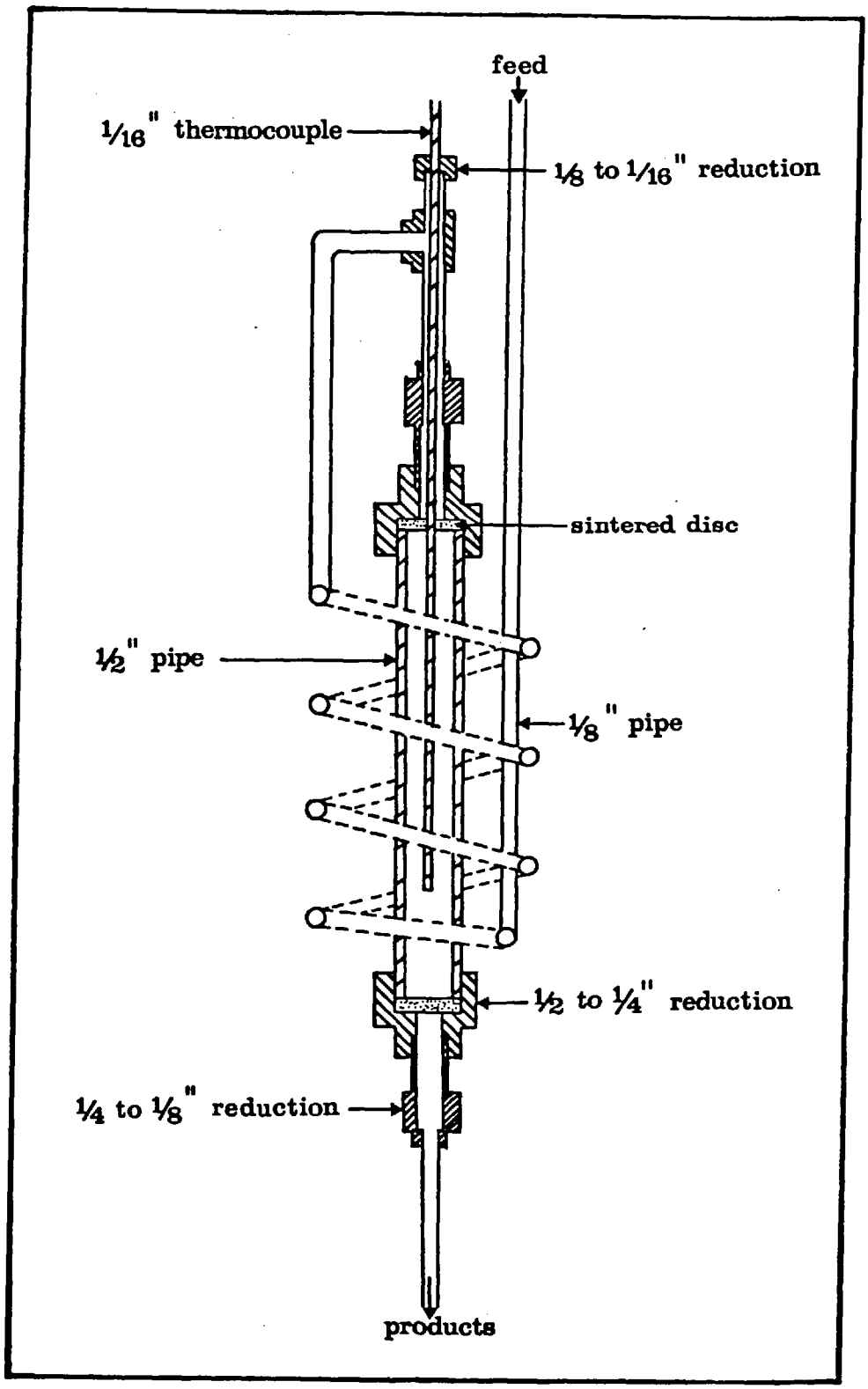

FIGURE 2.2 THE TRICKLE-BED REACTOR

controlled the gas flow through the reactor. A 4 cm^3 capacity high pressure sampler placed upstream to the accumulator allowed the extraction of samples for analysis during a run.

2.2.2 Procedure

Typically, 8 g of a 0.30 - 0.40 mm particle diameter catalyst was placed in the reactor, and the reactor was pressure tested up to 10.3 MPa with nitrogen. The reactor was evacuated and placed in position in the rig, when the temperature was gradually increased up to the activation temperature of the catalyst while a flow of 186.4 $cm^3\ min^{-1}$(STP) at 680 kPa of nitrogen was passed through the reactor. Once the activation temperature was reached, a 465.9 $cm^3\ min^{-1}$ (STP) of hydrogen sulphide (or a 10% v H_2S/H_2 mixture) at 68.9 kPa was established through the reactor and the conditions maintained for the activation period (usually 1 hr).

After this period, the oil pump was started, a flow of 60 $cm^3\ hr^{-1}$ of oil was established, and the temperature of the reactor gradually increased to the reaction temperature. When liquid products were observed in the accumulator, the flow of activation gas was interrupted and the pressure of the reactor gradually increased to the desired value (usually 6.89 MPa) with hydrogen maintaining a flow of about 465.9 $cm^3\ min^{-1}$ (STP) through the reactor. Once the desired conditions of temperature and pressure were achieved (generally in a period of 1 - 2 hrs), the conditions of the catalyst test were established and sampling of the liquid products could begin after 1 hr of operation.

2.2.3 Feedstock

A standard feedstock was used for all high pressure activity

measurements, which was designed in such a way that the hydrogenation (HY), hydrocracking (HC), hydrodesulphurization (HDS), hydrodenitrogenation (HDN) and hydrodeoxygenation (HDO) functions of the catalysts could be assessed. Model compounds were chosen for the feedstock from those occurring in coal derived liquids but which give products that can be traced to individual reactions. The composition of the feedstock was selected to have a similar ultimate analysis to a coal extract (National Coal Board 1976), and details are given in Table 2.2. Dibutylsulphide, which is easily desulphurized, was

TABLE 2.2

Composition of Model Feedstocks

Components of coal	Model compound	Reaction expected	Feedstock use in: Reac. Mech. studies % w	Cat. testing % w
Multi-ring aromatics	phenanthrene	HY HC	10	8
Sulphur compounds	dibenzothiophene	HDS	8	-
	dibutylsulphide	HDS	5	5
Nitrogen compounds	quinoline	HDN	20	20
Oxygen compounds	dibenzofuran	HDO	7	7
Solvent	heptane	-	50	60
density (g cm^3)			0.91	0.85

added to the feed to provide an approximately constant distribution of sulphur through the catalyst bed. On the basis of the study of the reaction mechanisms, described in Chapter 3, it was decided to eliminate dibenzothiophene from the catalyst testing feedstock since it was completely hydrodesulphurized in the reactor.

2.2.4 Analysis

Liquid samples were collected at 2 hourly intervals during each run and analysed by GLC with a flame ionization detector using a 2 m long, 0.32 cm ($\frac{1}{8}$") O.D. 316 ss column, packed with OV-101 (Phase Separation Ltd.). The column was maintained at 313 K for 7 min after injection of the sample (0.5 μℓ) and then temperature programmed from 313 to 523 K at a rate of 4 K min^{-1}.

Product components were identified by the use of pure compounds where possible and by mass spectrometric analysis performed on some runs. The area factors were determined injecting solutions of known compositions using pure compounds, and for those not available using correlations given in the literature (Ambrose and Ambrose 1961). Table 2.3 shows the retention times and area factors of the main components of the liquid product. No analysis of gaseous products was made.

2.3 ATMOSPHERIC PRESSURE REACTION SYSTEM

2.3.1 Description

In addition to the catalyst testing in the high pressure trickle-bed reactor, an atmospheric pressure reaction system was employed to measure the HDS activity of the catalyst, since this system had the advantage of being less expensive to run and its results correlated well with those of the high pressure reactor, as shown in Chapter 5.

The experimental system used for the atmospheric pressure catalyst activity measurements employing thiophene is shown in Figure 2.3, and it was the same system employed in a previous work carried out by this Department (Laine 1977).

Hydrogen streams were purified by passing them through an Oxy-trap (Field Inst. Ltd.) and a molecular sieve dessiccator. The reactor

TABLE 2.3

GLC Analysis of liquid products

COMPONENT	FORMULA	AREA FACTOR	RETENTION TIME	
			min	sec
Butane	C_4H_{10}	1.0155	0	36
Benzene	C_6H_6	.9831	3	6
Cyclohexane	C_6H_{12}	.9798	3	14
Heptane	C_7H_{16}	1.0000	5	18
Methylcyclohexane	C_7H_{14}	.9789	6	18
Toluene	C_7H_8	.9194	7	48
Ethylcyclohexane	C_8H_{16}	.9799	12	03
Ethylbenzene	C_8H_{10}	.9270	13	02
Propylcyclohexane	C_9H_{18}	.9798	16	24
Propylbenzene	C_9H_{12}	.9328	17	12
Alkylcyclohexane A	-	.9500	17	42
Alkylcyclohexane B	-	.9500	18	18
Alkylcyclohexane C	-	.9500	19	50
Butylbenzene Isomer	$C_{10}H_{14}$	.9293	20	10
Alkylcyclohexane D	-	.9500	21	15
Dibutylsulphide	$C_8H_{18}S$	1.3044	23	48
Tetrahydro Naphthelene	$C_{10}H_{12}$	.9227	24	12
Naphthalene	$C_{10}H_8$	.8945	26	00
Quinoline	C_9H_7N	1.1615	27	48
O-Propylaniline	$C_9H_{13}N$	1.1548	27	54
Dicyclohexyl	$C_{12}H_{22}$	.9681	30	55
Cyclohexylbenzene	$C_{12}H_{16}$	.9320	31	40
Diphenyl	$C_{12}H_{10}$	.9086	33	05
Dibenzofuran	$C_{12}H_8O$	1.0745	37	42
Octahydraphenanthrene Isomer	$C_{14}H_{18}$	.9287	40	36
Dihydrophenanthrene	$C_{14}H_{12}$	.8985	43	04
Octahydrophenanthrene Isomer	$C_{14}H_{18}$	.9287	44	02
Tetrahydrophenanthrene Isomer	$C_{14}H_{14}$	.9086	45	10
Dibenzothiophene	$C_{12}H_8S$	1.2377	45	45
Phenanthrene	$C_{14}H_{10}$	.8885	46	20
Perhydrophenanthrene Isomer	$C_{14}H_{24}$	.9711	48	50

consisted of a 2.2 cm I.D. silica glass tube with a sintered glass disc in the middle of the tube in which the catalyst bed was supported. The thermocouple of the temperature controller reached the bed through a concentric well of 0.6 cm O.D., and the temperature of the bed was controllable within ± 2 K. All lines between the drechsel bottles and the exhaust were kept at about 423 K in order to avoid thiophene condensation or sulphur deposition on the walls.

The reactor input or output stream was diverted to the sampling-loop, according to the position of the five, two oblique-pattern valves, the reactants always passing through the catalyst bed. Analysis was carried out by GLC with a thermal conductivity detector using a 1.5 m long, 0.32 cm ($\frac{1}{8}$") O.D. 316 ss column packed with 13.5% bis-methoxyethyl adipate, 6.5% diethyl hexyl sebacate on Chromosorb P (Phase Separation Ltd.). At 373 K, the retention time for hydrogen was 15 sec and 2 min 10 sec for thiophene. H_2S, butane, 1-butane and 1,3 butadiene were elluted almost simultaneously (30 - 45 s). No selectivity studies were attempted and the conversion of thiophene was determined by its disappearance.

2.3.2 Procedure

The following standard procedure was followed for all the atmospheric pressure catalyst activity tests reported throughout this work.

Three grams of the 0.30 - 0.40 mm particle diameter catalyst was placed in the reactor. The temperature was gradually increased up to 573 K, with a flow of 279.5 cm^3 min (STP) of helium passing through the reactor. Once this temperature was reached (usually after about 15 min), the catalyst was activated by passing through it a flow of 465.8 cm^3 min^{-1} (STP) of a 10% v H_2S/H_2 mixture for 1 hr.

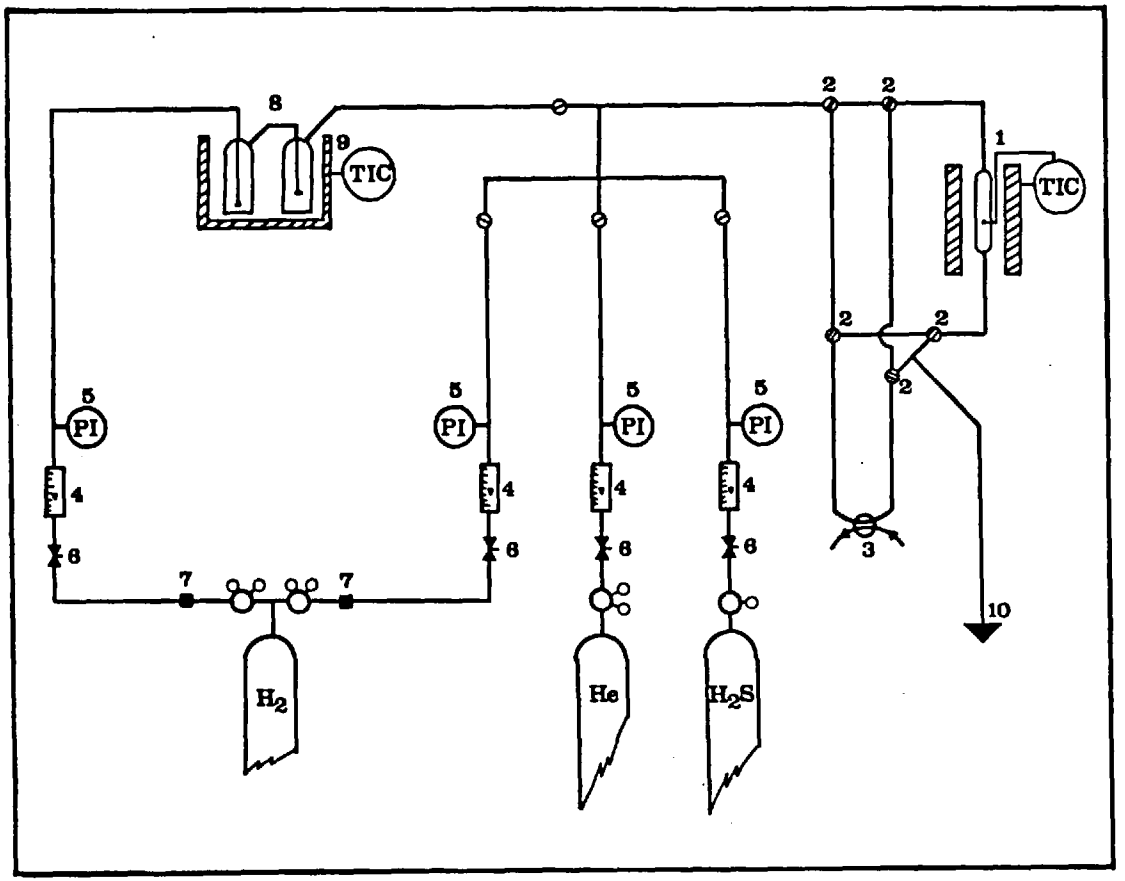

Legend

(1) Reactor
(2) Two oblique pattern valves
(3) Injection valve
(4) Float-meters
(5) Bourdon manometers
(6) Gas flow control valves
(7) Hydrogen purification traps
(8) Drechsel bottles
(9) Water bath
(10) Exhaust

FIGURE 2.3 ATMOSPHERIC PRESSURE REACTION SYSTEM

After this period the flow of reactants was started and the temperature increased to 623 K.

Tests were made to find the optimum conditions of operation to avoid mass transfer limitations in the reactor. The effect of the flow of reactants and the particle size was studied. It was found that a flow of 465.8 cm^3 min^{-1} (STP) of hydrogen (as measured in the float meters) with a hydrogen to thiophene molar ratio of 13 was necessary in order to have no mass transfer resistances in the reactor at 623 K.

The reported values of activity were taken during a 2 hr run and no decay in the catalyst activities were observed during this period for any catalyst.

When a sample of the used catalyst was required the reactor was cooled to room temperature passing the H_2S/H_2 mixture through the catalyst bed.

2.4 GRAVIMETRIC SYSTEM

2.4.1 Description

The gravimetric apparatus consisted of a microbalance associated with a vacuum line or with a flow system. Included in the system were means to measure pressure temperature, gas flows and to record the signals from the microbalance. This system was employed to measure surface area, pore size distribution and surface acidity, as well as the kinetics of the calcination, reduction and sulphidation of the catalysts in the flow mode. A schematic diagram of the system is shown in Figure 2.4, and it is similar to the one described by Bernardo (1977).

The vacuum line system consisted of a mechanical pump (Edwards Speedivac rotary pump) and a mercury diffusion pump giving an ultimate

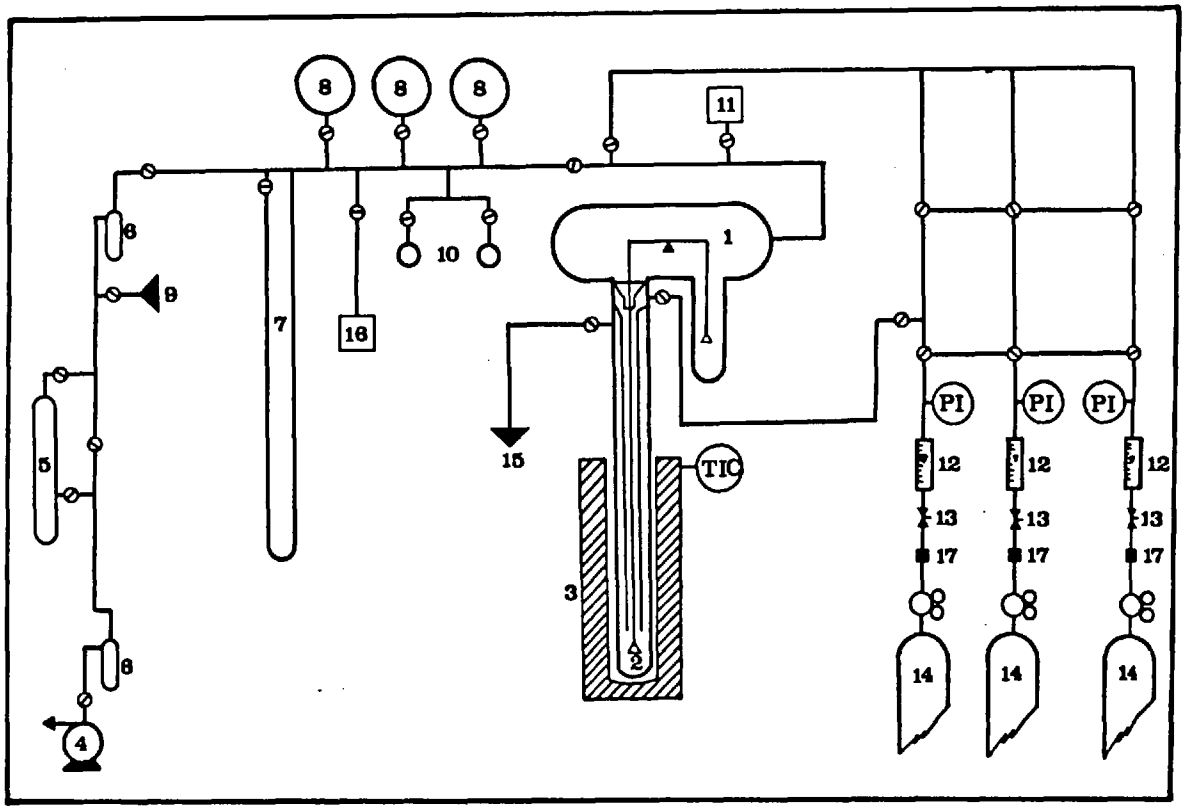

Legend

(1) Microbalance
(2) Catalyst basket
(3) Furnace
(4) Vacuum pump
(5) Hg diffusion pump
(6) Liquid nitrogen traps
(7) Manometer
(8) Gas containers
(9) Gas inlet
(10) Liquid containers
(11) Pirani vacuum head
(12) Float-meters
(13) Gas flow control valves
(14) Gas cylinders
(15) Gas outlet
(16) McLeod gauge
(17) Purification traps

FIGURE 2.4 GRAVIMETRIC GAS ADSORPTION AND FLOW SYSTEM

vacuum of about 1.33 mPa. Low pressures were measured by means of Pirani and MacLeod gauges. Three storage bulbs of about 3.5 litres were used to store gases and two 50 cm^3 bulbs to store liquids. The liquid nitrogen trap at the outlet of the mercury diffusion pump allowed also the purification of the gases employed in the adsorption experiments.

The head of the microbalance (C.I. Electronics MK23) was fitted inside a special vacuum bottle and connected to the vacuum line. It was capable of recording changes in weight from 0 to 100 mg in five ranges (from 0 - 25 μg, 0 - 250 μg, 0 - 2.5 mg, 0 - 10 mg and 0 - 100 mg) with a sensitivity of about 0.5% of the corresponding range. The maximum sample weight is 1 g.

The reactor, which was also used as a sample container in the vacuum experiments and was connected to the vacuum glass bottle of the microbalance, is represented in Figure 2.5. The funnel was used to prevent the presence of corrosive gases in the microbalance head, by means of a flush gas (usually nitrogen) passing through it. The inner tube assured the circulation of the gases through the sample. A water cooled jacket was used to cool down the lower glass conical connection.

The reactor was placed inside an electric furnace and the thermocouple of the temperature controller was located adjacent to the outer wall of the reactor tube, in front of the sample basket. It was established that the temperature near the sample was within 3 K of the temperature measured outside the reactor when a total flow of 112.9 $cm^3\ min^{-1}$ (STP) of gas passed through the reactor.

For the flow experiments, gases were supplied from cylinders through two-stage pressure regulators, purification traps, a series of rotameters (calibrated for each individual gas) and five control needle valves. Each line had a mercury manometer and the pressure

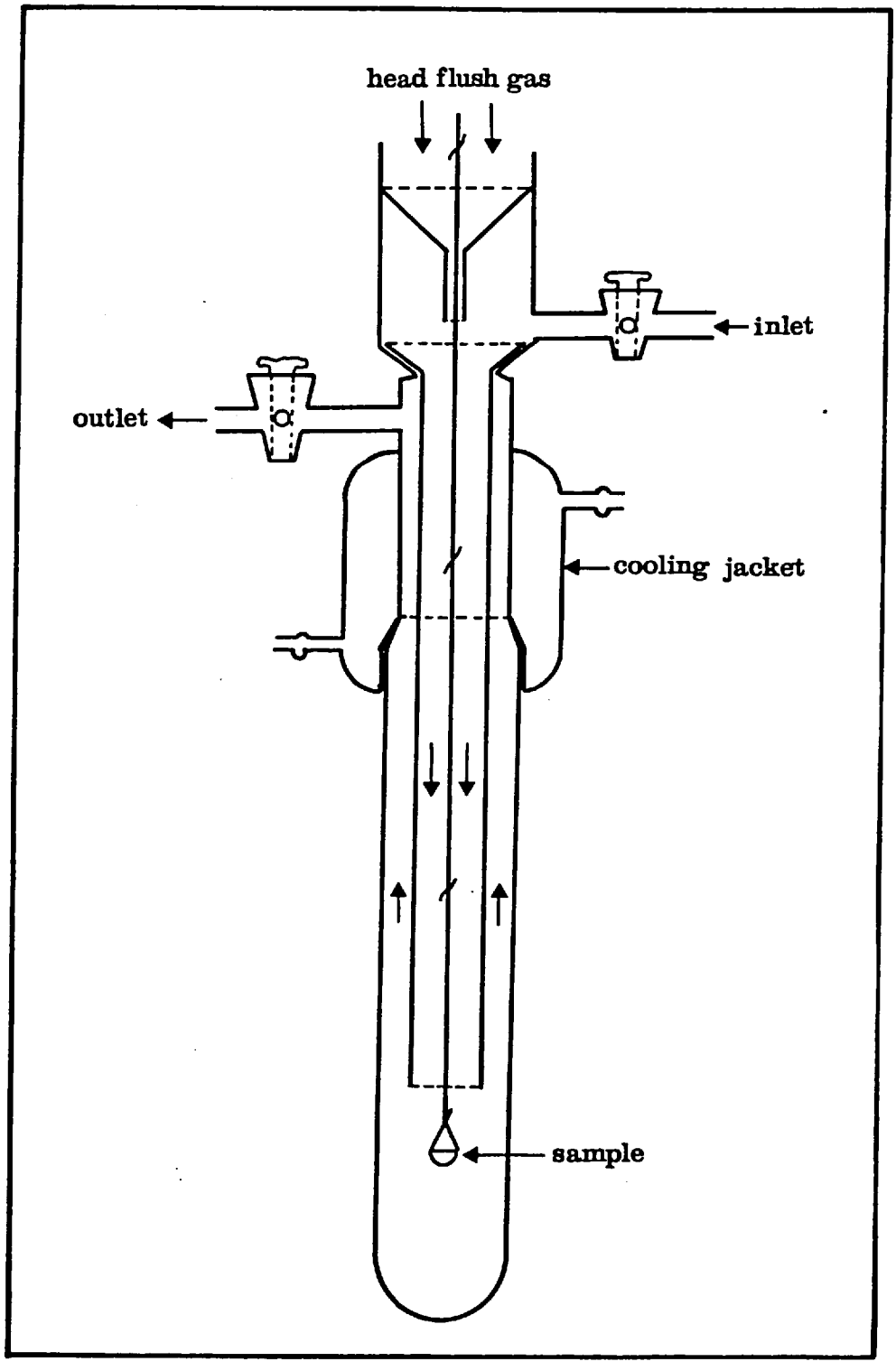

FIGURE 2.5 GRAVIMETRIC SYSTEM REACTOR

was always maintained at the same level so that corrections to the float meter readings were unnecessary.

2.4.2 Surface Area and Pore Size Distribution

For the surface area and pore size distribution determinations, the gravimetric system was used in the vacuum mode. Typically, about 100 mg of the catalyst (for a high surface area catalyst) were placed in the sample basket, the exact weight having been measured in a separate balance (± .1 mg). The basket was fitted in the system, the sample counterweighted within 2 mg, and the temperature increased to the desired degasing value (around 673 K). Evacuation was then carried out until no change either in pressure (around 1.33 mPa) or weight was observed (usually for about 2 - 3 hours).

After this period the furnace was replaced by a dewar flask containing liquid nitrogen (78 K) and nitrogen from the gas storage bulbs was admitted stepwise, recording both pressure and change in weight at each step. For the determination of pore size distribution the pressure was increased up to about 99.3 kPa, and then the pressure was reduced stepwise to obtain the desorption isotherm. Weights measured were corrected for the buoyancy effect, determined by carrying out the same process with an approximately equal volume of glass beads (negligible surface area). For high surface area samples this effect is of no significance.

The results were processed by a computer program SURPOR described in Appendix A, in which surface areas are obtained employing the BET equation (Thomas and Thomas, 1967), and pore size distributions employing the Kelvin equation following the procedure described by Gregg and Sing (1967). The thermodynamic basis and the validity of the results obtained by these methods have

been recently discussed (Broeckhoff 1978), and it is beyond the scope of the present research to discuss them in detail.

2.4.3 Surface Acidity

The determination of surface acidity was carried out using the gravimetric system in the vacuum mode, employing the method proposed by Richardson and Benson (1957). Gaseous pyridine was used as the basic adsorbate, the measure of the acidity being taken from the weight of pyridine chemisorbed on the surface. This method gives an estimation of the total acidity of the surface, since pyridine chemisorbs either by the transfer of electrons to the surface (Lewis acidity) or through the transfer of a proton from the surface (Brønstead acidity) (Forni 1974). It was always carried out after the determination of the surface area of the sample to refer the acidity as mg of chemisorbed pyridine per meter square of surface.

After the determination of the surface area, the temperature of the sample was increased to the degasing temperature and the sample evacuated for 1 hr at 13.3 mPa. After this period the sample was cooled down to room temperature, the reactor immersed in a temperature controlled water bath at 298 K, and about 0.20 kPa of pyridine admitted inside the vacuum system. These conditions were maintained until the balance reached a steady state (usually around 30 - 40 min) and then the sample evacuated. The weight of pyridine adsorbed at about 13.3 mPa was taken as a measure of the total surface acidity of the sample.

2.4.4 Kinetics of Activation Reactions

The determination of the kinetics of the activation reactions of the catalyst, i.e. calcination and sulphidation, was carried out in the flow mode of the gravimetric system employing 50 - 150 mg of

the catalyst. In the calcination studies, the dried sample was kept at 353 K and a flow of 118.1 cm^3 min^{-1} (STP) of dry air in order to eliminate the weakly adsorbed water. After this period, in which a weight loss around 3 - 5%w was observed, the temperature was gradually increased (at an approximately linear rate of 3.5 K min^{-1}) to 673 K and kept under these conditions for 4 hours while continously recording the changes in weight.

For the sulphidation studies, the already calcined samples were kept at the sulphidation temperature (573 K) under a flow 118.1 cm^3 min^{-1} (STP) of dry air until no change in weight was observed. Then the air flow was replaced by a 188.2 cm^3 min^{-1} (STP) of the 10% v H_2S/H_2 mixture, and the weight increase recorded. To protect the microbalance head during the sulphidation studies, a continuous flow of 10.9 cm^3 min^{-1} (STP) of nitrogen was maintained through it.

2.5 SPECTROSCOPIC METHODS OF SURFACE CHARACTERIZATION

In order to gain information about the surface structure and composition of the catalysts, ESCA and u.v.-reflectance spectroscopy was employed.

2.5.1 U.v.-reflectance Spectroscopy

U.v. reflectance spectra of the catalysts were measured by the diffuse-reflectance technique in a Beckman DK-2 spectrophotometer with an integrating sphere coated with Ba SO_4. The samples were analysed against the Norton 6175 γ-alumina support as standard and MgO was employed as a reference for pure compounds (Gajardo 1978).

2.5.2 X-ray Photoelectron Spectroscopy (ESCA or XPS)

Spectra were obtained with a Vacuum Generators ESCA III spectrometer using an Al X-ray anode and computerised data system. Samples

were mounted on double-sided adhesive tape. The binding energy scale was calibrated using carbon contamination with C_{1S} = 284.3 eV or Al_{2p} = 74.5 eV in those cases where the carbon contamination peak was poorly resolved (Carlson 1975).

2.6. CATALYST PREPARATION

Catalysts were prepared in order to study the influence of the preparation procedure on catalytic activity. This research began initially as a catalyst development study in which the aim was to establish the conditions of preparation (based on impregnation of the active components from solutions containing the ions) which give the highest activity in coal hydrogenation. However, in order to achieve this fully it became necessary to study the different stages of the preparation process in detail.

The first method of impregnation adopted was the one proposed by Laine (1977) and it consisted of co-impregnation employing the pore filling technique. That is, the volume of the impregnating solution (containing both Ni and Mo ions) was just enough to fill the pore volume of the support and the excess moisture was eliminated by evaporation. This method was employed in the studies to select the support for use throughout the catalyst preparation studies of the present research, reported in Section 4.4.

This method, although having the advantage that it can be used for any support, does not ensure a good dispersion of the active components over the surface of the support (Fenelov et al 1978). Therefore, employing a volume of solution in excess of that of the pore volume of the support is desirable to have better control of the variables (pH, concentration) during the impregnation. Moreover, in the case of alumina it is possible to select the conditions (pH)

in order to have an adsorption of the active ions on the support, leading to a higher degree of dispersion, and this will be discussed more fully later. But the latter method requires knowledge of the adsorption isotherms of the ions on the support prior to its use. For this reason, and also to investigate the nature of the impregnation process itself, the impregnation of Ni and Mo on the support was studied in detail. The selected pH conditions were such as to have the surface of the support positively or negatively charged (pH 2 and pH 8), although in fact the impregnations were carried out in a range of pH rather than the initial value. This will be discussed in Chapter 5.

On the basis of this study the effect of the impregnation conditions (pH, order of impregnation) employing a volume of solution in excess of the pore volume of the alumina support was studied, on a series of catalysts having the same loading 4%w NiO - 15%w MoO_3 . Calcination conditions were the same for the whole series (673 K, air). This effect was subsequently studied on a series of catalysts employing the best method of impregnation.

The experimental details of the impregnation studies as well as the catalyst preparation methods are presented next, including the procedure used to modify the pore structure of the support.

2.6.1 Impregnation Studies

γ-alumina (Norton SA-6175, particle diameter 030 - 0.40 mm, BET surface area 259 m^2g^{-1}, water pore volume 0.55 $cm^3\ g^{-1}$) was impregnated at room temperature (293 K) with the following solutions:

a) Mo from ammonium molybdate (BDH-Analar grade) at pH = 8 and pH = 2.

b) Ni from nickel nitrate at pH = 8 and pH = 2.

c) Mo and Ni simultaneously at pH = 2 and pH = 7.

Typically, 3g of the support was placed in a 2.5 × 10 cm polyethylene stoppered tube and 30 cm^3 of the solution of the required concentration and pH was added. The samples were shaken in a bath at 293 ± 1 K for 40 hours. The pH of the suspension was periodically adjusted (every 20 min during the first few hours of the adsorption run) to the desired value using concentrated HNO_3 or NH_4 OH. After this period, the samples were filtered keeping both liquid and solid phases, and the impregnated alumina was dried for 24 hours at 393 K in air. Changes in the pH of the suspension were observed in the first few hours of the adsorption run. XRF analyses were performed to determine Ni and Mo compositions of the impregnated alumina and of the solutions to obtain the equilibrium concentration.

2.6.2 Pore-filling Co-impregnation

This method is based on the results of Laine (1977) and it was used to prepare the catalyst employed to study the effect of the surface acidity of the support in the performance of the Ni-Mo/γ-alumina coal hydrogenation catalyst (4.4, Chapter 4). The preparation procedure was as follows:

1. The requisite amount of Mo salt was dissolved in 27 cm^3 of warm water (323 K).
2. The Mo solution was cooled to 293 K and the Ni salt was dissolved in the solution.
3. 20g of the support was added, the mixture stirred for 45 minutes, and the formation of a precipitate of a Ni-Mo complex (light green) began.
4. The pH of the solution was adjusted to 10, by addition of a concentrated NH_4 OH solution, and the mixture was stirred

for 2 hours under these conditions.

5. The catalyst was dried at 353 K for one hour and at 383 K for 14 hours.

2.6.3 Impregnation under Excess Volume

On the basis of the results from the impregnation studies (5.2, Chapter 5), the catalysts were prepared by impregnation using a volume of solution 30% in excess of the total pore volume of the support. For the impregnation condition in which the pH of the solution was such that no adsorption took place, the volume of the solution employed in preparing the catalysts was 5% in excess of the pore volume.

Typically, 20g of the support was placed in a beaker, the necessary volume of the solution of the required concentration and pH was added and the suspension shaken in a bath at 293 ± 1 K for 24 hours. The pH was periodically adjusted to the desired value. After this period, the catalyst was filtered and dried for 24 hours at 393 K. For the catalysts prepared in successive impregnations, the support was impregnated with the first cation/ion, dried and calcined before it was impregnated with the second cation/ion by the same procedure. Catalyst nomenclature throughout is that Mo(A) - Ni(B) = Mo first at pH = 2 and then Ni at pH = 8, NiMo(A) = co-impregnation at pH = 2.

2.6.4 Calcination

The catalysts were calcined in a 5.0 cm ID silica tube placed inside an electrical furnace (the temperature of which was controllable within 3 K) and supported inside the tube by means of two silica wool plugs in the apparatus described by Bernardo (1977). For small samples (below 10g) a silica boat was employed. Calcinations were carried

out for a period of 8 hours at the set temperatures; the heating rate (from room temperature) was about 6 K min^{-1} while the cooling rate was about 10 K min^{-1}. The standard calcination conditions were 673 K and a flow of 372.7 cm^3 min^{-1} (STP) of dry air, in which case the catalyst nomenclature is that of the previous section. For catalysts calcined under different conditions of temperature or atmosphere (Chapters 6 and 7), the nomenclature is that Ni773A - Mo873WA = Ni first at pH = 8 and calcined at 773 K in dry air followed by Mo impregnated at pH = 2 and calcined in air saturated in water (at 293 K) at 873 K; 673 N designate calcinations at 673 K under nitrogen.

2.6.5 Modification of the Pore Structure of the Support

Modification of the pore size distribution of the Norton 6175 γ-alumina support, for those catalysts employed in 4.3, Chapter 4, was carried out with an aqueous ammonium carbonate solution (25%w) at 423 and 448 K, following the procedure described by Pearson et al (1977). It was carried out in a 100 cm^3 316 ss pressured vessel for 20 hours at the set temperature. The heating time was about 3 hours and the cooling time about 4 hours.

2.7 MATERIALS

The type, purity and use of all chemicals employed throughout this research are listed in Table 2.4. With the exception of the gases employed in the adsorption experiments, they were used as received.

TABLE 2.4

Purity, Use and Supplier of the Chemicals Employed

Chemical	Purity %	Use	Supplier
Heptane	> 99.5	diluent	BDH
Dibutylsulphide	97.0	reactant	Aldrich
Quinoline	96.0	reactant	Aldrich
Dibenzofuran	98.0	reactant	Aldrich
Dibenzothiophene	95.0	reactant	Aldrich
Phenanthrene	95.0	reactant	BDH
Thiophene	99.0	reactant	BDH
γ-Alumina	> 80.3	catalyst support	Norton SA3232
γ-Alumina	> 99.75	catalyst support	Norton SA6175
γ-Alumina	> 99.9	catalyst support	BDH
γ-Alumina	> 99.9	catalyst support	BDH
Nickel nitrate	> 98.0	cat. preparation	BDH-Analar
Ammonium molybdate	> 99.0	cat. preparation	BDH-Analar
Molybdenum trioxide	> 98.0	cat. characterization	BDH-Analar
Sodium molybdate	> 98.0	cat. characterization	UCB-Analar
Ammonium carbonate	> 95.0	cat. preparation	BDH-Analar
Ammonia solution	35.0	cat. preparation	BDH-Analar
Nitric acid	69 - 72	cat. preparation	BDH-Analar
Pyridine	> 99.5	cat. characterization	BDH-Analar
Nitrogen	> 99.9	carrier, cat. preparation	BOC
Hydrogen	> 99.9	reactant, cat. activation	BOC
Air	-	cat. preparation	BOC
Hydrogen sulphide	> 99.6	cat. activation	BOC
10%v H_2S/H_2	-	cat. activation	BOC
Helium	> 99.9	diluent	BOC
AKZO-1535	—	catalyst	AKZO CHEMIE

CHAPTER THREE: HYDROPROCESSING OF THE MODEL FEEDSTOCK ON A Ni-Mo/γ-Al_2O_3 CATALYST

3.1 INTRODUCTION

Most modern coal-conversion processes are based on catalysts containing molybdenum compounds promoted by nickel or cobalt, usually supported on aluminas. Their mode of action is, however, subject to considerable doubt. Part of the problem arises from the complexity of the reactions involved in the hydrotreating of coal. The major reactions involve the hydrocracking of multi-ring aromatics and the removal of the heteroatoms O, N and S as H_2O, NH_3 and H_2S. Many of the studies have been focussed on coal or on single feedstocks such as thiophene. In the first case the complexity of the product spectra tends to obscure the underlying mechanisms while in the second case, the absence of cross-interactions between components of coal leaves the results open to question.

This study has been focussed on the hydrogenation of a model feedstock containing compounds typical of those occurring in coal derived liquors, but which give products that can be traced to individual reactions, over a Ni-Mo/γ-Al_2O_3 catalyst.

3.2 REACTOR DATA

A model feedstock consisting of 8%w dibenzothiophene, 7%w dibenzofuran, 20%w quinoline and 10%w phenanthrene dissolved in heptane (50%w) was hydroprocessed over a commercial Ni-Mo/γ-Al_2O_3 catalyst (AKZO 153-S) in the trickle-bed reactor, under the conditions described in Table 3.1. Overall conversions of the feed compounds are shown in Table 3.2 and product compositions at the steady state

are given in Table 3.3. A comparison of the equilibrium and the observed hydrogenation ratios is presented in Table 3.4. Equilibrium values were calculated using equations available in the literature (Frye 1962, Satterfield et al 1978).

TABLE 3.1

EXPERIMENTAL CONDITIONS

Weight of catalyst*	2g
Weight hourly space velocity	10 g h^{-1} g-cat^{-1}
Hydrogen flow rate	465.9 cm^3 min^{-1} (STP)
Pressure	6.89 MPa
Temperature	673 and 753 K

*particle size 0.15 - 0.21 mm, diluted in a 1:1 ratio with ground silica glass.

TABLE 3.2

FEED OVERALL CONVERSIONS

Conversions	Temperature	
	673 K	753K
Dibutylsulphide	100	100
Dibenzothiophene	100	100
Quinoline (HDN)*	50.56	95.79
Phenanthrene total	68.44	86.99
Phenanthrene (hydrogenation)	61.31	5.66
Dibenzofuran	14.56	78.84

*based on nitrogen removal from organic ring.

TABLE 3.3

PRODUCT COMPOSITIONS

Component		Temperature 673K %w*	753K %w*
1. C_4H_{10}	Butane	2.49	1.87
2. C_6H_6	Benzene	0.01	0.35
3. C_6H_{12}	Cyclohexane	0.28	0.90
4. C_7H_{16}	Heptane	49.58	49.58
5. C_7H_{14}	Methyl Cyclohexane	tr	0.07
6. C_7H_8	Toluene	tr	0.16
7. C_8H_{16}	Ethyl Cyclohexane	0.05	0.14
8. C_8H_{10}	Ethyl Benzene	tr	0.14
9.	n-paraffin	0	tr
10. C_9H_{18}	Propyl Cyclohexane	9.95	4.35
11. C_9H_{12}	Propyl Benzene	1.01	5.71
12.	Alkyl Cyclohexane A	0.09	tr
13.	Alkyl Cyclohexane B	0.54	tr
14. C_9H_{12}	Isopropyl Benzene	0	0.07
15. C_9H_{10}	Indan Isomer	0	0.30
16.	Alkyl Cyclohexane C	0.01	tr
17. $C_{10}H_{14}$	ButylBenzene Isomer	0	0.15
18.	Alkyl Cyclohexane D	tr	tr
19. $C_{11}H_{16}$	Pentyl Benzene Isomer	0	tr
20. $C_8H_{18}S$	Dibutyl Sulphide	0	0
21. $C_{10}H_{12}$	Tetrahydro Naphthalene	tr	0.07
22. $C_{10}H_8$	Naphthalene	0.01	0.04
23. $C_{12}H_{18}$	Hexylbenzene Isomer	0	tr

TABLE 3.3 (continued)

Component		Temperature 673K %w*	753K %w*
24. C_9H_7N	Quinoline	0	tr
25. $C_9H_{13}N$	O-Propyl Aniline	3.15	0.38
26. $C_{12}H_{22}$	Dicyclohexyl	0.18	0.21
27. $C_{12}H_{16}$	Cyclohexyl Benzene	0.79	1.98
28. $C_{12}H_{10}$	Acenaphthene	0	tr
29. $C_9H_{11}N$	Tetrahydroquinoline	0	tr
30. $C_{12}H_{10}$	Diphenyl	5.96	2.67
31. $C_{12}H_{12}$	Ethyl Naphthalene Isomer	0	tr
32. $C_{13}H_{12}$	Methyl Diphenyl Isomer	0	tr
33. $C_{14}H_{24}$	Perhydrophenanthrene Isomer	tr	tr
34. $C_{12}H_8O$	Dibenzofuran	5.53	1.37
35. $C_{14}H_{14}$	Tetrahydrophenanthrene Isomer	tr	tr
36. $C_{14}H_{18}$	Octahydrophenanthrene Isomer	0.61	0.03
37. $C_{14}H_{12}$	Dihydrophenanthrene Isomer	0.89	0.18
38. $C_{14}H_{16}$	Hexahydrophenanthrene Isomer	0	tr
39. $C_{14}H_{18}$	Octahydrophenanthrene Isomer	1.97	0.02
40. $C_{14}H_{14}$	Tetrahydrophenanthrene Isomer	1.84	0.21
41. $C_{15}H_{16}$	Trimethyl Diphenyl Isomer	0	tr
42. $C_{12}H_8S$	Dibenzothiophene	0	0
43. $C_{14}H_{10}$	Phenanthrene	2.94	1.21
44. $C_{14}H_{24}$	Perhydrophenanthrene Isomer	0.73	tr
45. $C_{18}H_{34}$	Dicyclohexyl Hexane Isomer	tr	tr
46. $C_{18}H_{28}$	Unknown	tr	tr

tr: trace

* %w corrected to 100% mass balance using heptane as internal standard

TABLE 3.4

EQUILIBRIUM AND OBSERVED HYDROGENATION RATIOS

REACTION	TEMPERATURE 673 K		753 K	
	eq	obs	eq	obs
C_9H_{18}/C_9H_{12}	53.45	9.80	2.96	0.76
$C_{12}H_{16}/C_{12}H_{10}$	18.0	0.13	0.26	0.74
$C_{12}H_{22}/C_{12}H_{10}$	72.5	0.03	0.01	0.08
$C_{14}H_{12}/C_{14}H_{10}$	0.39	0.30	0.15	0.149
$C_{14}H_{14}/C_{14}H_{10}$	1.51	0.63	0.14	0.14
$C_{14}H_{18}/C_{14}H_{10}$	2.14	0.88	0.02	0.018
$C_{14}H_{24}/C_{14}H_{10}$	8.8	0.25	0.001	0.001

3.3 HYDRODESULPHURIZATION (HDS)

It is apparent from the complete conversion of dibenzothiophene and dibutylsulphide that HDS is the most facile of all the reactions considered. Most hydrodesulphurization studies have been carried out at atmospheric pressure (Weisser and Landa 1973, Bartsch and Tanielian 1974, Massoth 1977, Lee and Butt 1977). Under these conditions dibenzothiophene yields diphenyl as a product, although some ring saturation has been reported at higher pressures (Landa and Monkova 1966). Rollman (1977) has reported cyclohexyl benzene formation from dibenzothiophene over Co-Mo catalysts under similar conditions and that diphenyl added to the feed was not hydrogenated to cyclohexyl benzene.

In principle, it is not possible to distinguish in the present work between diphenyl, cyclohexyl benzene and dicyclohexyl produced from either dibenzothiophene or dibenzofuran. However, at 673 K

a molar balance on the diphenyl produced showed that its production can be ascribed almost entirely to the converted dibenzothiophene. This suggests that there is no substantial further hydrogenation of the diphenyl produced and this was further substantiated in experiments in which no dibenzothiophene was present in the feed and only small amounts of diphenyl (from hydrocracking of phenanthrene) was observed. This might be expected since Hall and Crawley (1939) found that over MoS_2 hydrogenation of diphenyl to cyclohexyl benzene occurred only at pressures in excess of 20 MPa. At 753 K the amount of diphenyl produced is higher than that derived from dibenzothiophene alone, indicating that the difference may come either from the dehydrogenation of cyclohexyl benzene or from the hydrocracking of phenanthrene.

Thus, the general reaction path for the dibenzothiophene HDS appears to be:

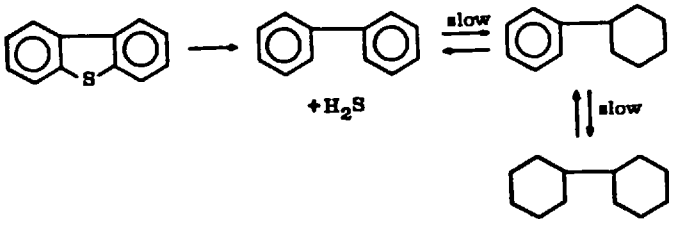

where, under the present conditions, there is no significant reaction beyond diphenyl. The hydrogenolysis of sulphide compounds is much faster than that of thiophenes and the reaction path for dibutyl sulphide could be represented as:

$$C_4H_9\text{-}S\text{-}C_4H_9 \xrightarrow[H_2]{\text{fast}} 2C_4H_{10} + H_2S$$

If these observations are general for the commercial HDS of coal-derived materials, then it is apparent that, since sulphur can be removed without saturation of the ring structure, such reactions consume relatively little hydrogen and there is no significant loss

of aromaticity of the product as a result of hydrodesulphurization alone. The fact that the formation of cyclohexyl benzene from dibenzothiophene occurs on Co-Mo catalysts indicates an advantage of the Ni-Mo system in terms of reduced hydrogen consumption in commercial hydrodesulphurization.

3.4 HYDRODENITROGENATION (HDN)

In the HDN of quinoline (Q), only traces of Q and tetrahydroquinoline (THQ) (at 753 K) were detected among the products of the reactor and, although quinoline and o-propyl aniline (OPA) were eluted almost simultaneously from the gas chromatograph, mass spectrometry failed to detect any quinoline in the reaction products at 673 K. Thus it appears that the production of o-propylaniline is much faster than the subsequent breaking of the C-N bond and that the latter is rate-determining in nitrogen removal. This is in agreement with the proposal made by Rollman (1977) for the reaction path of indole at higher temperatures but seems, at first sight, to be contrary to the studies of Satterfield et al (1978). Using a similar catalyst, the latter reported that quinoline was hydrogenated to a near-equilibrium concentration of phenyl-tetrahydroquinoline (PyTHQ) and to benzyl-tetrahydroquinoline (BzTHQ). They were, however, unable to distinguish BzTHQ from OPA in their experiments.

Although reaction mechanism is clearly complex, it may be represented by (Satterfield et al 1978):

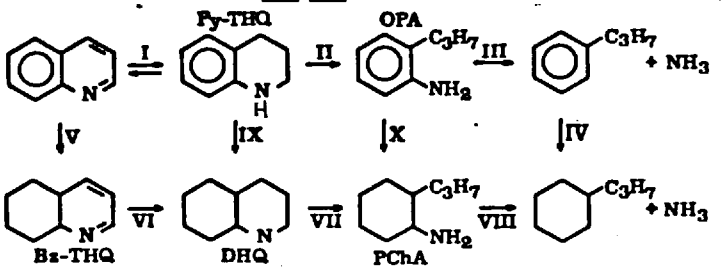

It seems that there may be two pathways. One involves the successive formations from quinoline of PyTHQ, OPA and then the breaking of the C-N bond with the formation of PBz and ammonia followed by the hydrogenation of PBz to PCh. These are shown as steps I, II, III and IV, and were the only products identified under the present conditions. A second pathway may involve the successive formation from quinoline of BzTHQ, decahydroquinoline (DHQ), propylcyclohexalamine (PChA) and then propylcyclohexane (PCh) and ammonia, shown as steps V , VI, VII and VIII. A complicating factor is that DHQ may be formed either from BzTHQ or PyTHQ (Step IX) and that PChA may be formed either from DHQ or from OPA (Step X). The fact that small amounts of Q and PyTHQ were observed only at the higher temperature suggests the rate of conversion of PyTHQ to OPA is relatively slower than Q to PyTHQ at 753 K compared with 673 K and that there is an equilibrium between Q and THQ under the reactor conditions in agreement with the results of Satterfield et al (1978). The fact that the ratio PCh/PBz decreases as the temperature increases indicates that this reaction is important in agreement with Shih et al (1977), with the results of Landa et al (1969) obtained over MoS_2 and with those of Aboul-Gheit and Abdou (1973) over Co-Mo catalysts.

It is apparent that, in contrast to sulphur removal, the nitrogen containing ring must be hydrogenated prior to the removal of nitrogen. The extent of further saturation depends upon process conditions and the catalyst.

3.5 HYDROGEOXYGENATION (HDO)

It has already been shown that diphenyl is unlikely to be a product of dibenzofuran HDO, and it might be expected that the sequence for oxygen removal would be analogous to that for nitrogen, i.e. via the formation of 2-cyclohexylphenol (CPHO):

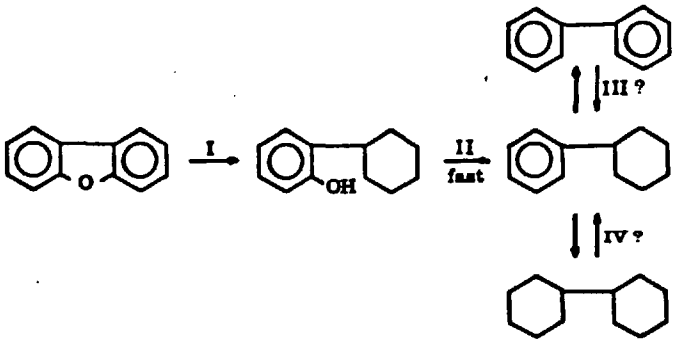

However, no 2-cyclohexyl phenol was detected in either temperature range and the rate-determining step may be the production of a possible CPHO intermediate (step I). Nevertheless, the present data does not allow discrimination between the several reaction paths proposed by Weisser and Landa (1973) for reaction over MoS_2.

At 673 K, a molar balance shows that the amount of cyclohexyl benzene produced is slightly higher than that of the converted DBF, suggesting that the further dehydrogenation of CBz to diphenyl (step III) or hydrogenation to dicyclohexyl (step IV, present in small amounts) are not important at this temperature, and that very small amounts of DPh, CBz and DCh arise from phenanthrene hydrocracking reactions. At 753 K, however, a molar balance on the DPh, CBz and DCh produced shows that it is much less than that derived from the conversion of DBF and dibenzothiophene, suggesting that hydrocracking of these molecules is occurring in significant amounts. The fact that the DCh/DPh and CBz/DPh ratios in the product are higher than the equilibrium values (Table 3.4) indicates that hydrogenation-dehydrogenation reactions are not occurring at this temperature.

Dibenzofuran HDO was the most difficult of the dehetero-atomization reactions studied. The main product of the reaction under the present conditions was cyclohexyl benzene. The need for ring saturation prior to oxygen removal is seen again, and this reaction consumes much hydrogen. In view of the high oxygen content of coals this is an important area of study - the more so because of the paucity of existing data (Hall and Cawley 1939, Weisser and Landa 1973).

3.6 HYDROGENATION AND HYDROCRACKING

Hydrogenation and hydrocracking of phenanthrene on sulphide catalysts yields a complicated mixture of hydroderivatives of the initial substance saturated to differing degrees of bicyclic and monocyclic aromatics, and of naphthalenes. The distribution of these species depends largely on the conditions employed. Sullivan et al (1964) reported that the prevailing products from hydrocracking of phenanthrene on a $NiS/\gamma-Al_2O_3$ catalyst at 566 K were tetralin and methylcyclohexane. However, Huang et al (1977), using a $Co-Mo/\gamma-Al_2O_3$ catalyst reported that the main products of the reaction were perhydro-phenanthrene isomers at 583 K and that hydrocracking became significant at temperatures in excess of 700 K.

It is evident from studies carried out using sulphide catalysts that higher temperatures (over 750 K) would be required to obtain substantial yields of cracked products. Catalyst deactivation as a result of carbon formation on the catalyst surface would probably be a problem under these conditions. The mechanism of the hydro-genation and hydrocracking of phenanthrene is complex, and, summarizing the literature, it appears that the observed reaction paths could be represented by (Wu and Haynes 1975):

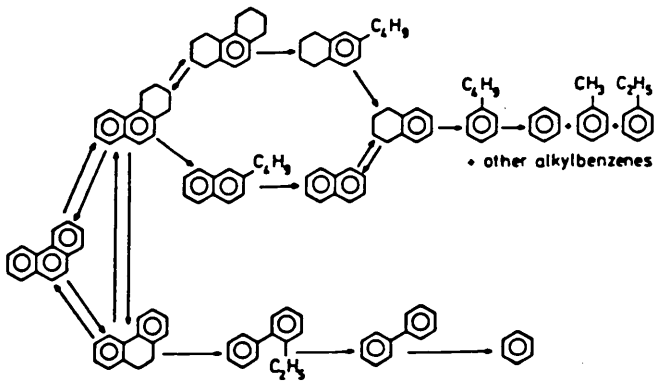

The phenanthrene hydrogenation conversions reported in Table 3.2 were calculated from the subtraction of the yields of phenanthrene hydroderivatives from the total conversion of phenanthrene, the difference being the total conversion to hydrocracked products (less than C_{14}). Under the present conditions of operation, hydrogenation may be expected to dominate at 673 K rather than hydrocracking, and the relative extent of hydrocracking to be much greater at 753 K. In agreement with this, the main products were a mixture of di-, tetra-, octa- and perhydrophenanthrenes in the first case, and dicyclic derivatives account for most of the hydrocracked products (although some alkyl cyclohexanes were also present in small amounts). In the second case (753 K), the main products were a complicated mixture of bi-, mono-cyclic aromatics, of naphthalenes, and also some phenanthrene hydroderivatives. Thus, it would appear that most of the pathways are operating at the higher temperature.

A comparison of the hydrogenation ratios with the equilibrium values (Table 3.4) indicates that at 753 K the phenanthrene hydroderivatives/phenanthrene ratios are at equilibrium, and that at 673 K only the dihydrophenanthrene/phenanthrene ratio is close to the equilibrium value. This is consistent with the fact that hydrogenation of the first aromatic ring proceeeds quite rapidly (Smith 1957).

Benzene is one of the most desired compounds from the coal hydrogenation products and the most direct pathway for the production is through the formation of di-hydrophenanthrene. The predominance of dicyclic products and the trace quantitites of diphenyl (which could be ascribed to hydrocracking of phenanthrene) suggest that, at 673 K, successive saturation and cracking of the central ring of phenanthrene was not significant. On the other hand, at 753 K, the presence of dicyclic products and benzene in significant amounts indicates that this pathway is more important. However, while no significant deactivation was apparent over the 8 hour run period, the pressure drop over the reactor, as a result of interstitial build-up of coke, increased more rapidly at 753 K than at 673 K. Therefore 753 K is unlikely to be a commercially operational temperature unless higher pressures are employed.

CHAPTER FOUR: THE INFLUENCE OF THE SUPPORT ON THE ACTIVITY OF THE CATALYST AND ON THE PERFORMANCE OF THE REACTOR

4.1 INTRODUCTION

The performance of a coal-hydrogenation catalyst depends largely on the fundamental physical properties such as surface area, pore size distribution and pore volume, as mass transfer resistances are important in the hydroprocessing of coal-derived liquors. In addition, in the absence of dopants, the surface acidity of the catalyst is largely determined by the acidity of the support. In this chapter the results of a study of the influence of the support characteristics (pore size distribution and surface acidity) in the overall performance of the catalyst is presented, including the results of the studies conducted to select the operation conditions for catalyst tests in the laboratory scale high pressure trickle-bed reactor employed in the present research.

4.2 THE PERFORMANCE OF THE TRICKLE-BED REACTOR

A process variable study was conducted to select the appropriate testing conditions for catalysts. The effect of the weight hour space velocity (WHSV) (to assess the external mass transfer resistances) and the particle size of the catalyst (to evaluate the internal mass transfer resistances) was studied on the performance of the reactor. The commercial catalyst AKZO-153S was used throughout the experiments, and the 1.27 cm ($\frac{1}{2}$ in.) O.D. reactor was employed. The catalyst was presulphided *in situ* as described in 2.2.2, Chapter 2. The model feedstock was used and the studies were carried out at 623 K and 6.89 MPa. Under these conditions

the main product of quinoline HDN was propylcyclohexane, cyclohexylbenzene from dibenzofuran HDO, and mainly hydroderivatives from phenanthrene hydroprocessing.

4.2.1 Effect of the Liquid Flow Rate

The effect of the liquid flow rate on the performance of the reactor was studied in order to evaluate the external mass transfer resistances. Eight grams of the 0.30 - 0.60 mm fraction of the ground commercial AKZO-153S catalyst was employed, and the hydroprocessing of the model feedstock (catalyst testing) was carried out at 623 K and a hydrogen flow rate of 465.9 $cm^3\ min^{-1}$ (STP). The results are shown in Figure 4.1. The broken lines represent no external mass transfer resistance for a pseudo-first order reaction mechanism for the reactions taking place with a plug flow pattern in the reactor.

From Figure 4.1 (a - c), it is evident that the external mass transfer resistance is important for values of WHSV below 2 (as shown by the deviation from the straight broken lines), but less important for values above 2. For dibenzofuran HDO, Figure 4.1(a), the straight line dependence indicates that the external mass transfer resistance is insignificant, as might be expected, since HDO is the slowest reaction. Pressure oscillations were observed at the reaction outlet at WHSV values higher than 4.0.

The flow patterns in trickle-bed reactors have been analysed by Satterfield (1975). At sufficiently low liquid and gas flow rates (WHSV in the range of 0.5 - 4.0) the liquid trickles over the packing in essentially a laminar film or in rivulets and the gas flow continuously through the voids in the bed; this is described as homogeneous flow. As gas and/or liquid flow rates are increased

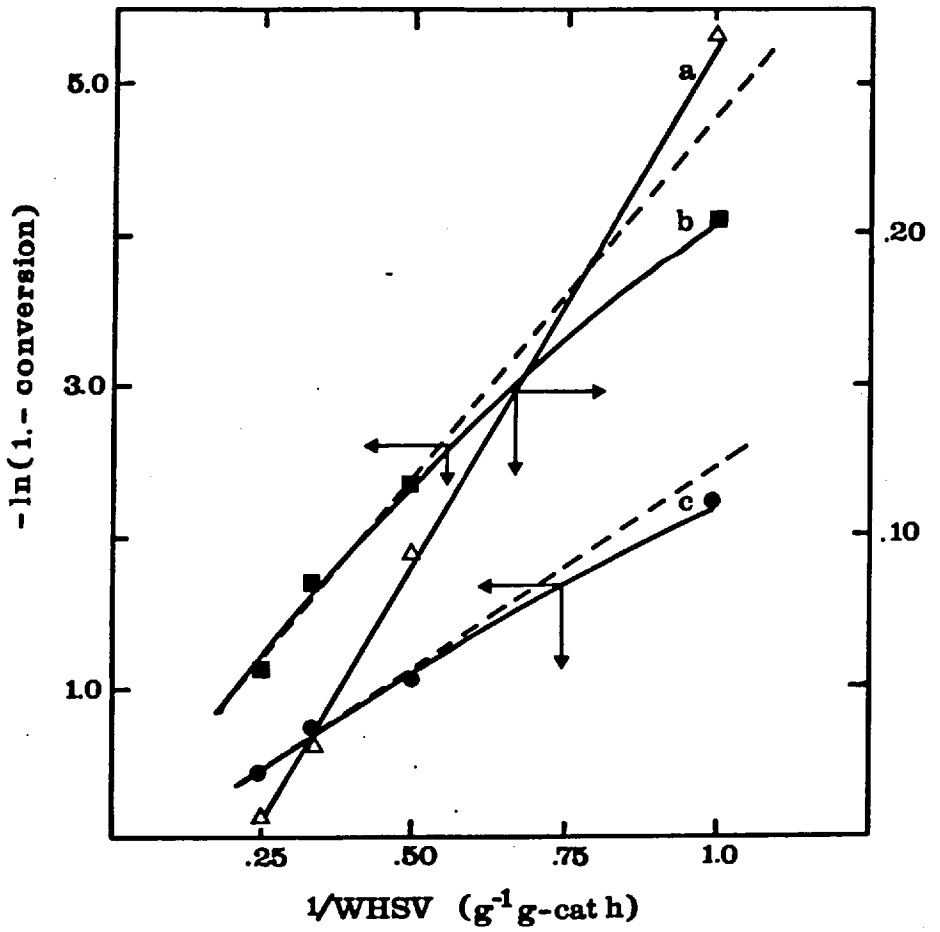

FIGURE 4.1: Effect of the liquid flow rate. Curves
(a) Dibenzofuran
(b) Phenanthrene hydrogenation
(c) Quinoline HDN.

one encounters a behaviour described as pulsing flow. At high liquid rates and sufficiently low gas rates, the liquid phase becomes continuous and the gas passes in the form of bubbles. Of particular importance in narrow diameter reactors (such as those employed in the present work) is the fact that liquid migrates to the wall of the reactor and the fraction of liquid flowing down the wall increases. This fraction may be as high as 30 - 60% even at ratios of reactor diameter to particle diameter of 10. The effect of the WHSV on the flow pattern of the ½ in. O.D. reactor was studied qualitatively, employing a model of the reactor made of glass with identical dimensions to the actual reactor. The same feedstock was used but γ-alumina (0.3 - 0.6 mm) was chosen instead of the catalyst and nitrogen rather than hydrogen. It was established that under the conditions of the test (WHSV: 2 - 4 and a nitrogen flow rate equivalent to a hydrogen flow rate of 465.9 cm^3 min^{-1} (STP) through the system) the flow pattern was that of homogeneous flow. By the addition of a colourant to the feed, it was found that the catalyst particles were completely surrounded by liquid and that the wall flow was minimised by employing a particle size of about 0.30 - 0.60 mm, i.e. a reactor diameter/particle diameter ratio of 20 - 40.

Therefore, the results presented in Figure 4.1 and the observations made in the glass model reactor indicate that, under the conditions normally employed, there is no significant diffusional resistance through the liquid film, in agreement with the general observation by Satterfield (1970) for commercial HDS. However, this resistance is likely to be more important in hydroprocessing of coal-derived liquids due to the higher heteroatom content of the feedstock (Stemberg et al 1976) and the higher temperatures needed

to obtain a substantial yield of hydrocracked products, since this in turn requires higher rates of hydrogen transfer through the liquid film than is required in HDS of petroleum feedstocks. Also, the fact that the rate of instertitial build-up of coke is large at temperatures above 750 K, as described in the previous Chapter, indicates that WHSV in excess of 4.0 may be desirable to remove this coke from the catalyst external surface more efficiently.

4.2.2 Effect of the Particle Size

The effect of the particle size was studied in order to evaluate the significance of the internal mass transfer resistance (pore diffusion). Three different fractions of the ground commercial AKZO-153S catalyst were used, at the same conditions as employed in the previous section and at a weight hour space velocity of 4.0. The results are shown in Figure 4.2 (a - c), and it can be seen that there is no significant difference between the conversions of dibenzofuran HDO (6.8 - 7.3%) Figure 4.2(c), for the particle size considered (0.70 - 0.60 mm) and only a slight variation for quinoline HDN, Figure 4.2(b) and for the total phenanthrene disappearance, Figure 4.2(a). No significant effect on the product distribution was observed under these conditions.

The pore diffusional limitation can be assessed in terms of an effectiveness factor (η) which is a function of the Thiele modulus (ϕ) and, for a pellet of spherical shape, is defined by (Satterfield 1970):

$$\eta = \frac{3}{\phi} \left(\frac{1}{\tanh\phi} - \frac{1}{\phi} \right) \qquad (4\text{-}1)$$

For a first order reaction mechanism, the Thiele modulus is given by:

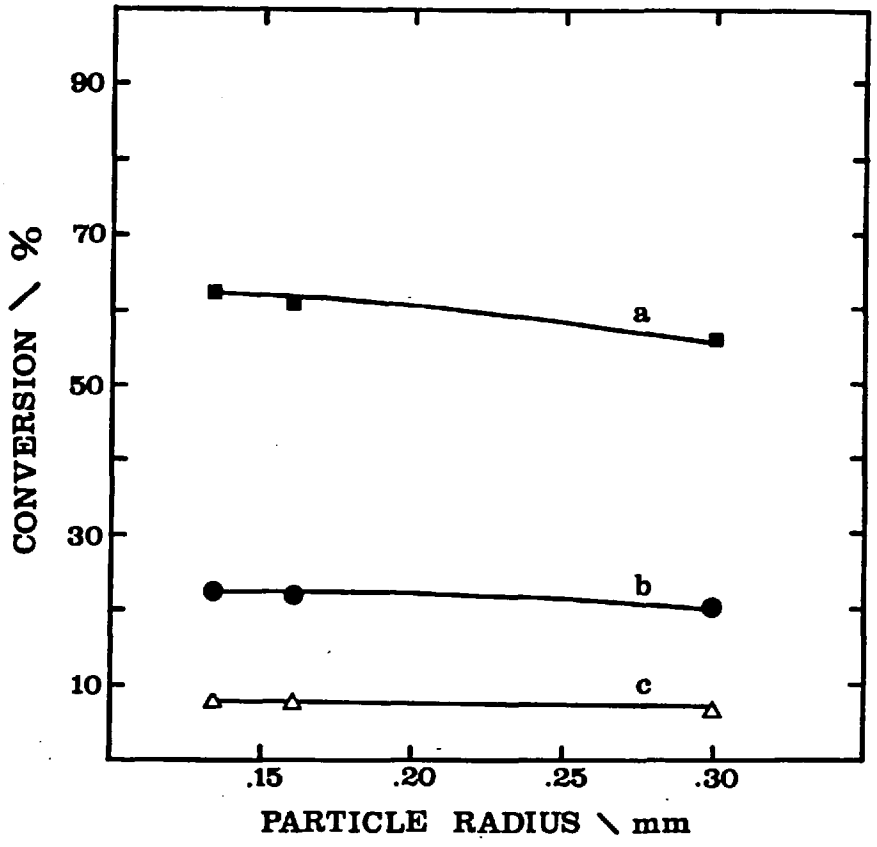

FIGURE 4.2: Effect of the particle size on the performance of the catalyst.
Curves:
(a) Phenanthrene hydrogenation
(b) Quinoline HDN
(c) Dibenzofuran HDO.

$$\phi = r \left(\frac{k_i}{D_{eff}} \right)^{\frac{1}{2}} \tag{4-2}$$

where r = pellet radius

k_i = intrinsic reaction kinetic constant

D_{eff} = effective diffusivity

When the values of the apparent kinetic constants are known for different particle sizes (as in this case), the effectiveness factor can be obtained (assuming that the intrinsic kinetic constant and the effective diffusivity is the same). Using the ratios of the observed apparent kinetic constants (k_r) and particle radii, in the knowledge that:

$$\frac{\eta_{r_1}}{\eta_{r_2}} = \frac{k_{r_1}}{k_{r_2}} = \frac{\phi_{r_2}}{\phi_{r_1}} \frac{\left(\coth\phi_{r_1} - \frac{1}{\phi_{r_1}} \right)}{\left(\coth\phi_{r_2} - \frac{1}{\phi_{r_2}} \right)} \tag{4-3}$$

$$\frac{\phi_{r_1}}{\phi_{r_2}} = \frac{r_1}{r_2} \tag{4-4}$$

the values of the Thiele modulus and the effectiveness factors may be calculated from (4-3) and (4-4). The results are presented in Table 4.1, and it can be seen that effectiveness factors vary from 0.8 to 1.0, indicating that the pore diffusion is not significant under the conditions for catalyst testing employed in the present work. The standard conditions of the high pressure trickle-bed reactor employed throughout the present research are shown in Table 4.2.

TABLE 4.1

EFFECTIVENESS FACTORS

	REACTION	CATALYST PARTICLE SIZE/mm 0.135	0.30
CONVERSIONS (%)	Dibenzofuran	7.2	6.4
	Quinoline HDN*	23.1	20.4
	Phenanthrene	62.5	57.4
APPARENT KINETIC CONSTANTS (k_r) g-mol g-cat^{-1} h^{-1}	Dibenzofuran	0.30	0.27
	Quinoline HDN*	1.05	0.91
	Phenanthrene	3.92	3.41
$\frac{\phi_{.30}}{\phi_{.135}} = \frac{.30}{.135}$		-	2.22
$\frac{\eta_{.135}}{\eta_{.30}} = \frac{k_{.135}}{k_{.30}}$	Dibenzofuran	-	1.11
	Quinoline HDN*	-	1.15
	Phenanthrene	-	1.17
EFFECTIVENESS FACTOR	Dibenzofuran	0.97	0.87
	Quinoline HDN*	0.96	0.83
	Phenanthrene	0.95	0.81

*based on N removal from organic ring

TABLE 4.2

STANDARD CONDITIONS OF

THE TRICKLE-BED REACTOR FOR CATALYST TESTS

Catalyst load *	8.0 g
Hydrogen flow rate	465.9 cm^3 min^{-1} (STP)
Liquid hourly space velocity (WHSV)	2-4 g h^{-1} g-cat^{-1}
Temperature	623 K
Pressure	6.89 MPa
Catalyst activation:	
10%v H_2S in H_2 mixture flow rate	458 cm^3 min (STP)
Temperature	523 K
Time on stream	1 hr

*0.15 - 0.20 mm particle radius

In general, there is very little information regarding mass transfer limitations in trickle-bed reactors. In commercial HDS values for the effectiveness factors have been reported in the range from 0.30 to 0.80 (Satterfield 1970, Smith 1970, Carberry 1976). Again, in the hydroprocessing of coal-derived liquors, due to the more severe conditions of operation and the presence of heavy molecules in the feedstock, mass transfer limitations in the pore system are a major inhibitor to higher catalyst effectiveness and values as low as 0.1 have been reported (Ochoa et al 1978). This indicates that catalyst efficient for petroleum upgrading may not be suitable for the hydrotreating of coal-derived liquors and there is a need to improve the catalyst through the optimization of the pore size distribution of the support, as discussed in the next section.

4.3 EFFECT OF PORE SIZE DISTRIBUTION

As indicated in the previous section, the pore size distribution of the catalyst is of great importance in the performance of catalysts employed in upgrading coal-derived liquors. Since high surface area catalysts are preferred for these processes (Weisser and Landa 1973, Consumano et al 1978), the high surface area Norton-6175 γ-alumina support was chosen (from those available for the present research) for this study. Three catalysts were prepared by successive impregnation under excess volume (2.5.3, Chapter 2) impregnating the Ni cations under basic and Mo anions under acid conditions. In two catalysts, the pore size distribution of the support prior to their impregnation was modified by a thermal treatment with a 25%w ammonium carbonate solution (Pearson et al 1977) in an autoclave at 423 K (catalyst Ni(B)-Mo(A)/M) and at 448 K (Ni(B)-Mo(A)/L), as described in 2.5.5, Chapter 2. The physical characteristics of the catalysts are given in Table 4.3, and pore size distributions are shown in Figure 4.3.

The conditions of the test were those described in Table 4.2, (WHSV = 4), but the temperature was increased to 673 K to increase the internal mass transfer limitations in the hydroprocessing of the model feedstock (catalyst testing composition). The overall conversions are given in Table 4.4. The effect of the pore diffusion resistance is clearly illustrated in the hydroprocessing of phenanthrene, though it is not significant for the hydrogenolysis of quinoline and dibenzofuran. This is in agreement with the results concerning the particle size of the catalysts presented in Figure 4.2.

TABLE 4.3

CATALYST CHARACTERISTICS

	CATALYST		
	Ni(B)-Mo(A)	Ni(B)-Mo(A)/M	Ni(B)-Mo(A)/L
MoO_3 (wt%)	15	15	15
NiO (wt%)	4	4	4
Surface area* m^2 $g\text{-}cat^{-1}$	260	221	177
Pore volume* cm^3 $g\text{-}cat^{-1}$	.56	.38	.29
Mean pore radius* nm	5.45	5.95	9.90

*by nitrogen adsorption

TABLE 4.4

FEED CONVERSIONS (%)

REACTION	CATALYST		
	Ni(B)-Mo(A)	Ni(B)-Mo(A)/M	Ni(B)-Mo(A)/L
Dibutylsulphide	100	100	100
Quinoline (HDN)*	84.6	78.9	72.5
Dibenzofuran	41.7	37.5	32.3
Phenanthrene hydrogenation	96.2	96.4	97.1
Phenanthrene hydrocracking	20.3	22.7	25.7

*based on nitrogen removal from organic ring

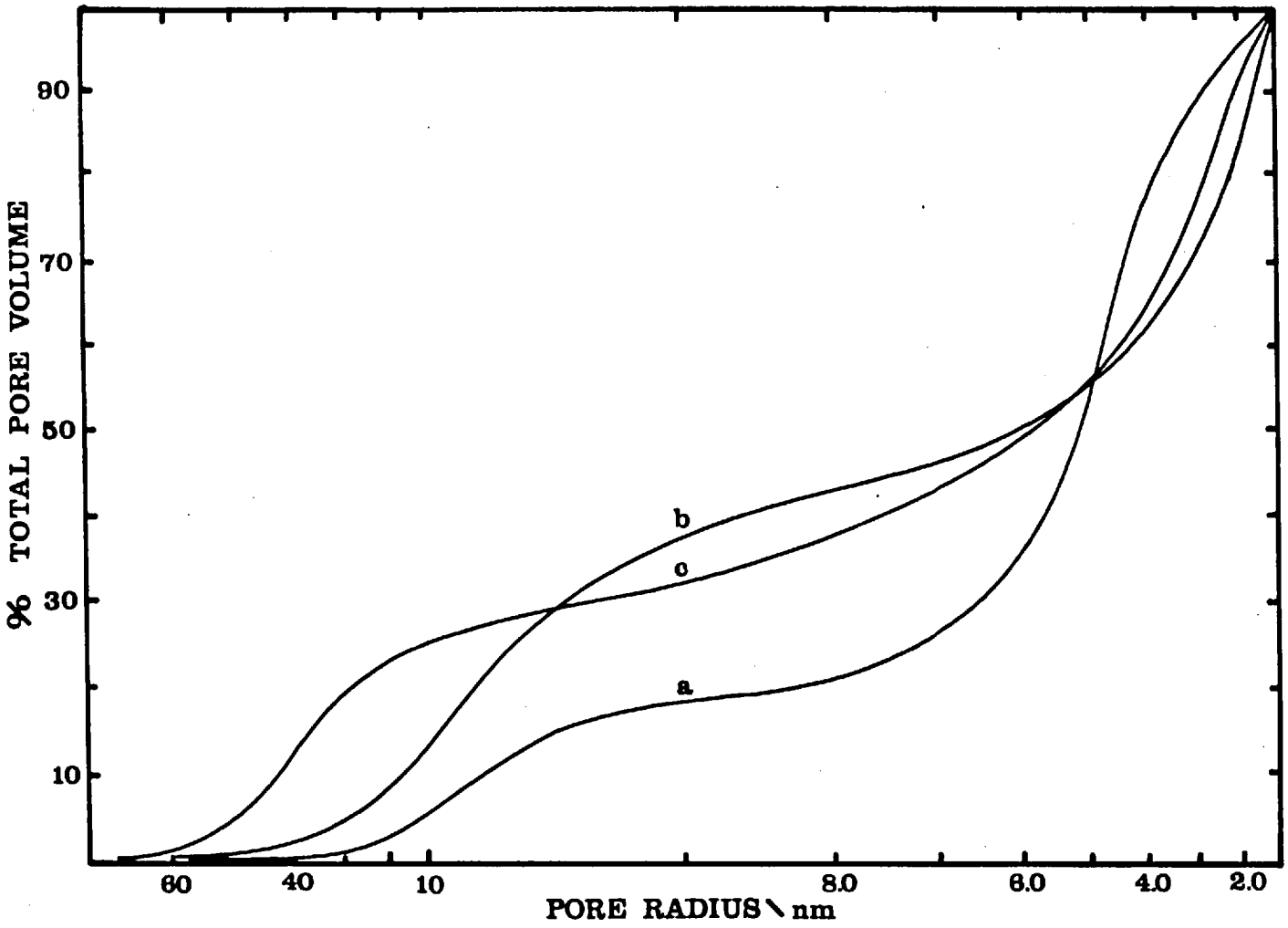

FIGURE 4.3: Pore size distribution.
Curves:
(a) Ni(B)-Mo(A); (b) Ni(B)-Mo(A)/M; (c) Ni(B)-Mo(A)/L

Catalyst Ni(B)-Mo(A), having a larger surface area than catalysts Ni(B)-Mo(A)/M and Ni(B)-Mo(A)/L, should have a higher phenanthrene hydroprocessing activity, but the results show otherwise. Since these catalysts should have identical chemical composition and surface structure since they were prepared in the same way, this difference must be related to the pore diffusional limitations. If internal mass transfer resistances are present, changes in pore size distribution leading to a reduction in the mean pore diameter can result in a decrease in the observed rate of reaction. Catalyst Ni(B)-Mo(A) has a mean pore diameter of 10.9 nm compared with 19.8 for catalyst Ni(B)-Mo(A)/L, even though the pore volume of Ni(B)-Mo(A) (0.56 cm^3 $g\text{-}cat^{-1}$) is greater than Ni(B)-Mo(A)/L (0.29 cm^3 $g\text{-}cat^{-1}$). As a result, the relative magnitude of the pore diffusion limitations is higher for catalyst Ni(B)-Mo(A). This effect is better shown in Table 4.5, in which the apparent kinetic constants (both per gram and per m^2 of catalyst surface) for the reactions were calculated from the overall conversion data, assuming pseudo-first order reaction mechanisms. For the hydrogenation and hydrocracking of phenanthrene, the overall mechanism was simplified to be (Huang et al 1977):

Phenanthrene → hydrogenation → hydrocracking

TABLE 4.5

APPARENT KINETICS CONSTANTS

REACTION	CATALYST					
	Ni(B)-Mo(A)		Ni(B)-Mo(A)/M		Ni(B)-Mo(A)/L	
	k_a	$k_{r_p} \times 10^2$	k_a	$k_{r_p} \times 10^2$	k_a	$k_{r_p} \times 10^2$
Quinoline (HDN)*	7.48	2.88	6.23	2.82	5.17	2.92
Dibenzofuran	2.16	0.90	1.88	0.85	1.56	0.88
Phenanthrene:						
hydrogenation	13.08	5.03	13.30	6.02	14.03	7.93
hydrocracking	0.07	0.03	0.08	0.03	0.08	0.03

$|k_a| = g\ g\text{-}cat^{-1}\ h^{-1}$

$\left|k_{r_p}\right| = g\ m^{-2}\ h^{-1}$

The Thiele modulus can be defined in terms of the intrinsic reaction kinetics constant per unit of surface (k_s) as (Satterfield 1970):

$$\phi = \frac{r}{3}\left(\frac{k_s}{\bar{r}_p D_{eff}}\right)^{\frac{1}{2}} \qquad (4\text{-}5)$$

where $\bar{r}_p$ is the mean pore radius of the support. Since all catalysts used had the same particle size, for the Thiele modulus of catalyst Ni(B)-Mo(A) to be the highest, the product $\bar{r}_p D_{eff}$ in Equation (4-5) should be the smallest (assuming the same intrinsic reaction rate). Under severe pore diffusional limitations, the effectiveness factor may be approximated to the inverse of the Thiele modulus and, if the ratio of the Thiele modulus of catalyst Ni(B)-Mo(A) to Ni(B)-Mo(A)/L is calculated only as the square root of the mean pore radius ratio

of these catalysts (1.348), the ratio of the effectiveness factor (Equation 4-4) comes out to be 1.310. This is lower than the observed ratio 1.577 for the hydroprocessing of phenanthrene and indicates that the effective diffusivity coefficient for phenanthrene of catalyst Ni(B)-Mo(A) must be lower than that of Ni(B)-Mo(A)/L.

In the case of a bulk diffusion mechanism, the effective diffusion coefficient is given by (Satterfield 1970):

$$D_{eff} = \frac{\theta D}{\tau} \qquad (4\text{-}6)$$

where θ = void fraction of the catalyst pellet

τ = tortuosity factor of the catalyst pellet

D = bulk diffusion coefficient.

A low value of D_{eff} for catalyst Ni(B)-Mo(A) suggests a higher tortuosity factor compared with that of Ni(B)-Mo(A)/L, since the void fraction of Ni(B)-Mo(A) (about 0.4) is higher than that of Ni(B)-Mo(A)/L (about 0.3). For an effectiveness factor ratio of 1.577 for the hydrogenation of phenanthrene the value of the ratio of the Thiele modulus for catalyst Ni(B)-Mo(A) to Ni(B)-Mo(A)/L should be 1.64, and a ratio of 1.19 can be estimated for the tortuosity factors of Ni(B)-Mo(A) to Ni(B)-Mo(A)/L (Equation 4-5). Satterfield (1975) has reported that the value of τ is usually around 4.0, extreme values for the usual catalyst structures being about 2 - 7.

However, when the solute molecular diameter becomes significant with respect to the pore diameter, the concentration of the solute within pores of equilibrium becomes less than that in the bulk of a geometrical exclusion effect (Knudsen diffusivity) and the effective diffusivity becomes less than in the bulk diffusion mechanisms. Several empirical correlations have been attempted to describe this effect, and the effective diffusivity may be assumed to be (Satterfield

1975):

$$D_{eff} = \frac{\theta D}{\tau} 10^{-2.0\lambda} \qquad (4\text{-}7)$$

where λ is the ratio of the critical molecular diameter to the pore diameter. Assuming that the ratio of the Thiele modulus in the present case should be 1.65, then using Equations (4-5) and (4-7) (with no significant difference in the tortuosity factors), the diffusing molecules should be of the order of 1.0 nm. Since the diameter of the phenanthrene molecule is about 0.5 nm, this indicates that Knudsen diffusivity effect is more important in catalyst Ni(B)-Mo(A) than in Ni(B)-Mo(A)/L, as expected from the larger percentage of micropores.

In general, the pore structure of coal hydrogenation catalysts is of great importance to their performance due to the larger molecules present in the feed (Steinberg et al 1976), which reduces their effective diffusion coefficient through the catalyst pores. Of particular importance in coal derived liquids is the presence of asphaltene molecules, which have diameters from 1 to 3 nm and contain most of the metals (e.g. Ni, V, etc.) and some of the heteroatoms (O, N, S) present in the feed (Yen et al 1961). These molecules are the main cause of catalyst deactivation since they are the principal precursors of coke formation (McColgan and Parsons. 1974, Stanulisis et al 1976) which covers the catalyst surface and blocks the pore, and of metal deposition on the active sites (Kovach et al 1978). As a result, catalysts with mean pore diameters higher than 10 nm and with surface areas above 150 $m^2\ gr^{-1}$ are desirable (Sooter and Crynes 1975).

Chiou and Olson (1978), based on theoretical considerations, established that values of λ (in Equation 4-7) below 0.1 would be

necessary to avoid plugging of the catalyst pores.

Catalysts such as employed in coal hydrogenation always have a distribution of pore sizes. There are micro-, meso- and macro-pores present and a selective pattern can exist for the diffusion of the reactants in the pore structure (Ahmed and Crynes 1978). Polynuclear aromatics have a tendency to undergo chemical changes forming lower molecular weight compounds. These species can diffuse into the smaller pores which are unavailable to their parent compounds. Hence, a bimodal pore size distribution is desirable to ensure a sufficient amount of large pores for the large molecules to react (Kang and Gendler 1978), bearing in mind that the active surface in these pores is the one in which the catalyst activity is decaying faster.

4.4 EFFECT OF SURFACE ACIDITY

Another important characteristic of catalysts for hydroprocessing coal-derived liquors is the surface acidity and, in the absence of dopants, it is largely determined by the acidity of the support. Surface acidity is very important for the hydrocracking capability of the catalyst (Anderson 1975). In order to study this effect, four catalysts were prepared on four different alumina supports, employing the pore-filling co-impregnation procedure described in 2.5.2, Chapter 2. In addition, the commercial AKZO-153S catalyst was tested for comparison. The physical characteristics (including the surface acidity measured as mg m^{-2} of chemisorbed pyridine) are given in Table 4.6.

Since the main objective was to measure the effect of the surface acidity on the intrinsic activity and the overall performance of the catalysts in the reactor, the model feedstock (reaction

TABLE 4.6

CATALYST CHARACTERISTICS

	CATALYST				
	AKZO-153S	NiMo-AB	NiMo-AS	NiMo-AA	NiMo-SA
MoO_3 w%	15	12	12	12	12
NiO w%	3	4	4	4	4
Surface area[a] $m^2\ g^{-1}$	230	98	214	60	27
Pore volume[a] $cm^3\ g^{-1}$	0.48	0.25	0.33	0.15	0.05
Mean pore diameter[a] nm	8	7	10	5	5
Surface acidity[b]	0.178	0.244	0.263	0.274	0.396
Support origin	-	BDH-100% $A\ell_2O_3$	Norton SA-6175	BDH-100% $A\ell_2O_3$	Norton SA-3232

[a] by nitrogen adsorption

[b] as mg m^{-2} of chemisorbed pyridine

mechanisms studies) was hydroprocessed at 673 K rather than 623 K to increase the hydrocracking yields. As the mean pore diameter of the catalysts (Table 4.6) decreases in the order: NiMo-AS > AKZO-153S > NiMo-AB > NiMo-AA ∿ NiMo-SA, the effectiveness factors of the catalyst under the testing conditions would decrease in the same order, as discussed in the previous section. No attempt was made to evaluate the effectiveness factor for each catalyst, but the expected values should lie in the range from 0.6 to 1.0. Values of the apparent kinetic constants for the various reactions calculated from the conversion data are shown in Table 4.7. No significant difference was observed in the product spectra among the tested catalysts and, since dibenzothiophene and dibutylsulphide were completely converted in the reactor, no attempt was made to evaluate the HDS activities.

In spite of the fact that the internal mass transfer limitations were neglected in calculating the apparent kinetic constants, Table 4.7, it can be seen that the rate of the various reactions increased as the surface acidity of the catalyst increased. Catalyst NiMo-SA showed higher rates per unit of surface area despite having the lowest effectiveness factor. However, when considered per unit volume, catalyst NiMo-AS gives the best results for the deheteroatomization reactions. Thus, it is clear that the choice of the support depends on the surface acidity, in addition to pore structure. While no significant deactivation was apparent over the 8 hr run periods, the pressure drops over the reactor (as a result of interstitial build-up of coke) increased rapidly with surface acidity. Therefore, the high acidity catalysts, while possessing the highest initial activities, are unlikely to be successful commercial catalysts in trickle-bed operations under the

TABLE 4.7

APPARENT KINETIC CONSTANTS

REACTION	CATALYST									
	AKZO-153S		NiMo-AB		NiMo-AS		NiMo-AA		NiMo-SA	
	k^a	k_s^b	k^a	k_s^b	k^a	k_s^b	k^a	k_s^b	k^a	k_s^b
Quinoline (HDN) [c]	7.04	3.06	4.28	4.37	7.23	3.38	3.85	6.42	2.09	7.74
Dibenzofuran	1.57	0.68	0.74	0.76	o.98	0.93	0.78	1.30	0.47	1.74
Phenanthrene hydrogenation	11.53	5.01	6.74	6.87	14.27	6.67	8.70	14.50	5.57	20.62
Phenanthrene hydrocracking	1.87	0.81	3.23	3.29	4.33	2.02	5.90	9.83	5.28	19.56
Hydrocracking/hydrogenation ratio	0.16		0.47		0.30		0.67		0.94	

(a) k: g-mol g-cat^{-1} h^{-1}

(b) k_s: g-mol 100 m^2 h^{-1}

(c) based on nitrogen removal

conditions employed. They may be effective in operations at lower temperatures, since they showed a significantly higher hydrocracking/ hydrogenation selectivity.

Little has been published on the influence of surface acidity on the performance of coal hydrogenation catalysts (Wu and Haynes 1975). The preparation of alumina supports with different surface acidities usually involves the calcination of the $Al(OH)_3$ precipitate at different temperatures (Tanabe 1970) or by co-precipitation of alumina and silica. In the latter case, the surface acidity of the support is a function of the SiO_2 content of the surface (Anderson 1975). The fact that no significant differences in the product spectra were observed indicates that in the present case, it was the total acidity which varied, and the nature of the acid sites remain unchanged. The modification of the surface acidity of alumina by either calcining at different temperatures or by the addition of silica usually leads to quite different pore structures of the final support (Inogushi et al 1971), which in turn affects the performance of the catalysts as far as internal mass transfer limitations is concerned. SiO_2-Al_2O_3 supports, such as Norton SA-3232, are usually of lower surface areas and mean pore diameters than Al_2O_3 supports, such as Norton SA-6175, as shown in Table 4.6. Controlling the surface acidity of alumina supports by the addition of dopants such as phosphorous or chromia (rather than SiO_2) should enhance the activity and selectivity of coal hydrogenation catalyst without modifying the desired surface area and pore size distribution of the support.

Finally, it is evident from the results presented in Table 4.7, together with the conclusions from the previous section of this Chapter, that the support which gives the highest overall performance

(from those available for the present research) is the Norton SA-6175 γ-alumina, and this was used in preparing the catalysts employed throughout the catalyst preparation studies presented in the next chapter.

CHAPTER FIVE: A STUDY OF THE IMPREGNATION AND THE INFLUENCE OF THE IMPREGNATION PROCEDURE ON THE ACTIVITY OF Ni-Mo/γ-Al_2O_3 CATALYSTS

5.1 INTRODUCTION

In this Chapter a study of the impregnation stage of the preparation of Ni-Mo/γ-Al_2O_3 catalysts (by impregnation from aqueous solutions) is presented. In addition an attempt has been made to relate the hydrogenation activity of the catalysts, measured both at atmospheric pressure (using thiophene) and at high pressure (employing a model coal-derived oil), to the impregnation procedure through characterization of the structure of the catalysts in their oxidic state. ESCA and u.v. reflectance spectroscopy were the principal methods of surface characterization. Since the formation of the oxidic state of the catalyst involves the impregnation and calcination of the active components on the surface of the support, in this study catalysts prepared employing different impregnation procedures were calcined under similar conditions. Therefore, the correlation presented between the surface structures of different impregnation conditions and the activity of the catalyst is in the fully oxidic state (after calcination). A study of the calcination and the effect of the calcination conditions on the activity of the catalyst is presented in the next Chapter.

The variables considered in the impregnation process were the pH of the solution and the order of impregnation. The former affects the surface charge of the support and therefore, the incorporation of Ni and Mo on to the support was studied in two ranges of pH, namely one above and one below the ZPC* of the alumina, from solutions containing Ni, Mo and Ni-Mo ions.

ZPC : zero point of charge

5.2 INFLUENCE OF pH ON THE ALUMINA SURFACE AND ITS EFFECT ON IMPREGNATION

Solid oxides such as γ-Al_2O_3 in aqueous suspensions are generally electrically charged as may be observed in electrophoresis experiments (Parks 1965). The surface charge has long been attributed to one of two apparently indistinguishable mechanisms: (a) amphoteric dissociation of surface M-OH groups, and (b) adsorption of metal hydroxo complexes derived from the hydrolysis products of material dissolved from the solid or additional cations/anions. Both mechanisms can explain qualitatively the pH dependence of the surface charge and the existence of a pH resulting in zero net surface charge, called the zero point of charge (ZPC). For aluminum oxides and hydroxides, ZPC values from 9.5 to 5.0 have been reported (Parks 1965) and this depends on the method of preparation, temperature of calcination and impurities present in the solid. The Norton SA-6175 γ-Al_2O_3 support employed in the present study contained 0.2%w SiO_2 and 0.08%w Fe_2O_3, and since the ZPC values for these two compounds are about 1.8 and 6.0 respectively (Parks 1965), the ZPC of this support should be lower than that of pure γ-aluminas and lie in the range of 6 - 8, as reported by Anderson (1975) and Brunelle (1978).

In the present study an attempt was made to control the pH of the impregnation solution to a desired value by periodic manual adjustment over 40 hours. The two impregnation conditions of interest are at pH above and below that necessary to produce a zero net charge on the alumina surface and thus initial values for the pH of impregnation solutions were set at 8 and 2. However, accurate control is made impossible by the tendency of γ-Al_2O_3 to buffer the pH of its environment to a constant value (Pourbaix 1966, Perrin and Dempsey 1974) and by the release of H^+ or OH^- ions from the alumina

surface due to adsorption of metal ions (Amphett 1974, Anderson 1975). In order to study this effect, 20 gms of the support material were placed in 200 cm^3 of water at pH = 1.7 and the pH of the solution continuously monitored. The result is presented in Figure 5.1.

It can be seen in Figure 5.1(a) that the pH rises rapidly on addition of γ-alumina reaching a value of about 4.5 after one hour. When the pH is restored to the initial value approximately, the pH rises again but stabilises at a lower value ($\sim$ 3). Repetition of this process results in a smaller rise still, and after 6 hours the pH remains sensibly constant. This phenomenon can be explained by the dissolution of the support according to the equilibrium (Pourbaix 1966):

$$2Al^{3+} + 3H_2O \rightleftarrows Al_2O_3 + 6H^+$$

This causes the pH to rise until the equilibrium concentration of Al^{3+} is reached. However, it cannot rise above about pH = 5 because this represents the minimum solubility of Al^{3+} (Pourbaix 1966).

Similar behaviour was observed, Figure 5.1(b), when γ-alumina was added to 200 cm^3 of a 20 gr solution of ammonium molybdate at pH = 1.7, although the rise in the pH was smaller than for the γ-Al_2O_3/water system (Figure 5.1(b). However, curves (a) and (b) may be superimposed if the initial, almost instantaneous, rise in pH for the γ-Al_2O_3/water case is ignored. This is entirely consistent with the observation (Ianibello et al 1978, Ianibello and Mitchell 1978) that when γ-Al_2O_3 is added to ammonium heptamolybdate at pH $\simeq$ 7 there is an initial rapid decrease in pH, followed by a slow increase. This has been attributed to the exchange of ammonium ions with protons present on the alumina (Ianibello and Mitchell 1978). In the present experiments this exchange would act to suppress the fast initial rise in pH when γ-Al_2O_3 is added to water at pH = 1.7, and would result

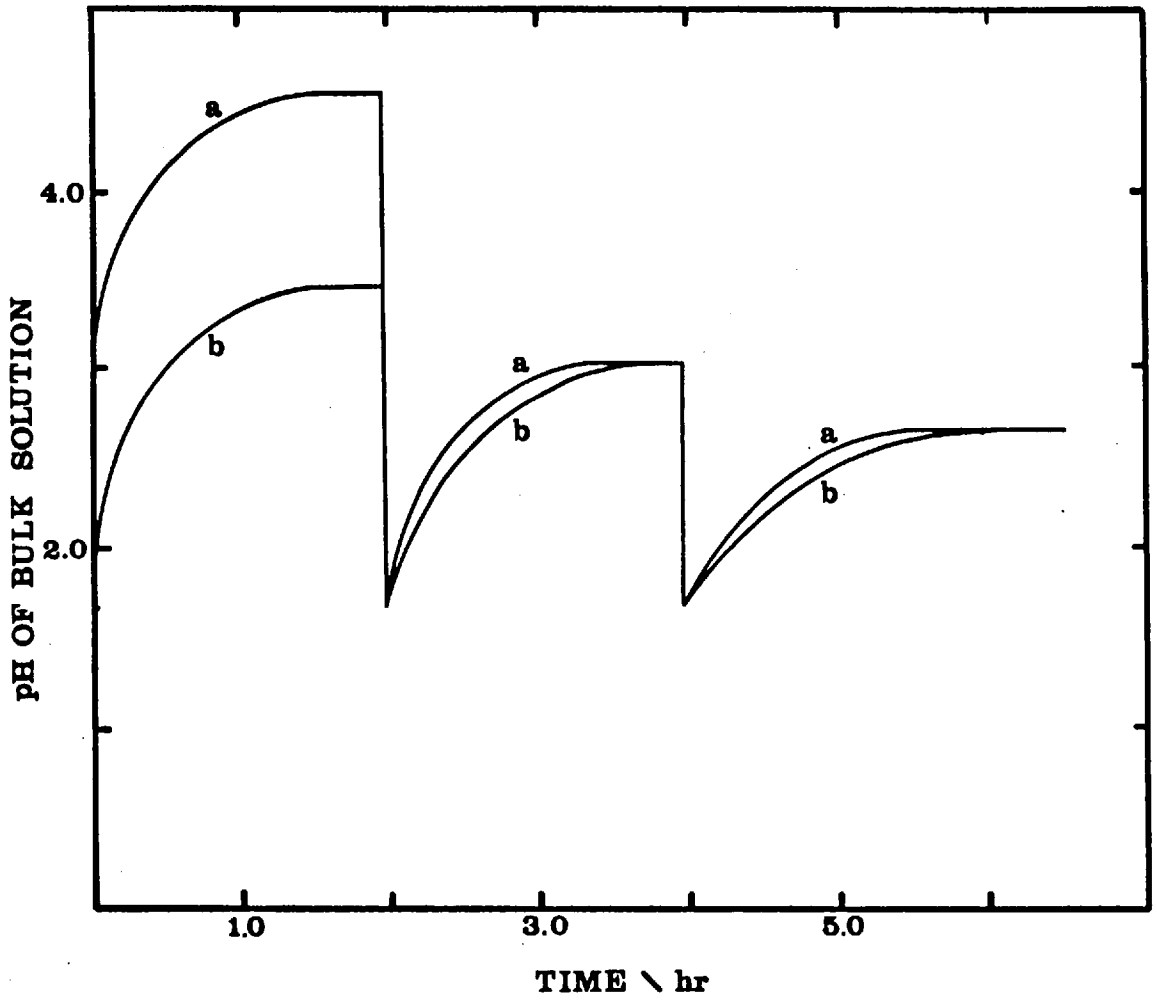

FIGURE 5.1: Effect on bulk pH of adding γ-$A\ell_2O_3$ to:

(a) water at pH = 1.7; (b) a 12 g dm^{-3} Mo solution at pH = 1.7. The pH is re-adjusted at 2 and 4 hours.

in the observed smaller increase in pH.

In basic conditions the pH of the solution was observed to fall slightly when γ-Al_2O_3 was added to ammonium molybdate at pH = 8, reaching pH = 7.5 after 6 hours. However, with periodic adjustment it was possible to keep the pH within a narrow range. Therefore, in the experiments described below the pHs of the impregnating solutions were not constant, and adsorption of Ni and Mo took place in a range of pH rather than at the initial pH of the solutions. Since the ranges of pH stated refer to the bulk solution, it is clear that the variation of pH within the pores of the support must be greater, although this cannot be quantified easily.

5.3 Mo/γ-Al_2O_3

The equilibrium adsorption curves for Mo on the γ-alumina support have been obtained for the two pH ranges considered, namely pH = 2 - 4 and pH = 7.5 - 8. The results are shown in Figure 5.2. Curves (a) and (b) represent the total uptake of Mo (expressed as MoO_3) by the support at pH = 2 - 4 and pH = 7.5 - 8 respectively, where the amount of Mo was determined by XRF analysis of the solid phase and the equilibrium concentration was determined by XRF of the solution. Curve (d) shows the amount of Mo which would be deposited on the support if no adsorption took place. This was calculated from the known pore volume of the support and the measured equilibrium concentration. The "adsorption isotherm", curve (c), was obtained by correcting curve (a) for the amount of Mo contained in the solution which fills the pore volume of the support, i.e. by subtracting (d) from (a) in Figure 5.2. An exactly similar curve may be obtained from the decrease in the concentration of the impregnating solution.

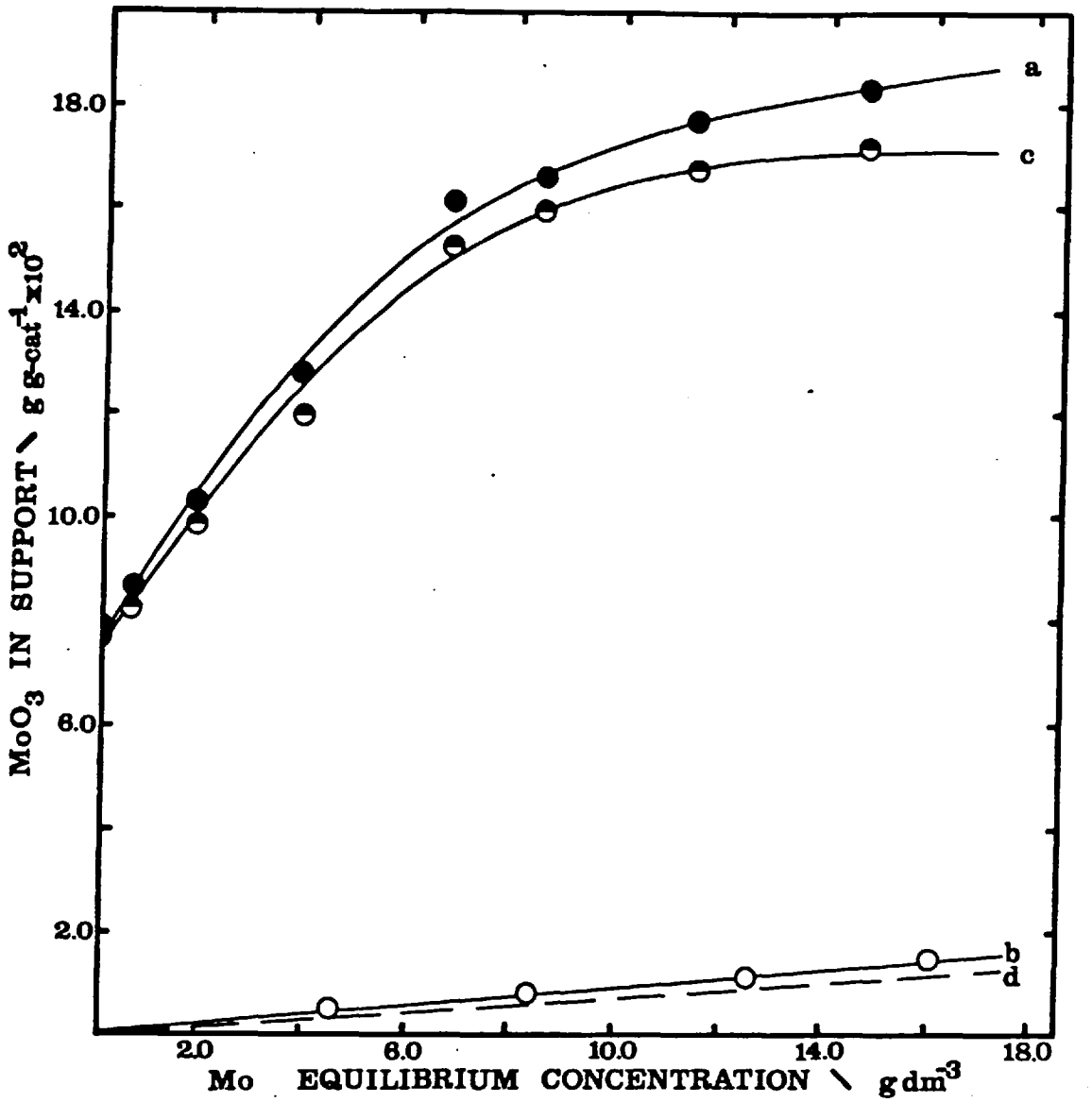

FIGURE 5.2: Impregnation of γ-$A\ell_2O_3$ by Mo at 293 K.

(a) total uptake of Mo at pH = 2 - 4

(b) total uptake of Mo at pH = 7.5 - 8

(c) adsorption isotherm at pH = 2 - 4

(d) total Mo uptake calculated from the pore volume assuming no adsorption.

From Figure 5.2 it can be seen that two different processes of impregnation are taking place. In the pH range 2 - 4, there is an adsorption mechanism which accounts for most of the Mo uptake. The maximum uptake by adsorption, ca 16%w as MoO_3, is in agreement with published results (Ianibello and Trifiro 1975). At pH = 7.5 - 8 no adsorption takes place and the Mo on the support arises simply from the solution contained in the pore volume.

The nature of the Mo ions present in a solution is strongly pH dependent (Cotton and Wilkinson 1972). In a basic environment the predominant species is MoO_4^{2-} and at pH < 6 the molybdate ions condense to form polymolybdate ions in definite steps, according to:

$$\times\ MoO_4^{2-} + nH^+ \rightleftarrows |Mo_xO_y|^{m-} + \frac{n}{2} H_2O$$

At pH < 4.8 the predominant species is $Mo_7O_{24}^{6-}$, although other polyions may also be formed (Pourbaix 1966).

Figure 5.3 shows the u.v. reflectance spectra obtained from the $Mo/\gamma\text{-}Al_2O_3$ surfaces and model Mo compounds. The octahedral Mo compounds MoO_3 (a) and ammonium heptamolybdate (c), are characterised by a strong peak in the range 300 - 360 nm, while the tetrahedral Mo compound, Na_2MoO_4 (b), has a strong peak at 250 - 270 nm. Figure 5.3 (f) and (g) show the spectra of $Mo/\gamma\text{-}Al_2O_3$ prepared at pH = 2 - 4 with Mo loadings of 8%w and 15%w respectively. Clearly the spectra for different Mo loadings are virtually identical. Comparison of spectra (f) and (g) with those of the pure compounds (a - c) indicates that the $Mo/\gamma\text{-}Al_2O_3$ surfaces produced in acid conditions consist largely of octahedral Mo(VI) species. The spectra are ill-defined compared to the pure compounds suggesting a mixture of octahedral structures with the possible presence of a small amount of a tetrahedral species, as will be discussed in the next Chapter.

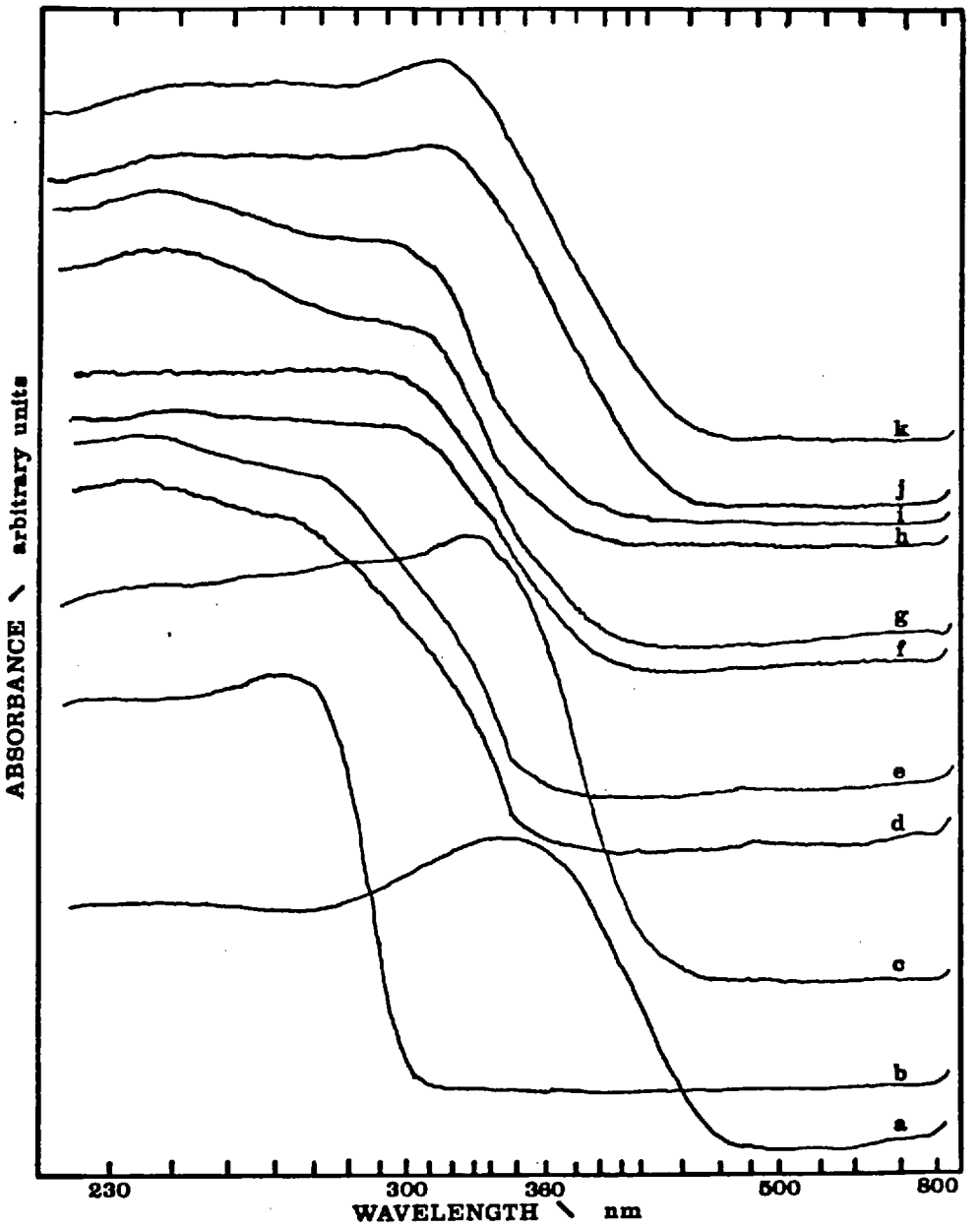

FIGURE 5.3: U.v.-reflectance spectra of Mo/γ-Al_2O_3 and unsupported pure compounds. (a) MoO_3; (b) Na_2MoO_4; (c) ammonium heptamolybdate; (d) 4%w MoO_3, pH = 7.5 - 8, dried at 393 K; (e) 8%w MoO_3, pH = 7.5 - 8, dried at 393 K; (f) 8%w MoO_3, pH = 2 - 4, dried at 393 K; (h) 4%w MoO_3, pH = 7.5 - 8, calcined 673 K; (i) 8%w MoO_3, pH = 7.5 - 8, calcined 673 K; (j) 8%w MoO_3, pH = 2 - 4, calcined 673 K; (k) 15%w MoO_3, pH = 2 - 4, calcined 673 K.

Spectra (d) and (e) were obtained from Mo/γ-Al_2O_3 prepared at pH = 7.5 - 8 with loading of 4%w and 8%w respectively and, again, there are no differences produced by variation of the Mo loading. For these samples the main absorption peak lies in the region of 230 nm indicating that the major surface species is a tetrahedral Mo structure, though some octahedral Mo species is clearly present. The predominance of tetrahedral Mo species produced by impregnation under basic conditions is expected from the stability of the MoO_4^{2-} anion (Pourbaix 1966) referred to above and from the finding that no adsorption takes place under basic conditions.

Therefore, the u.v. reflectance results of the dried samples indicates that Mo is adsorbed at the surface as polymolybdate ions under acid conditions. This may be by means of an electrostatic double layer mechanism (Kruyt 1952) or by chemisorption involving the exchange of OH^- groups from the surface with the polymolybdate anions of the solution (Giordano et al 1975 , Ianibello and Mitchell 1978). The fact that under acid conditions the adsorption is essentially irreversible (Ianibello and Triffiro 1975, Ianibello and Mitchell 1978) would indicate a strong chemisorption, but no definitive conclusions can be drawn as to the way in which the Mo anions are adsorbed at the surface.

Figure 5.3 (h - k) shows the u.v. reflectance spectra obtained after the samples had been calcined in dry air at 673 K. Compared to the spectra obtained before calcination, all the surfaces show sharper features which may be taken as an indication of more well-defined surface structures. The spectra for different Mo loadings are virtually identical. For samples prepared in acid conditions the spectra (j) and (k) show that the surface consists mainly of an octahedral Mo species. The fact that these spectra appear remarkably

similar to that of $Mo_7O_{24}^{6-}$ suggests that the surface contain structures which are similar to a polymolybdate. Some tetrahedral Mo is present, but samples prepared under acid conditions are clearly characterised by a high octahedral/tetrahedral Mo ratio. On the other hand, samples prepared in basic conditions are characterised by a low octahedral/tetrahedral Mo ratio, Figure 5.3 (h) and (i).

The calcined $Mo/\gamma\text{-}Al_2O_3$ samples and the pure Mo compounds were also characterised by ESCA and the results are given in Table 5.1. There is a measured difference of 0.6 eV between the Mo $3d_{5/2}$ binding energies for octahedral and tetrahedral Mo compounds, and this should be sufficient to distinguish between these species in $Mo/\gamma\text{-}Al_2O_3$. However, the Mo $3d_{5/2}$ binding energies for 15%w and 8%w samples prepared in acid conditions and the 8%w samples prepared in basic conditions are not significantly different, despite the fact that u.v. reflectance studies indicate a much higher octahedral/tetrahedral ratio in the former. The Mo 3d spectra were considerably broader than those of the pure compounds which could indicate a mixture of structures, and this is a possible reason why the Mo 3d binding energy appears insensitive to the octahedral/tetrahedral ratio. Variation in surface charging across the $Mo/\gamma\text{-}Al_2O_3$ surface would also lead to broadish spectra. Interesting information is obtained from the Mo $3d_{5/2}$/Al $2p_{3/2}$ peak area ratios. For the two samples prepared in acid conditions, this ratio appears to increase in direct proportion to the Mo loading which is consistent with a monolayer model (Schuit and Gates 1973) for the adsorbed Mo species, or at least a small particle size which remains constant with loading. At 15%w Mo loading the $\gamma\text{-}Al_2O_3$ surface (240 $m^2\ g^{-1}$) would still not be completely covered by a monolayer Mo species, and a coverage fraction of about

TABLE 5.1

Binding Energies (eV)[a] and Peak Area Ratios from ESCA

Compound or Catalyst[b]	Mo $3d_{5/2}$	Ni $2p_{3/2}$	Mo/Aℓ	Ni/Aℓ
MoO_3	232.8	-	-	-
$Mo_7O_{24}^{6-}$	232.8	-	-	-
$NiMoO_4$	232.2	-	-	-
8%w Mo(B)	233.2	-	0.64	-
8%w Mo(A)	233.2	-	1.50	-
15%w Mo(A)	233.2	-	2.6	-
4%w Ni(A)	-	856.2	-	0.61
4%w Ni(B)	-	856.2	-	1.00
Ni(B)-Mo(A)[c]	233.1	856.0	2.04	1.01
Ni(A)-Mo(A)[c]	232.9	856.1	1.92	0.71
NiMo(A)[c]	233.1	855.9	1.79	0.41
Ni(B)-Mo(B)[c]	233.1	855.8	1.50	1.00
NiMo(N)[c]	233.1	856.0	1.76	0.74
Mo(A)-Ni(B)[c]	233.0	856.1	1.99	1.05
Mo(A)-Ni(A)[c]	233.1	856.1	1.91	0.81
Mo(B)-Ni(A)[c]	233.1	856.0	1.73	0.79
AKZO-153S[d]	233.2	856.0	1.47	0.62

(a) Binding energies referred to C_{1S} = 284.3 eV or Aℓ $2p_{3/2}$ = 74.5 eV

(b) (B) = basic (A) = acid (N) = neutral

(c) 15%w MoO_3 and 4%w NiO

(d) 15%w MoO_3 and 3%w NiO

0.52 - 0.65 can be expected if the surface area occupied by one MoO_3 molecule is 20 or 25 A^2 respectively (Sonnemans and Mars 1973). The Mo 3d /Aℓ 2p ratio for the Mo/γ-$A\ell_2O_3$ sample prepared in basic conditions is much lower than the ratio for the sample with the same loading prepared in acid conditions. This indicates that the mean particle size produced in basic conditions must be greater than in acid conditions. Clearly the Mo species present in samples prepared in basic conditions cannot be completely in monolayer form. This is consistent with there being no adsorption in basic conditions.

Comparison of the above results with those previously published (Ashley and Mitchell 1968, Giordano et al 1972, Ianibello and Trifiro 1975, Ianibello and Mitchell 1978, Gajardo 1978) is not straightforward because of the different methods of preparation, although some parallels can be drawn. It has been reported that the amount of Mo taken up decreases as the pH increases (Ianibello and Trifiro 1978), and this is consistent with the present finding that no adsorption takes place in basic conditions. The present results indicate that the surface structure remains the same for any Mo loading provided the pH is controlled within a small range, but that different structures are produced depending on the pH. If the pH is allowed to vary freely during impregnation, then the pH condition within the pores of the support will be a function of the Mo concentration of the impregnating solution and the method employed, e.g. equilibrium adsorption or pore-filling. Under these conditions the surface structure would vary with Mo loading, which has been observed (Giordano et al 1975, Ianibello and Mitchell 1978, Voro'bev et al 1978). The suggestion that a high local pH in the pores during

impregnation by pore-filling (Ianibello and Mitchell 1978) results in MoO_4^{2-} species and a low degree of dispersion compared to impregnation by equilibrium adsorption (Lipsh and Schuit 1969) is consistent with the present finding that impregnation in controlled basic conditions results in a lower degree of dispersion than in acid conditions.

5.4 Ni/γ-Al_2O_3

Figure 5.4 shows the incorporation of Ni on to the γ-alumina support in the two ranges of pH considered. Curves (b) and (a) are the total uptake of Ni (expressed as NiO) at pH = 2 - 4 and pH = 7.5 - 8 respectively, as measured by XRF analysis of the solid phase. Equilibrium concentrations were determined by XRF of the solutions. The broken line (d) represents the amount of Ni which would be deposited in the support if no adsorption took place and is calculated from the measured equilibrium concentration and the pore volume of the support. The adsorption isotherm, Figure 5.4(c), was obtained by correcting curve (a) for the amount of Ni contained in the solution; filling the pore volume of the support, i.e. subtracting (d) from (a).

Again, two different processes are occurring during the impregnation. In the pH range 2 - 4 no adsorption takes place and the Ni present arises from the solution within the pore volume, while at pH 7.5 - 8 there is adsorption which accounts for most of Ni on the support up to an equilibrium concentration of ca 20 g dm^3 of Ni, where a maximum adsorption of ca 3.2%w Ni (as NiO) is reached. No adsorption isotherms have been reported for Ni on γ-Al_2O_3, although the values for uptake are similar to those of Co (Ashley and Mitchell 1968) and some reported values for Ni (Cervello et al 1976).

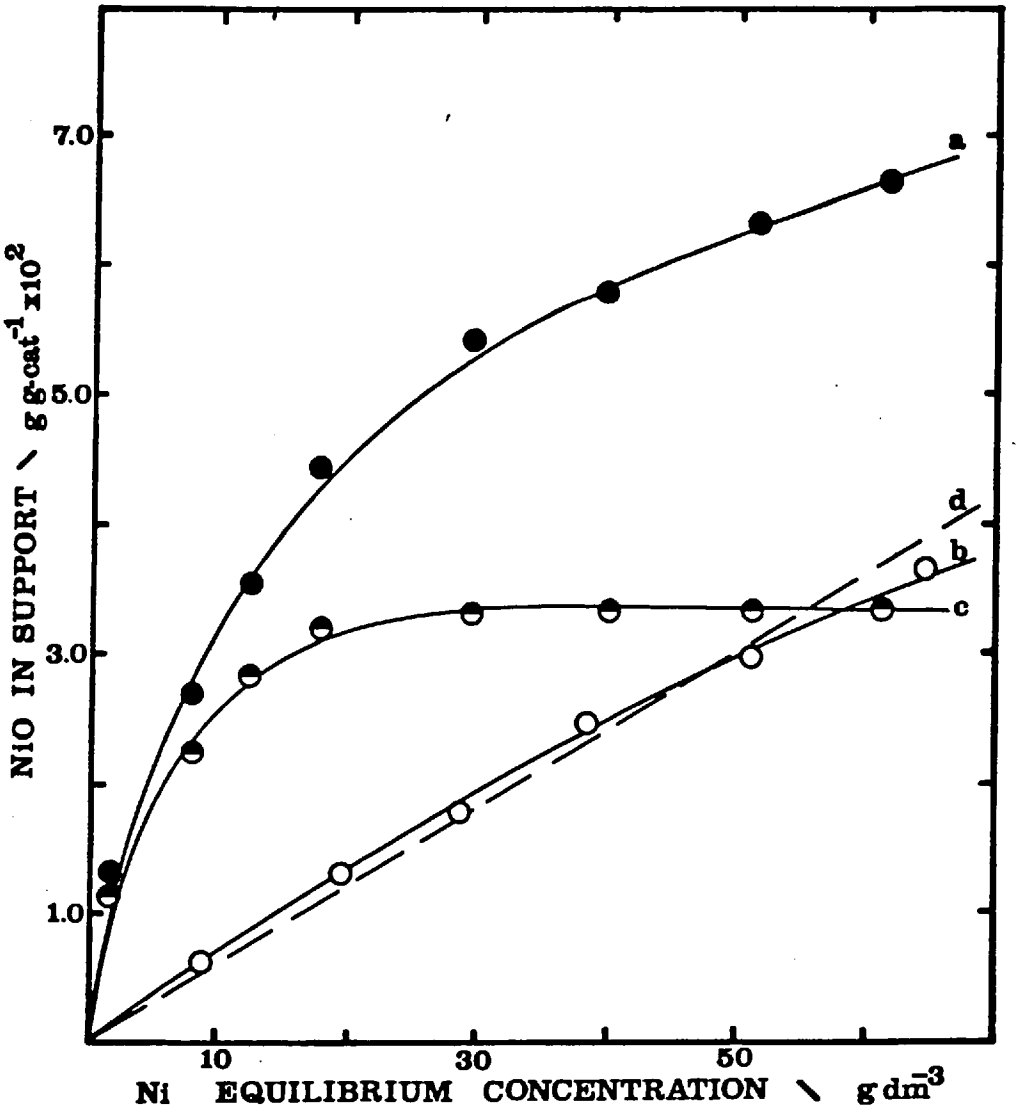

FIGURE 5.4: Impregnation of γ-$A\ell_2O_3$ by Ni at 293 K.

(a) total uptake of Ni at pH = 7.5 - 8.

(b) total uptake of Ni at pH = 2 - 4.

(c) adsorption isotherm at pH = 7.5 - 8.

(d) total uptake calculated from the pore volume, assuming no adsorption.

The Ni cation present in the solutions is $|Ni(H_2O_6)|^{2+}$ in the whole range of pH employed in the present work (Pourbaix 1966, Cotton and Wilkinson 1972). Above pH = 7.5 - 8 the surface of the alumina is slightly negative charge (Amphett 1974) and therefore a small adsorption is to be expected.

Figure 5.5(a - c) shows the u.v. reflectance spectra of the $Ni/\gamma\text{-}A\ell_2O_3$ surfaces after drying at 383 K for 60 hours. The spectra are similar to that of $|Ni(H_2O)_6|^{2+}$ (Cotton and Wilkinson 1972). There are slight differences between the spectrum of the sample prepared in acid conditions (a) when no adsorption takes place, and those obtained from samples prepared in neutral and basic conditions, (b) and (c). The similarity of the latter spectra is interesting since in basic conditions Ni exists as an amino complex (Cotton and Wilkinson 1972).

After calcination in dry air at 673 K, all the samples developed a strong peak at about 600 nm in the u.v. reflectance spectrum, Figure 5.5 (d - f), which corresponds to the $^3T_1(F) \rightarrow {}^3T_1(P)$ transition of tetrahedral nickel (II) (Lo Jacomo et al 1971, Cotton and Wilkinson 1972). However, it is only the samples prepared in neutral or basic conditions which show the characteristic spin-orbit splitting of this transition, indicating a well-defined tetrahedral environment. The very broad adsorption between 370 - 450 nm, Figure 5.5 (d - f), probably arises from octahedral nickel species with the presence of some free NiO (Lo Jacomo et al 1971). Comparison of the spectra from calcined and dried samples shows that the intensity of the nickel transitions is reduced in the calcined samples. Since the molar absorbance of the 600 nm transition in tetrahedral nickel is 10 - 20 times greater than that of any octahedral nickel transition (Cotton and Wilkinson 1972), it must be concluded that the nickel concentration

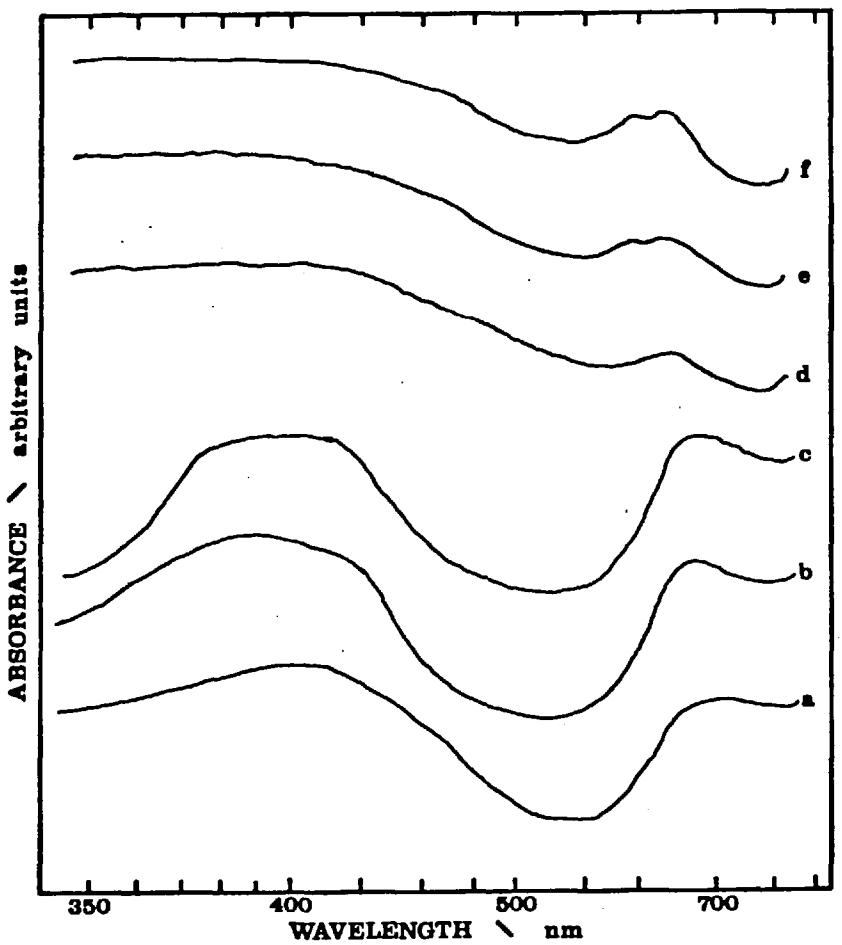

FIGURE 5.5: U.v.-reflectance spectra of Ni/γ-Al_2O_3

(a) pH = 2 - 4, dried 393 K
(b) pH = 6 - 8, dried 393 K
(c) pH = 9 - 10, dried 393 K
(d) pH = 2 - 4, calcined 673 K
(e) pH = 6 - 8, calcined 673 K
(f) pH = 9 - 10, calcined 673 K

Loading in all samples was ≈ 4%w NiO.

at the surface is reduced on calcination by diffusion into the bulk alumina.

These results are consistent with the formation of a Ni Al_2O_4 surface spinel phase as has been previously suggested (Lo Jacomo 1971). In a recent Mössbauer study of Co-Mo/Al_2O_3 catalysts (Topsoe et al 1978), it was concluded that for low Co loading (< 1%) the Co was diffused into the alumina occupying a distribution of sites and that this was independent of the presence of Mo. In addition it was found that for higher Co loadings, some Co_3O_4 was also formed (Topsoe et al 1978). These findings are entirely in agreement with the present results.

The results of the ESCA analysis of the calcined Ni/γ-Al_2O_3 samples are given in Table 5.1 The Ni $2p_{3/2}$ binding energies for the samples impregnated under basic and acid conditions are similar, suggesting the formation of similar surface compounds in agreement with the u.v. reflectance studies. The fact that the Ni 2p / Al 2p peak area ratio is much higher for the sample impregnated under basic conditions indicates that Ni is much dispersed on the surface under this condition of impregnation, consistent with the fact that Ni is adsorbed on the surface under basic conditions whereas no adsorption takes place under acid conditions.

5.5 CO-IMPREGNATION OF Ni AND Mo

Figure 5.6 shows the incorporation of Ni on to the γ-alumina support, in the pH ranges 2 - 4 and 6 - 7. Figure 5.6 (a) and (b) represent the total uptake of Mo (given as MoO_3) at pH = 2 - 4 and 6 - 7 respectively and curve (c) represents the adsorption isotherm of Mo in the pH = 2 - 4 range and results from subtracting from the total uptake the amount of Mo contained in the solution which fills the pore volume as described above. The broken line (d) represents

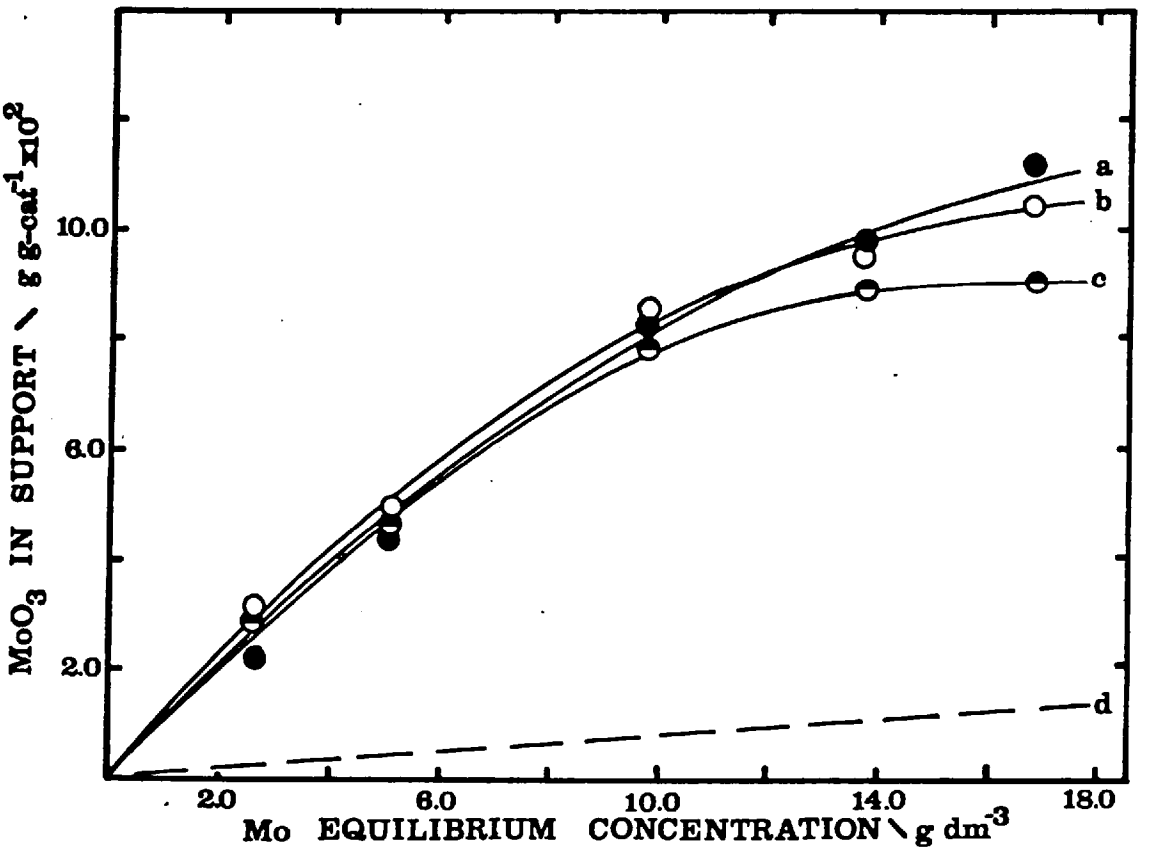

FIGURE 5.6: Co-impregnation of γ-$A\ell_2O_3$ by Mo and Ni at 293 K at an initial Ni concentration of 50 gdm^{-3}.

(a) total Mo uptake at pH = 2 - 4 (3%w NiO)

(b) total Mo uptake at pH = 6 - 7 (6%w NiO)

(c) adsorption isotherm at pH = 2 - 4 and 6 - 7

(d) total Mo uptake calculated from the pore volume assuming no adsorption.

the amount of Mo which would be deposited on the support if no adsorption took place. The initial concentration of Ni was 50 g dm^{-3} in both series and the total uptake of Ni in the support was ca 3%w and 6%w (as NiO) respectively, in agreement with the results presented in Figure 5.4 and independent of the Mo uptake. This indicates that Mo does not interfere with the Ni adsorption/deposition on the surface under the conditions employed.

From Figure 5.6 it can be seen that in both pH ranges the total Mo uptake is similar. However, at pH = 2 - 4 the amount of Mo adsorbed on the surface is decreased in the presence of Ni compared with that for Mo alone (Figure 5.2), whereas in the pH range 6 - 7 the presence of Ni greatly enhances the Mo uptake of the support compared to that of Mo alone. The lack of influence of Mo on the behaviour of Ni is readily explained by the large excess of Ni ions present in the impregnating solution. The behaviour of Mo is clearly not straightforward. In the pH range 2 - 4 the reduced adsorption could possibly be explained by occupation of adsorption sites by Ni, and this would give a total metal loading (on an atom basis) close to the maximum uptake observed for Mo alone. However, it cannot explain the discrepancy in Mo uptake at low equilibrium concentrations and in addition no adsorption was observed for Ni alone under these pH conditions. Thus either the presence of Ni interferes with polymolybdate formation or the high concentration of Ni cations within the pores neutralises the net negative charge of the molybdate anions reducing their ability to adsorb on the alumina surface at pH = 2 - 4.

The situation at pH = 6 - 7 is more complex. Solutions made from ammonium heptamolybdate and nickel nitrate have pH = 4 - 5 in the range of concentrations employed in the present work and when the pH was increased by the addition of ammonium hydroxide to above

pH = 7 the formation of insoluble molybdate (Climax Molybdenum Co. 1973) occurred immediately. At pH = 6 - 7 the formation of a gel was observed 2 - 4 hours after the addition of alumina, depending on the Mo concentration. However, it is clear from Figure 5.6 that the measured Mo uptake arises from adsorption. The fact that the Mo uptake is greater than for Mo alone at pH = 7.5 - 8 when no adsorption takes place, Figure 5.2(c), but less than that observed at pH = 2 - 4, Figure 5.2(a), is expected from surface charge considerations and is in agreement with previous results which suggest a decreasing Mo uptake with increasing pH (Ianibello and Trifiro 1975). An additional factor tending to increase the Mo uptake may be the adsorption of Ni cations which shift the net surface charge allowing the adsorption of molybdic anions.

The u.v. reflectance spectra of the co-impregnated surfaces after drying at 393 K are shown in Figure 5.7 (a) and (b). The spectra of samples prepared in different pH conditions are virtually identical in agreement with the similarity in the equilibrium adsorption data. The transitions at 700 - 800 nm and 380 - 550 nm corresponding to octahedral Ni(II) are clearly observed. Comparison with Figure 5.3 indicates that the strong absorption around 300 nm arises from octahedral Mo whereas no well-defined absorption from tetrahedral Mo species is apparent. Spectra from the calcined samples are shown in Figure 5.7 (c) and (d) where, again, there is virtually no difference between the two samples. Looking at the region 230 - 360 nm, where the Mo transitions occur, it can be seen that in these co-impregnated samples the Mo behaves in a similar manner to Mo impregnated alone at pH = 2 - 4, Figure 5.3 (f)(g)(j)(k), producing a surface with a high octahedral/tetrahedral Mo ratio. Turning to the nickel transitions, the changes in the 600 - 800 nm

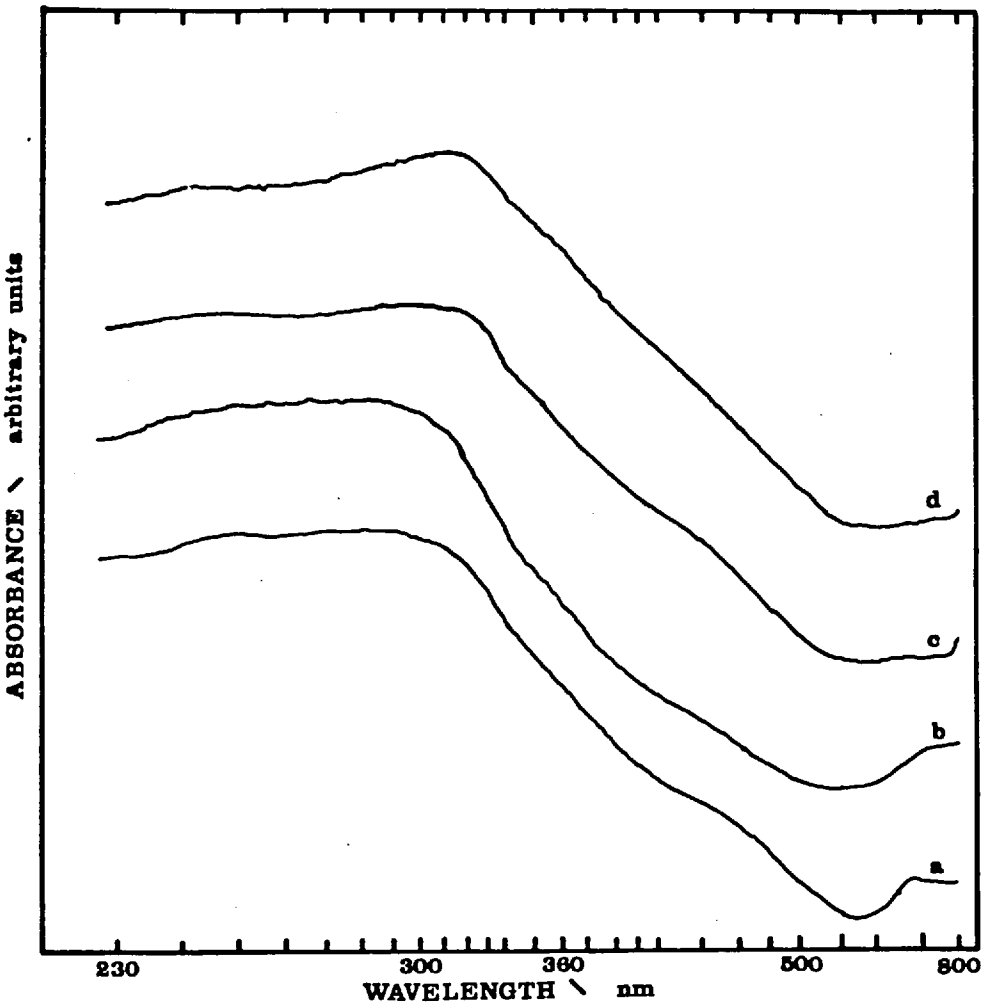

FIGURE 5.7: U.v.-reflectance spectra of co-impregnated Ni Mo/ γ-Al_2O_3 (4%w NiO and 15%w MoO_3)

(a) pH = 6 - 7, dried at 393 K

(b) pH = 2 - 4, dried at 393 K

(c) pH = 6 - 7, calcined at 673 K

(d) pH = 2 - 4, calcined at 673 K.

region suggest the formation of some tetrahedral Ni(II), while the strong absorption in the range 360 - 550 nm indicates the presence of octahedral Ni(II) and possibly some free NiO (Lo Jacomo et al 1971) at increased levels compared to samples prepared by impregnation of Ni alone, Figure 5.5. This is consistent with a recent finding for the Co-Mo/γ-Al_2O_3 system that the presence of Mo influences the extent of Co_3O_4 formation (Topsoe et al 1978).

The results of the ESCA analysis of the calcined NiMo/γ-Al_2O_3 samples are given in Table 5.1. The Mo $3d_{5/2}$ and Ni $2p_{3/2}$ binding energies for the samples prepared in neutral and acid conditions are similar, in agreement with the findings from the u.v. reflectance studies. The Mo $3d_{5/2}$/Al $2p_{3/2}$ peak area ratios are not significantly different, indicating a similar degree of dispersion of Mo on the surface and suggesting that Mo is adsorbed on the surface by a similar mechanism; the degree of dispersion is, however, lower than that of Mo(A) but greater than Mo(B) samples. The fact that the Ni $2p_{3/2}$/Al $2p_{3/2}$ peak area ratios are much higher for the sample impregnated under basic conditions is consistent with an adsorption of Ni cations on the surface leading to a higher dispersion under these conditions in agreement with the results of the Ni/γ-Al_2O_3 surfaces presented in the previous Section.

5.6 INFLUENCE OF THE IMPREGNATION PROCEDURE ON CATALYST ACTIVITIES

5.6.1 Catalyst Activities

On the basis of the impregnation studies previously described a series of catalysts were prepared varying the pH of the impregnating solutions and the cycle of impregnation in order to study the effect of these variables on catalyst activity. A constant loading of 15%w Mo and MoO_3 and 4%w Ni as NiO on the same γ-alumina support was chosen for this comparative study. In addition, a commercial catalyst

AKZO-153S was included in the study. Details of the preparation procedures and nomenclature were given in the Experimental Chapter (Section 2.5.3). It was found that the uptake of Ni by γ-alumina previously impregnated with Mo was identical to the uptake in the absence of Mo (see Figure 5.4). On the other hand, the uptake of Mo on the support containing Ni was found to be similar to that measured for the co-impregnation method (Figure 5.6).

The catalysts were tested initially for HDS activity in the atmospheric reaction system under the conditions described in the experimental section. The measured values of the apparent kinetic constant for thiophene HDS assuming a pseudo-first order reaction mechanism (Massoth 1977) are given in Table 5.2. No decay in activity was observed for any of the catalyst during a 2 hour run.

TABLE 5.2

Catalyst Activity for Thiophene HDS at Atmospheric Pressure

Catalyst[a]	Apparent kinetic constant/g-mol $(g\text{-cat})^{-1} hr^{-1} \times 10$
Ni(B)-Mo(A)	4.7
Ni(A)-Mo(A)	4.5
Ni Mo(A)[b]	4.2
Ni(B)-Mo(B)	4.0
Ni Mo(N)[b]	3.8
Mo(A)-Ni(B)	3.7
Mo(A)-Ni(A)	3.6
Mo(B)-Ni(A)	3.5
AKZO-153S	3.5

a (A) = acid conditions; (B) = basic conditions; (N) = neutral

b prepared by co-impregnation

Within the experimental error of the results (± 0.2) presented in Table 5.2, the following generalisations may be drawn concerning the activity for HDS in relation to the method of preparation.

(i) Higher initial activities are achieved when γ-$A\ell_2O_3$ is impregnated with Ni first.

(ii) When Ni is added first higher activities are obtained if Mo is added at pH = 2 - 4 rather than at pH = 7.5 - 8 but the effect is insignificant if Mo is added before Ni.

(iii) The pH at which alumina is impregnated with Ni is not critical, although basic conditions do give rise to a slight increase in activity whatever impregnation cycle is used.

(iv) Co-impregnation produces catalysts with slightly reduced activity compared with separate impregnation steps.

Once having established an activity ranking of the catalysts with the atmospheric pressure apparatus, it was important to test whether this pattern was still valid at high pressure. Three representative catalysts and the commercial catalyst were chosen for the high pressure measurements. These were Ni(B)-Mo(A), Mo(A)-Ni(B) and Mo(B)-Ni(A) which showed high, medium and low activity respectively in the atmospheric pressure tests. Values of the apparent kinetic constants obtained by the procedures described in Chapter 4 are given in Table 5.3. Since HDS was complete on all four catalysts, no attempt was made to evaluate kinetic data. The results in Table 5.3 demonstrate that the trend in activity observed in the atmospheric pressure experiments is valid in the high pressure test with model synthetic feedstock. Catalyst Ni(B)-Mo(A) showed the highest activity for all

the hydrogenation reactions. The present results confirm the finding by other workers (Laine 1977, Mone and Moscou 1977, Ochoa et al 1978) that higher activities are obtained when the impregnation of alumina is carried out with Ni before Mo.

TABLE 5.3

Catalyst Activity at High Pressure

Catalyst	Apparent kinetic constants/g-mol (g-cat)$^{-1}$hr^{-1}			
	HDO	HDN	Phenanthrene hydrogenation	Phenanthrene hydrocracking
Ni(B)-Mo(A)	0.46	1.64	4.05	0.88
Mo(A)-Ni(B)	0.31	1.04	3.33	0.50
Mo(B)-Ni(A)	0.27	0.91	3.57	0.72
AKZO-153S	0.28	1.01	3.60	0.71

5.6.2 Catalyst Characterization

During the impregnation studies previously described, u.v. reflectance spectroscopy and ESCA were used successfully to identify preparation dependent surface structural features. Similar features were anticipated in the catalyst used in the activity tests, and so the catalysts were studied in detail with the above two techniques.

The results of ESCA studies on the calcined catalysts are given in Table 5.1. The measured Mo $3d_{5/2}$ binding energies for the catalysts are the same within experimental error and they are also in agreement with the measured values for the Mo/γ-$A\ell_2O_3$ samples. Comparison with results from MoO_3 and $Mo_7O_{24}^{6-}$ indicates that the Mo is largely in an octahedral environment. The Ni $2p_{3/2}$ binding

energies show no significant variation. More interesting are the Mo 3d /Aℓ 2p and Ni 2p /Aℓ 2p peak area ratios which give a measurement of the relative surface composition. The Mo/Aℓ ratios for the catalysts are lower than that measured for the Mo/γ-$Aℓ_2O_3$ sample with the same 15%w Mo loading and for some catalysts it approaches the value obtained from an 8%w Mo sample. Not all of this reduction in Mo/Aℓ ratio can be explained by attenuation of the Aℓ 2p signal by an overlayer of Ni, and it would appear that the degree of Mo dispersion in the catalysts is lower than in the Mo/γ-$Aℓ_2O_3$ samples. The variation in the Mo/Aℓ ratio shows no correlation with the activity pattern in Tables 5.2 and 5.3, but the values are generally higher for catalysts in which Mo is impregnated under acid conditions compared with those under basic conditions, in agreement with the findings in the preparation of the Mo/γ-$Aℓ_2O_3$ samples.

Turning to the Ni 2p /Aℓ 2p peak area ratios, large variations are observed in the measured values (Table 5.1). Catalysts in which Ni is impregnated under basic conditions show a consistently higher Ni/Aℓ ratio when when Ni is impregnated under acid conditions, for the same conditions for the impregnation of Mo, leading to a higher activity. This is also consistent with the fact that Ni is adsorbed on the surface under basic conditions leading to a higher degree of dispersion on the surface of the alumina.

The u.v. reflectance spectra of the catalysts are shown in Figure 5.8(a-g) which are in the order of activity, i.e. the spectrum of the most active catalyst is in Figure 5.8(a). The Mo transitions occur below 360 nm. Comparison with the spectra of pure Mo compounds and Mo/γ-$Aℓ_2O_3$ samples (Figure 5.3) reveals that

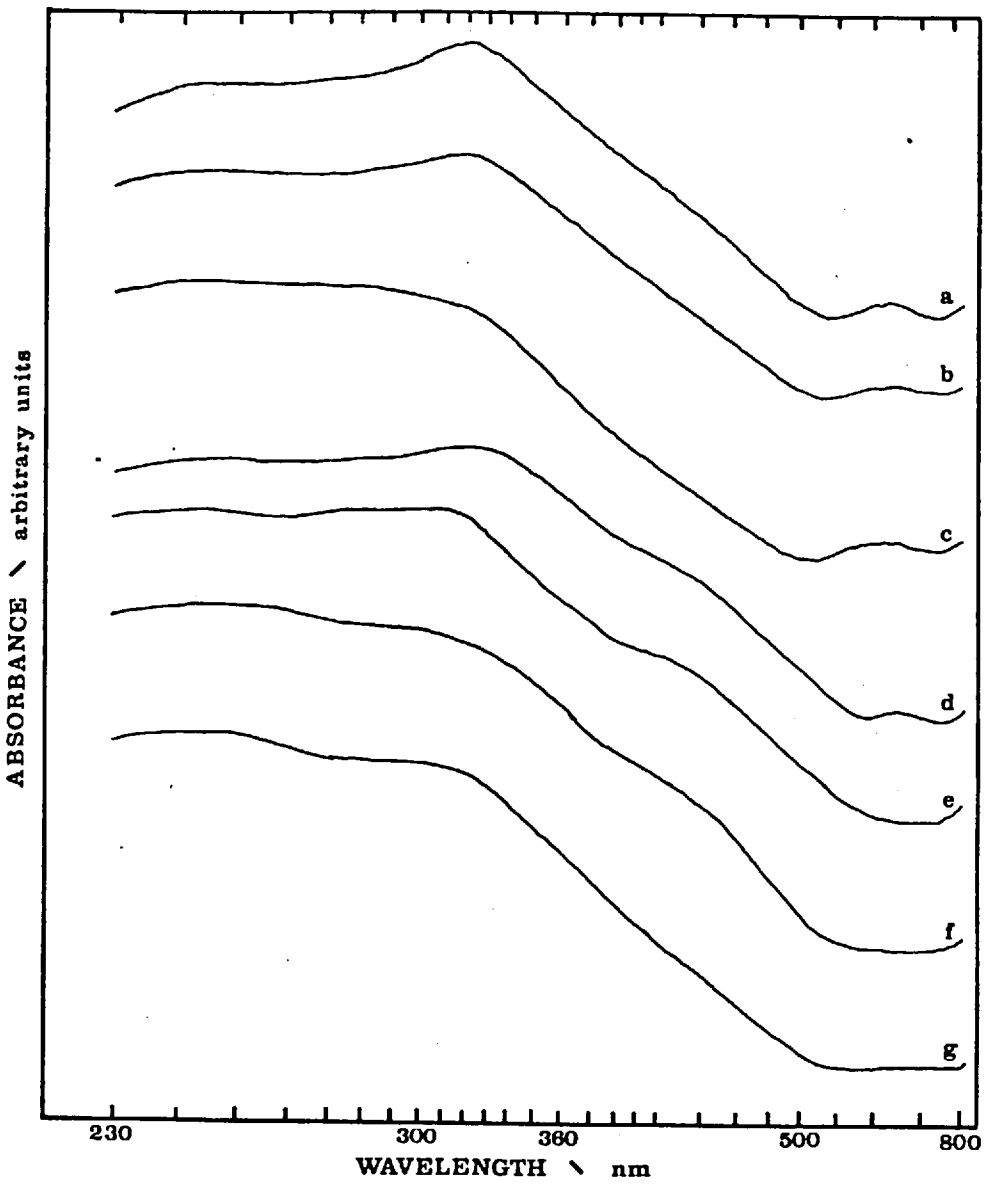

FIGURE 5.8 U.v.-reflectance spectra of catalysts (4%w NiO and 15%w MoO_3)
(a) Ni(B)-Mo(A) (b) Ni(A)-Mo(A) (c) Ni(B)-Mo(B)
(d) Mo(A)-Ni(B) (e) Mo(A)-Ni(A) (f) Mo(B)-Ni(A)
(g) AKZO-153S

catalysts in which Mo is impregnated under acid conditions are characterized by a higher octahedral/tetrahedral Mo(III) ratio than those under basic conditions. Indeed, the 340 nm adsorption of octahedral Mo is very pronounced in the spectrum of the Ni(B)-Mo(A) catalyst, Figure 5.8(a), while the spectrum of the Mo(B)-Ni(A) catalyst, Figure 5.8(f), presents a strong adsorption in the 240 nm region, typical of Mo tetrahedral compounds. Therefore, the octahedral/tetrahedral Mo ratios are in agreement with the results obtained for the Mo/γ-$A\ell_2O_3$ system with respect to the pH of the impregnated solution, except that the preparation conditions for AKZO-153S are unknown.

The region 400 - 800 nm contains the transitions of Ni(II). A striking feature is that the adsorption around 400 - 500 nm, which arises from octahedral Ni(II) and possibly some free NiO, is characteristic of the low active catalysts, Figure 5.8(d-f), while the transition of tetrahedral Ni(II) at 600 nm becomes more pronounced as the activity increases, Figure 5.8(d-a). This characteristic of the spectrum of an active Ni-Mo(W) catalyst has been described in a U.S. patent as a method to determine the activity of the catalyst prior to its use in a hydrotreating process (Johnson 1976) by comparing the relative reflectance of the transition of Ni(II) in the region of 580 -630 nm of a given catalyst to that of a standard catalyst with known activity. However, comparison of the spectra of catalysts Ni(B)-Mo(B) and Ni(A)-Mo(A), Figure 5.8(c)(b), indicates that, although the absorbance in the 580 - 630 nm region of the first is slightly higher, the activity is 12% lower (Table 5.2). Turning to the Mo transitions, it can be seen that catalyst Ni(A)-Mo(A) presents a better defined Mo(VI) octahedral species on the surface.

The spectra of the catalysts imply that the following features are correlated with increasing activity:

i) a high octahedral/tetrahedral Mo(VI) ratio

ii) an increased tetrahedral/octahedral Ni(II) ratio

iii) an increased Ni content or Ni dispersion in the catalyst surface.

Comparison of the u.v. reflectance spectra of the co-impregnated samples, Figure 5.7, with those for the catalyst prepared by successive impregnation, Figure 5.9, indicates that according to the above criteria the co-impregnated catalysts should have medium activity. Reference to Table 5.2 shows this to be the case.

CHAPTER SIX: A STUDY OF CALCINATION AND THE INFLUENCE OF THE CALCINATION PROCEDURE ON THE ACTIVITY OF Ni-Mo/γ-Al_2O_3 CATALYSTS

6.1 INTRODUCTION

In the studies of the influence of the impregnation procedure on the activity of Ni-Mo/γ-Al_2O_3 catalysts presented in Chapter 5, a "best" impregnation procedure was developed, but calcinations were carried out at 673 K under dry air throughout these studies. As the conditions of the calcination, namely temperature and atmosphere, are important for the activity of the catalyst, in this Chapter the results of a study of the calcination and the influence of the calcination conditions on the activity of the catalyst is presented. An attempt has been made to relate the hydrogenation activity, measured for thiophene HDS at atmospheric pressure, to the calcination procedure through characterization of the catalyst surfaces by ESCA and u.v. reflectance spectroscopy.

6.2 CALCINATION OF Ni, Mo AND Ni-Mo/γ-Al_2O_3

The formation of the oxidic state of the catalyst involves three steps: impregnation from solutions, drying and calcination. As indicated in the previous Chapter, when the impregnation is carried out under acid conditions Mo is adsorbed at the surface in what appears to be polymolybdate structures such as $Mo_7O_{24}^{6-}$, and is deposited on the surface in structures such as MoO_4^{2-} when the impregnation is carried out under basic conditions. This was explained in terms of the effect of the pH of the solution on the nature of the Mo species present in the solution and on the surface charge of the support. Similarly, Ni is adsorbed on the surface

under basic conditions and deposited under acid conditions. In order to gain more information on the nature of the interaction between the active components and the support in the oxidic state of the catalyst, the weight loss during the calcination at 673 K under dry air of γ-$A\ell_2O_3$ containing Ni and/or Mo impregnated under basic or acid conditions was measured in the gravimetric flow system described in 2.4, Chapter 2. The results are shown in Figure 6.1 (b-h) and since during the calcination process the temperature of the sample increased from 383 to 673 K, the rate of temperature increase (measured by a thermocouple placed adjacent to the samples) is represented in Figure 6.1(a).

During the calcination process the observed weight loss arises not only from the possible decomposition or condensation reactions of the impregnated species but also from the support since it is capable of absorbing a considerable amount of water (de Boer et al 1963). In fact, aluminas adsorb water in two ways: a species weakly bound (physisorbed) to the surface that can be removed by drying at 383 K and a chemisorbed water, strongly bound to the surface (Peri and Hannan 1960, Peri 1965) which is partially removed during calcination to an extent which depends on the temperature of calcination. The latter process is represented in Figure 6.1(b), in which the support was first wetted and dried in the same way as the samples. The surface of the alumina can be assumed to be completely covered by OH groups after drying (Peri 1965). Assuming that each hydroxide ion occupies an area of about 0.1 nm^2 (Peri 1965), a rough calculation based on the observed weight loss of the alumina sample (about 27 mg g^{-1}), Figure 6.1(h), shows that the OH coverage fraction is about 60% of a monolayer in the present conditions, i.e. after calcination in dry air at 673 K.

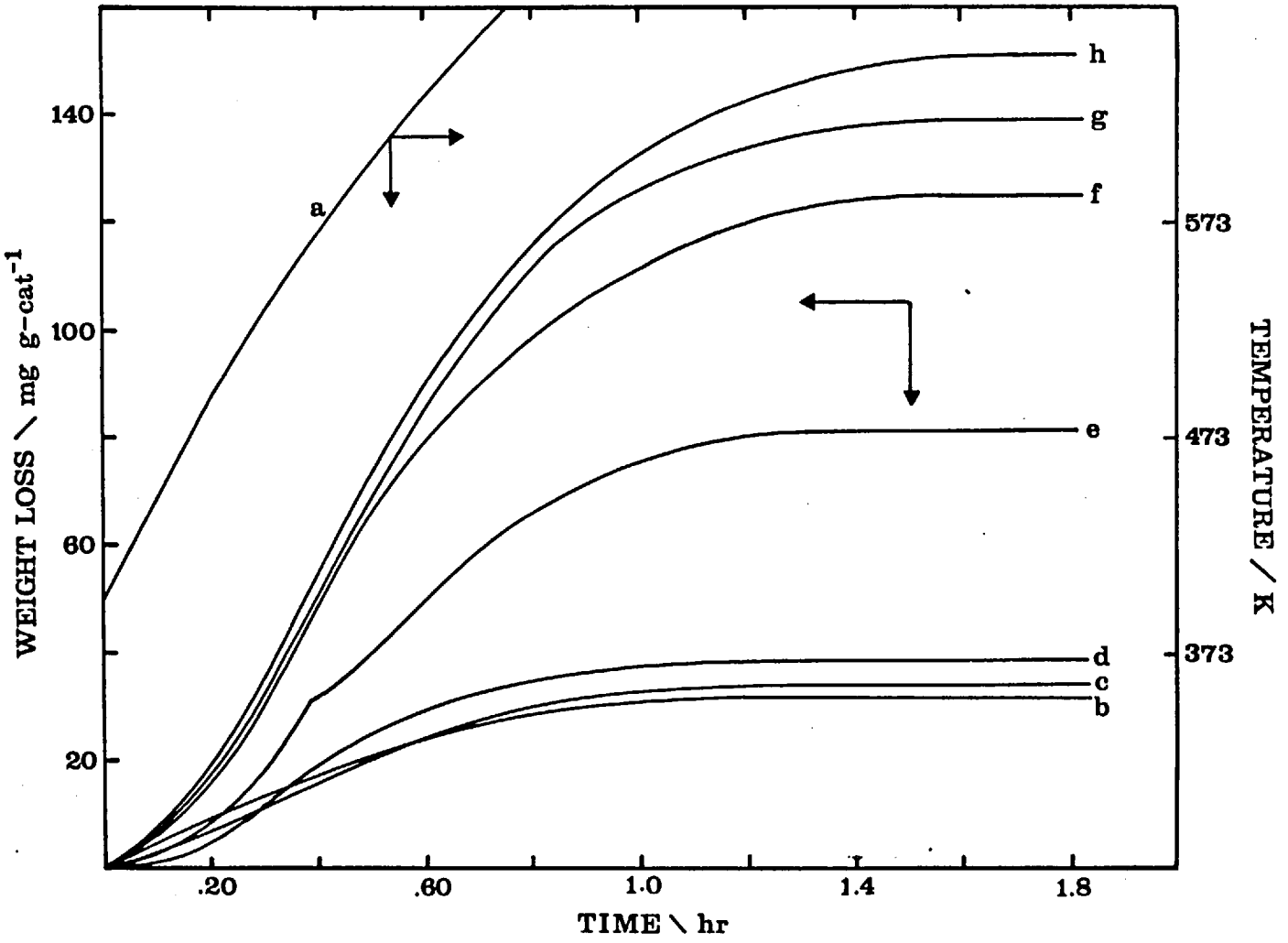

FIGURE 6.1: Kinetics of calcination under dry air

(a) rate of temperature increase; (b) γ-$A\ell_2O_3$;
(c) Mo(A); (d) Mo(B); (e) Ni(B); (f) Ni(A);
(g) NiMo(B); (h) NiMo(A)

Comparison of the weight losses of the Mo/γ- $A\ell_2O_3$ samples, Figure 6.1(c)(d), indicates that the weight loss of the sample impregnated under basic conditions is about 15% larger than that under acid conditions. As indicated in the studies of the impregnation of Mo on to the support (5.3, Chapter 5), under acid conditions Mo is adsorbed on the surface probably as a polymolybdate, whereas under basic conditions, Mo is deposited on the support as a Mo salt (after drying) in which Mo is tetrahedrally surrounded as in a MoO_4^{2-} ion. Therefore, the observed difference in the weight loss of samples impregnated under basic and acid conditions during the calcination is consistent with these findings.

In the case of the sample impregnated under basic conditions, the weight loss arises from the decomposition of the Mo salt deposited on the surface, probably $(NH_4)_2\ MoO_4.2H_2O$ (Climax Molybdenum Co. 1962), whereas in the second case, it arises from the condensation reactions of the $Mo_7O_{24}^{6-}$ ion on the surface (Dupuis and Duval 1950), in addition to the weight loss from the alumina surface. In fact, $(NH_4)_2\ MoO_4.2H_2O$ decomposes at about 413 K (Dupuis and Duval 1950), and this is the temperature about which a maximum in the rate of calcination of the Mo(B) sample, Figure 6.1(d), is observed. On the other hand, $Mo_7O_{24}^{6-}$ is only stable at temperatures below 331 K, and above this temperature condensation of the ion to complex polymolybdate compounds such as Mo_8O_{23}, $Mo_{17}O_{47}$, etc., occurs (Dupuis and Duval 1950).

Comparison of the weight losses of the Ni/γ-$A\ell_2O_3$ samples, Figure 6.1(e)(f), indicates that the weight loss of the sample prepared under acid conditions is much larger than that prepared under basic conditions (125 and 82 mg $(g\text{-cat})^{-1}$ respectively) and

in the latter case, the rate of calcination shows a maximum at about 558 K. As $Ni(H_2O)_6^{2+}$ ions are adsorbed on the surface under basic conditions and deposited on the surface under acid conditions, probably at $Ni(NO_3)_2.6H_2O$, 5.4, Chapter 5, this large difference is consistent with these findings since NiO is formed mainly from adsorbed $Ni(H_2O)_6^{2+}$ in the first case and from $Ni(NO_3)_2.6H_2O$ in the second case.

Turning to the co-impregnated samples, Figure 6.1(g)(h), it can be seen that the sample impregnated under acid conditions showed a larger weight loss than that impregnated under basic conditions, but this difference is much lower than that which will arise if the Ni and Mo ions are considered separately. This is in agreement with the fact that there is a chemisorption (or precipitation) of Mo ions under both conditions when Ni and Mo are co-impregnated (2.5, Chapter 5).

Finally, no attempt was made to employ this gravimetric technique to characterize the nature of the compounds on the surface at different calcination conditions, due to the interference in the weight loss measurements by the desorbed water from the support.

6.3 THE INFLUENCE OF THE CALCINATION CONDITIONS ON THE SURFACE STRUCTURES ON Ni and Mo/γ-Al_2O_3 SURFACES

6.3.1 Mo/γ-Al_2O_3

U.v. reflectance spectroscopy was successfully employed in the impregnation studies to characterise Ni and Mo/γ-Al_2O_3 surfaces. Figure 6.2(a-e) shows the u.v. reflectance spectra of the Mo(A)/γ-Al_2O_3 surfaces of samples containing 15%w Mo as MoO_3 (bulk composition) impregnated under acid conditions (pH 2-4), after calcination for 8 hours at 673, 773 or 873 K under air (A), air saturated in

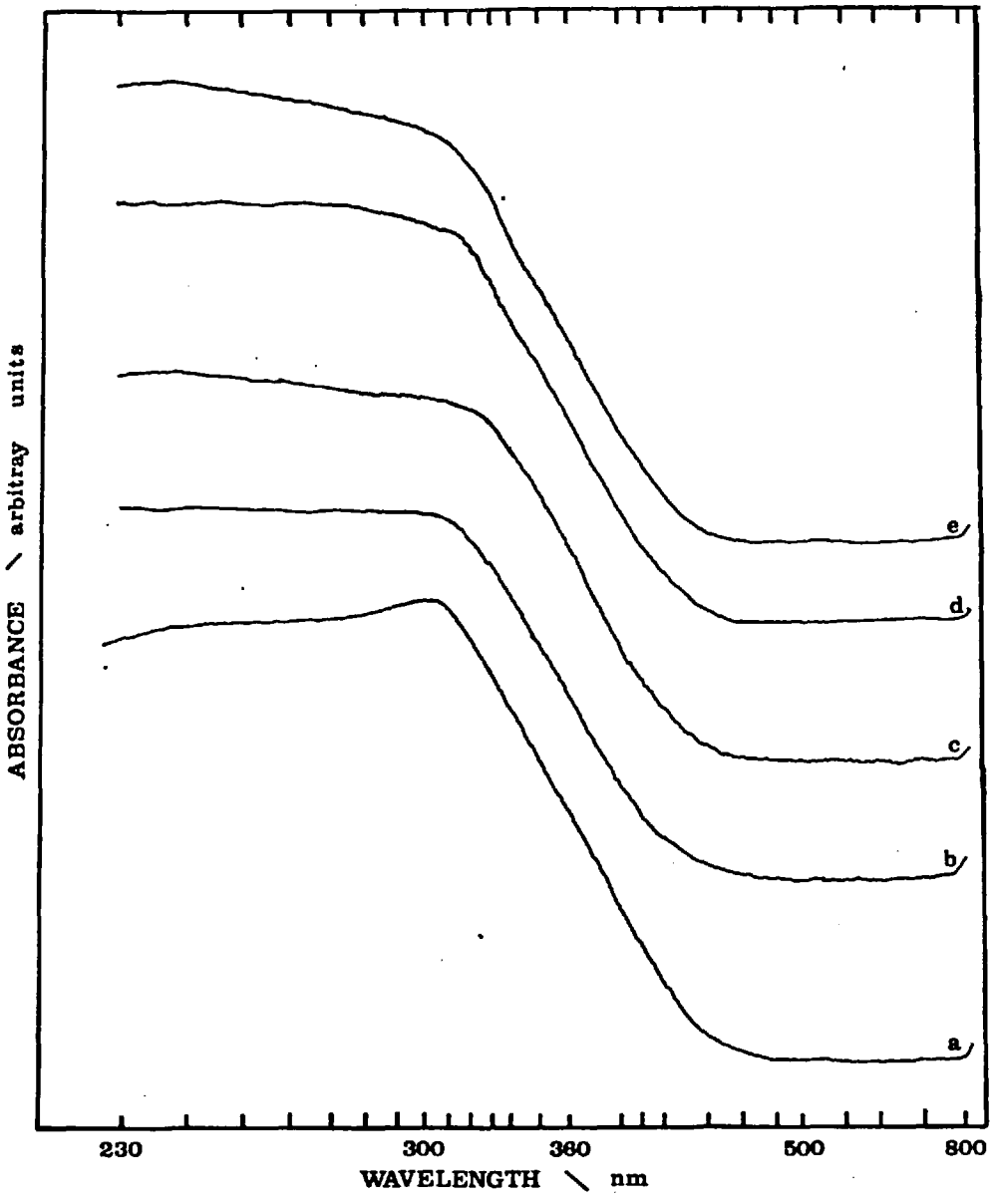

FIGURE 6.2: U.v. reflectance spectra of $Mo/\gamma\text{-}Al_2O_3$ (15%w MoO_3)

Conditions of calcination: (a) 673 K, air; (b) 773 K, air; (c) 773 K, nitrogen; (d) 773 K, air-water; (e) 873 K, air.

water at 298 K (AW) or nitrogen (N). All spectra show two strong absorption bands, the maximum of which are saturated between 300 - 360 nm and 240 - 260 nm and, as indicated in the previous Chapter (Section 5.3), these correspond to the electronic transitions of Mo(VI) in octahedral and tetrahedral structures respectively. Therefore, the spectra indicate that the Mo(VI) configurations on the surface consist of mixtures of tetrahedral and octahedral species, the ratio of which depends on the conditions of the calcination. The octahedral/tetrahedral Mo(VI) ratio of the samples in Figure 6.2 decreases in the order: 673A(a) > 773A(b) $\sim$ 773N(c) $\sim$ 773AW(d) > 873A(e). This result is in agreement with those of Vorob'ev et al (1978) and with those of Giordano et al (1975), and it appears that there is no significant difference in the structural features of the Mo/γ-Al_2O_3 surface when the atmosphere of the calcination is varied, Figure 6.2(b-d). The fact that the octahedral/tetrahedral Mo ratio decreases as the temperature increases suggests that there is a condensation process of the Mo components on the surface leading to an increased occupancy of Mo in tetrahedral sites in the Mo surface structures. The fact that the spectrum of the sample calcined at 873 K under air, Figure 6.2(e), presents a well defined peak at about 230 - 250 nm may indicate the occurrence of a chemical interaction between Mo and the support leading to the formation of a $Al_2(MoO_4)_3$ phase, as observed by Asmolov and Krylov (1970), in addition to structures in which Mo is present in octahedral and tetrahedral sites.

A more precise assignment of the absorption bands in the u.v. region to particular structures in the case of Mo is difficult. The interpretation of spectra by comparison with spectra of model compounds

as in the present work, has been widely applied (Ashley and Mitchell 1968 - 1969, Asmolov and Krylov 1970, Giordano et al 1975, Gajardo 1978), but does not allow one to draw a definitive conclusion concerning the surface species present on the support. The reason for this lies in the complexity of Mo chemistry (Cotton and Wilkinson 1972) and the fact that there is a superimposition of the absorption bands of the various Mo compounds in the u.v. region (Figure 5.3, Chapter 5).

At this point, it is interesting to discuss the genesis and structure of the $Mo/\gamma\text{-}Al_2O_3$ surface starting from the impregnation stage. The interaction of Mo with the support undoubtedly involves the surface OH^- groups which are generally accepted as the reactive sites (Peri 1965, Giordano et al 1975, Ianibello and Mitchell 1978). As indicated by Peri (1965), the surface of the γ-alumina in the fully hydrated state (even after drying at 373 K) is completely covered by OH^- groups and in the case of impregnation under acid conditions, Mo is probably present in the solution as $Mo_7O_{24}^{6-}$ ions. Thus, the first step in the formation of $Mo/\gamma\text{-}Al_2O_3$ surface should be the formation of structures such as:

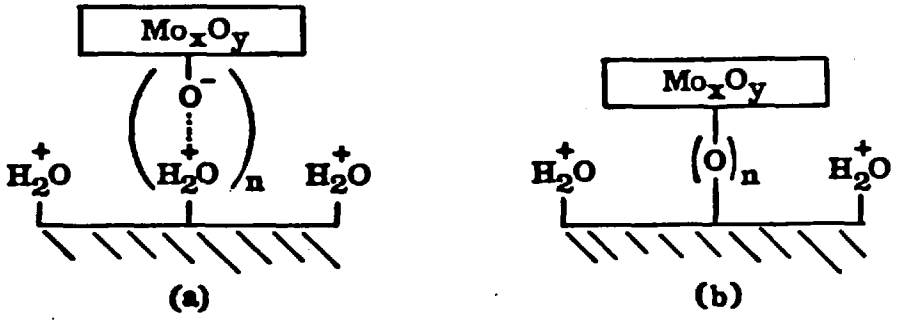

where (a) represents an electrostatic adsorption of the Mo anions on the positively charged surface and (b) an exchange of OH^- groups from the alumina with O^- ions present in the lattices of the $Mo_7O_{24}^{6-}$ ion.

As discussed before, the $Mo_7O_{24}^{6-}$ decomposes at temperatures above 331 K, forming compounds such as Mo_8O_{23}, $Mo_{17}O_{47}$, Mo_9O_{26}, Mo_4O_{11}, and therefore during drying and calcination these structures should be formed on the surface, being linked on the surface through Mo-O-Aℓ bonds, as indicated in structure (b) above. Since these components have complex structures in which Mo occupies both tetrahedral and octahedral sites (Wyckoff 1960), this explains the gradual shift of the adsorption bands to lower wavelength in the spectra of Mo/γ-$Aℓ_2O_3$ as the temperature of the calcination increases.

In the case of Mo impregnation under basic conditions, Mo is deposited on the surface after drying in structures similar to that of $(NH_4)_2MoO_4.2H_2O$, in which Mo is preferentially in tetrahedral surroundings (5.3, Chapter 5). On calcining, the deposited Mo compound decomposes on the surface, leading to structures in which Mo is preferentially in tetrahedral surroundings such as in MoO_4.

6.3.2 Ni/γ-$Aℓ_2O_3$

Figure 6.3(a-f) shows the u.v. reflectance spectra of the Ni/γ-$Aℓ_2O_3$ surfaces of samples containing 4% Ni as NiO (bulk composition) after calcination for 8 hours at 673, 773 and 873 K in air, air saturated in water at 298 K and nitrogen. All spectra are characterized by a strong adsorption peak in the region of 575 - 680 nm and by a broad peak at about 425 nm, consistent with the formation of a Ni $Aℓ_2O_4$ surface spinel phase (Lo Jacomo et al 1971, Lo Jacomo and Cimino 1976), as discussed in 5.4, Chapter 5. However, both the degree of inversion, i.e. the relative occupancy of tetrahedral and octahedral sites of Ni(II) in the surface spinel and the amount of free NiO present on the surface are affected by the conditions of the calcination.

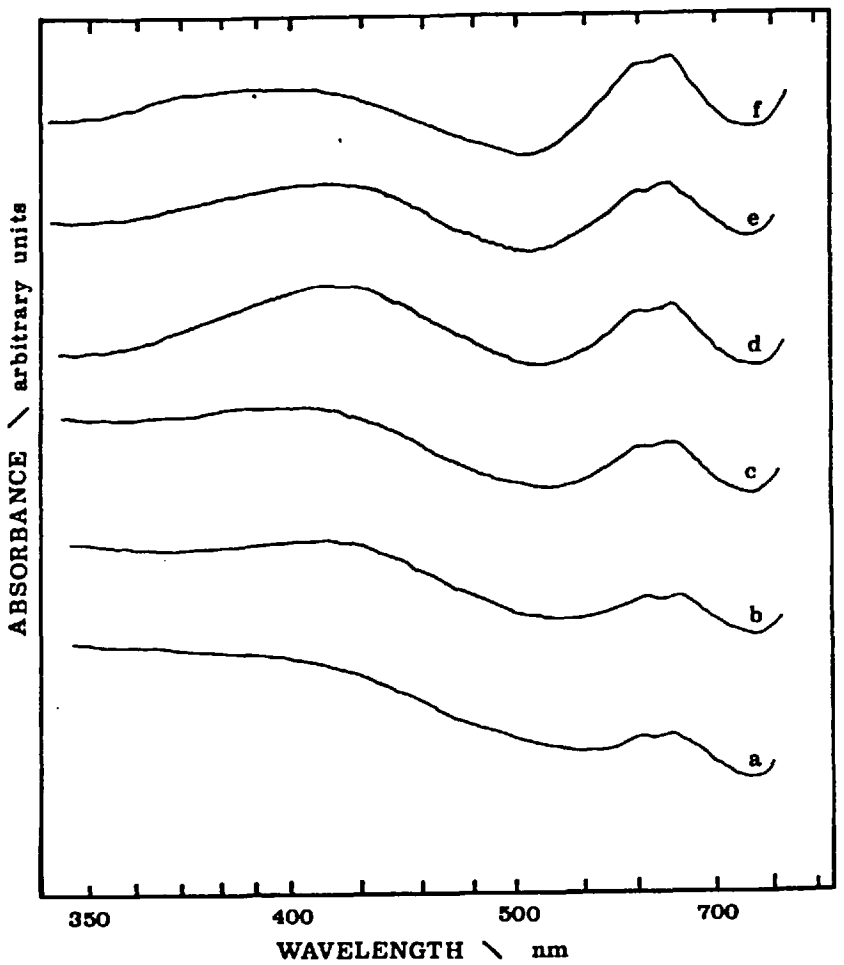

FIGURE 6.3: U.v. reflectance spectra of Ni/γ-Al_2O_3 (4%w NiO)

Conditions of calcination: (a) 673 K, air;
(b) 773 K, air; (c) 773 K, air-water;
(d) 873 K, nitrogen; (e) 873 K, air;
(f) 873 K, air-water.

Generally speaking, the tetrahedral/octahedral Ni(II) ratio, as indicated by the peaks at about 600 nm and the broad absorption between 370 - 450 nm increases as the temperature of calcination increases and with the atmosphere in the order: WA > A > N. The presence of the peak at about 370 - 450 nm reveals that, since the molar adsorbance of tetrahedral Ni(II) in this region is 10 - 20 times greater than that of octahedral Ni(II), as discussed in 5.4, Chapter 5, the octahedral sites Ni(II) must be also present in significant amounts. Lo Jacomo et al (1971) concluded from magnetic measurements that only 10 - 20% of the total Ni(II) is present in a tetrahedral coordination on the surface in samples calcined at 873 K. Adsorption in the region below 360 nm will arise if NiO is present at the surface (Lo Jacomo et al 1971). Comparison of the spectra of the samples indicates that the presence of NiO decreases as the temperature of calcination increases, and it is very small when the catalyst is calcined at 873 K under nitrogen.

According to these results, and recalling the findings of the studies of the impregnation of Ni on the support, (5.4, Chapter 5), the first step in the formation of the surface, when the impregnation is carried out under basic conditions, should be the adsorption of the $Ni(H_2O_6)^{2+}$ ions, as

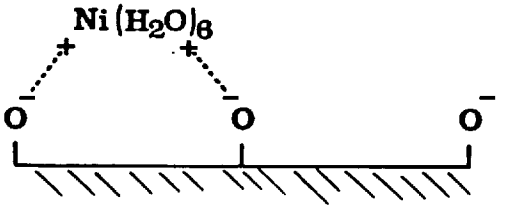

and during drying and calcination, the surface presents a structure similar to:

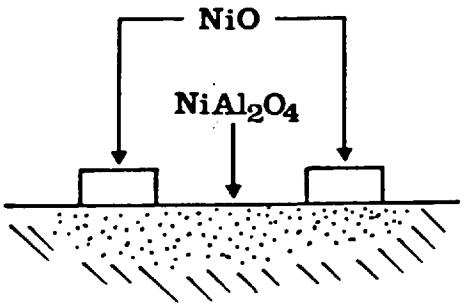

and in which the degree of inversion of the Ni Al_2O_4 spinel, i.e. the relative occupancy of Ni(II) in tetrahedral or octrahedral sites in the spinel, and the amount of NiO is determined by the conditions of the calcination. This picture is similar to that proposed for Co/γ-Al_2O_3 surfaces, in which the existence of both Co_3O_4 and Co Al_2O_4 has been observed (Schuit and Gates 1973, Gajardo 1978, Okamoto et al 1979).

6.4 INFLUENCE OF THE CALCINATION CONDITIONS ON THE CATALYST ACTIVITIES

6.4.1 Catalyst Activities

Catalysts containing 4%w Ni as NiO and 15%w Mo as MoO_3 were prepared employing the "best" impregnation identified in the impregnation studies (Chapter 5), i.e. the support was impregnated first from solutions containing Ni under basic conditions and calcined before impregnating Mo under acid conditions and final calcination, but in which the temperature and atmosphere of the calcination steps were varied in order to optimise further the preparation method. Two series of catalysts were prepared to study

the influence of the calcination conditions in the activity of Ni-Mo/γ-$A\ell_2O_3$ catalysts. In the first, the conditions of the final calcination (after Mo impregnation) were varied, impregnating a Ni/γ-$A\ell_2O_3$ surface already calcined at 673 K under air, and a second, in which the calcination conditions of the Ni/γ-$A\ell_2O_3$ surface were varied, final calcination carried out at 773 K under air (which gave the best results in the first series). Calcinations were carried out for 8 hours at either 673, 773 or 873 K under one of the following atmospheres: air (A), air saturated in H_2O at 298 K (AW) and nitrogen (N).

The catalysts were tested in the atmospheric pressure reaction system to compare their initial thiophene HDS activities under the standard conditions described in 2.4.2, Chapter 2. The values of the apparent kinetic constants at 623 K are given in Table 6.1. Since the surface area of the support is slightly affected by the calcination conditions (Srinivasan et al 1979) the surface area and the values for the kinetic constants are given both per gram and per unit of surface area of the support. It was also established that the surface acidity of the catalyst does not change significantly with the calcination conditions. Within the experimental error, the following generalisation can be drawn concerning the activity of the catalysts in relation to the method of calcination:

(i) higher initial activities are observed when the final calcination is carried out at 773 K under air

(ii) higher initial activities are observed when the first calcination (Ni/γ-$A\ell_2O_3$ surface) is carried out at temperatures above 673 K, the maximum being at 773 K under air saturated in water.

TABLE 6.1

CATALYST ACTIVITIES FOR THIOPHENE HDS AT ATMOSPHERIC PRESSURE

CATALYST (a)	SURFACE AREA $m^2\ g^{-1}$ (b)	APPARENT KINETIC CONSTANTS g-mol (g-cat)$^{-1}$ $hr^{-1} \times 10$	g-mol (m^2-cat^{-1} $hr^{-1} \times 10^3$
Ni 673A - Mo 773A	230	5.1	2.22
Ni 673A - Mo 673A	240	4.7	1.96
Ni 673A - Mo 773AW	210	4.5	2.14
Ni 673A - Mo 773N	225	4.2	1.86
Ni 673A - Mo 873A	203	3.6	1.77
Ni 773AW - Mo 773A	210	5.8	2.76
Ni 773A - Mo 773A	225	5.4	2.41
Ni 873AW - Mo 773A	185	4.8	2.61
Ni 873A - Mo 773A	196	4.9	2.55
Ni 873N - Mo 773A	204	4.7	2.30

(a) A: air; AW: air saturated in H_2O at 298 K;
N: nitrogen.

(b) by nitrogen adsorption.

Comparison of these results with those of the influence of the impregnation conditions (Table 5.2, Chapter 5) shows that an increase of about 14% (65% when compared with the commercial AKZO-153S catalyst) is achieved when the final calcination is carried out at 773 K (catalyst Ni 673A - Mo 773A and Ni 673A - Mo 673A) and a further 40% when the first calcination is carried out at 773 K under air saturated in water (catalyst Ni 773AW - Mo 773A and Ni 673A - Mo 673A). These results are in agreement with those of Laine (1977)

and Mone and Moscou (1975) and show that, for the final calcination (after Mo impregnation), temperatures in excess of 773 K have a detrimental effect on the activity of the catalyst leading to a lower performance.

6.4.2 Catalyst Characterization

The catalysts after the final calcination, were characterized by ESCA, and the results are given in Table 6.2. From Table 6.2 it can be seen that Mo $3d_{5/2}$ and Ni $2p_{3/2}$ binding energies are similar for all the catalysts and that both the Mo/Aℓ and Ni/Aℓ peak area ratios remained essentially constant.

TABLE 6.2

BINDING ENERGIES (eV)[a] AND PEAK AREA RATIOS FROM ESCA

CATALYST	Mo $3d_{5/2}$	Ni $2p_{3/2}$	Mo/Aℓ	Mo/Aℓ
Ni 673A - Mo 773A	233.1	856.1	2.05	1.10
Ni 673A - Mo 673A	233.1	856.0	2.04	1.08
Ni 673A - Mo 773N	232.9	856.0	2.06	1.09
Ni 673A - Mo 773AW	232.9	856.1	2.04	1.12
Ni 673A - Mo 873A	233.0	856.0	2.04	1.08
Ni 773AW - Mo 773A	233.2	855.8	2.02	1.16
Ni 773A - Mo 773A	232.8	856.1	2.05	1.10
Ni 873AW - Mo 773A	232.8	856.1	2.10	1.15
Ni 873A - Mo 773A	232.9	856.0	2.12	1.08
Ni 873N - Mo 773A	232.8	856.1	21.8	1.09

This implies a similar degree of dispersion of the active compounds on the surface of the support. Therefore, the degree of dispersion of both Ni and Mo are determined essentially by the impregnation conditions (under adsorption conditions), in agreement with the results of the impregnation studies (Chapter 5).

Figure 6.4(a-e) shows the u.v. reflectance spectra of the catalysts in which the atmosphere and temperature of the first calcination (after Ni impregnation) was varied. In all catalysts the final calcination was carried out at 773 K under air. Comparison of the spectra of the catalyst characterized in Figure 6.4 (a-e) indicates that the structures of Mo compounds on the surface are essentially similar, but the Mo structures present, in all cases, have a better defined absorption peak at about 320 nm, when compared with samples containing Mo alone calcined at the same conditions, Figure 6.2(b). This suggests that Ni affects the nature of the Mo species formed at the surface, increasing the Mo (octahedra) species at the surface.

Turning to the Ni transitions, from the absorption peak at about 575 - 680 nm, it can be seen that the absorbances increase in the order: 773A < 773AW < 873N ∿ 873A < 873AW, in agreement with the results from the Ni/γ-$A\ell_2O_3$ surfaces (Figure 6.3). However, this pattern does not correspond strictly to the order of activity of the catalysts, Table 6.1, since catalysts calcined at 873 K showed a lower activity than those at 773 K, although this pattern applied when comparing the activities of catalysts Ni 773A - and Ni 773AW - Mo 773A. Thus, the degree of inversion of the Ni $A\ell_2O_4$ spinel does not correlate strictly with the activity of the catalyst, though it appears that spinel formation is a condition for a high activity

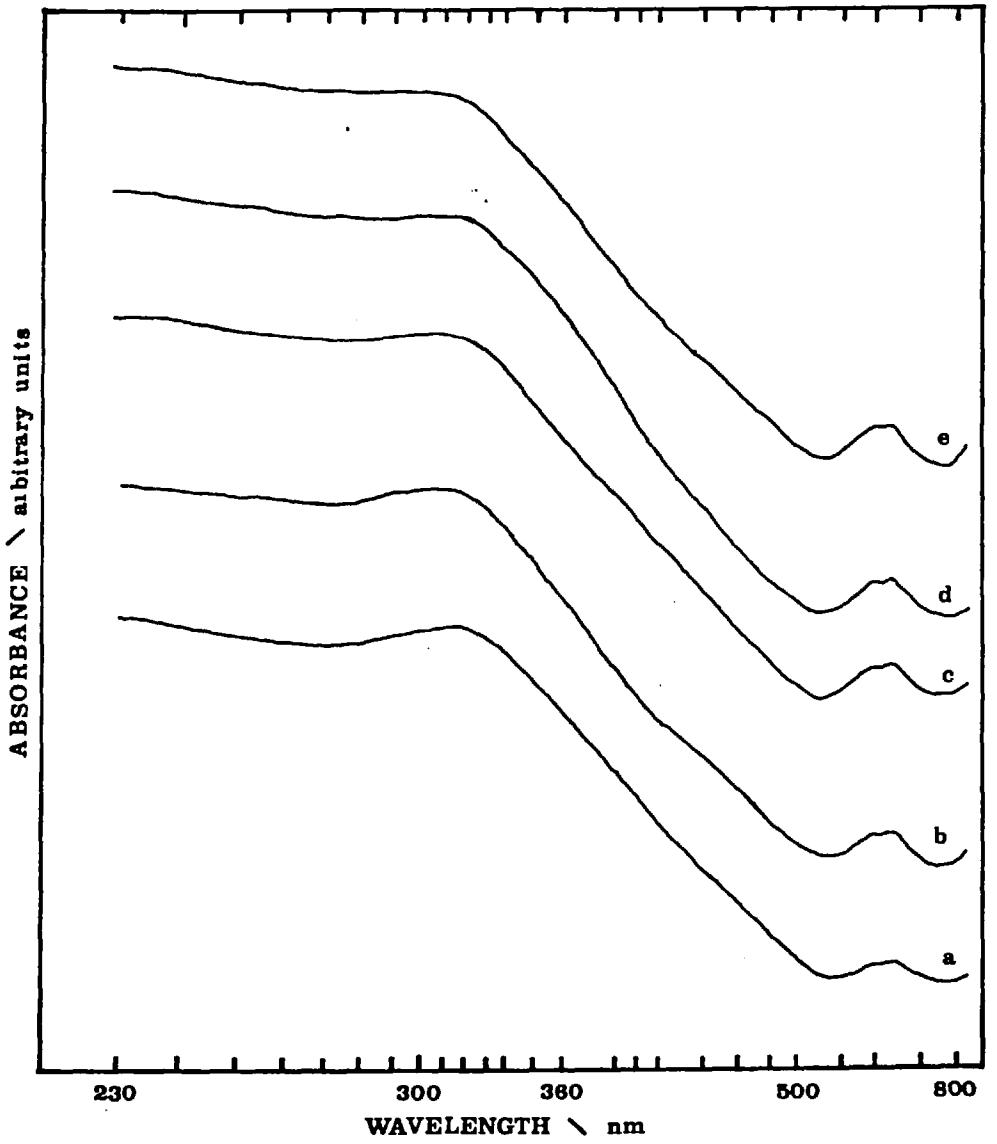

FIGURE 6.4: U.v. reflectance spectra of Ni-Mo/γ-Al_2O_3 catalysts

Final calcination at 773 K under air. Ni/γ-Al_2O_3 calcinations at: (a) 773 K, air; (b) 773 K, air saturated in water; (c) 873 K, nitrogen; (d) 873 K, air; (e) 873 K, air saturated in water.

catalyst.

Figure 6.5(a-e) shows the u.v. reflectance spectra of the catalysts in which the atmosphere and temperature of the final calcination (after Mo impregnation) was varied. In all catalysts, Mo was impregnated on to a $Ni/\gamma-Al_2O_3$ surface calcined at 673 K in air. It is obvious, looking at the spectra of the catalysts that the conditions of the final calcination of the catalyst affects the nature of both the Ni and Mo species at the surface, in agreement with the results when the active components are present separately on the surface. Moreover, the effect of the calcination conditions on the octahedral/tetrahedral Mo(VI) ratio in the structures present at the surface, as indicated by the absorption bands at 300 - 360 and 230 - 270 nm, is similar to that of $Mo/\gamma-Al_2O_3$ and reference to the activity measurements, Table 6.1, indicates that the catalyst in which this ratio is the lowest (Ni 673A - Mo 873A) present the lowest activity, in agreement with the conclusions from the study of the influence of the impregnation conditions (Chapter 5).

Summarizing the findings from the calcination studies, it appears that both the formation of Ni Al_2O_4 spinel and the presence of Mo preferentially on octahedral sites in the Mo structures present on the surface of the alumina are requirements for an active catalyst. Strictly speaking, there is not a direct connection between the degree of inversion of Ni in the Ni Al_2O_4 spinel and the activity of the catalyst, but the presence of Ni in tetrahedral sites is an indication of spinel formation and also good dispersion of the Ni phase.

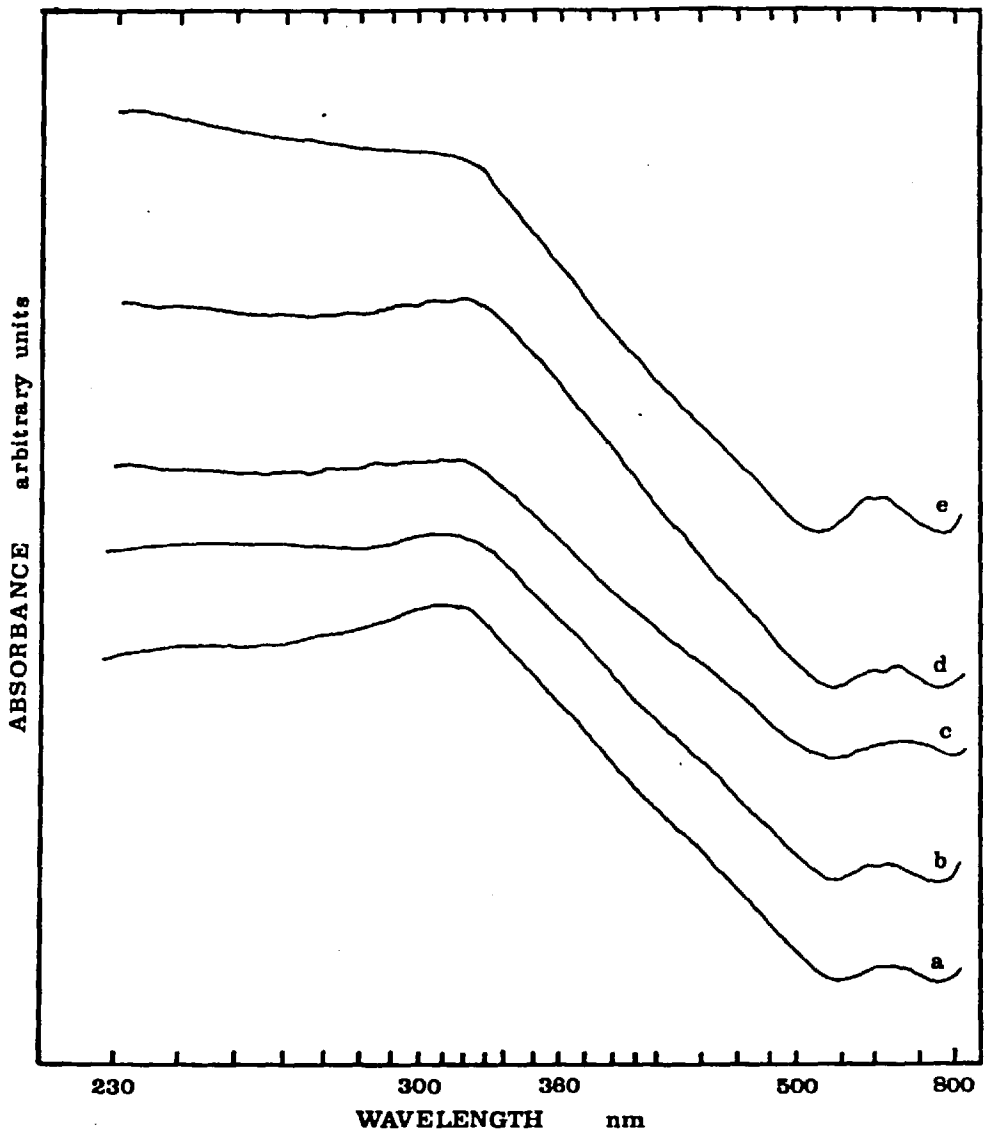

FIGURE 6.5: U.v. reflectance spectra of Ni-Mo/γ-Al_2O_3 catalyst

Ni/γ-Al_2O_3 surface calcined at 673 K, air. Final calcination at: 673 K, air; (b) 773 K, air; (c) 773 K, nitrogen; (d) 773 K, air saturated in water; (e) 873 K, air.

CHAPTER SEVEN: A STUDY OF THE SULPHIDED STATE OF Ni-Mo/γ-$A\ell_2O_3$ CATALYSTS

7.1 INTRODUCTION

In studies of the preparational aspects of the Ni-Mo/γ-$A\ell_2O_3$ catalyst reported in Chapters 5 and 6, the relationships between: (a) the method of preparation and the activity, and (b) the surface structure and the activity have been investigated, but the latter correlation has been established only between the features of the surface in the fully oxidic state, namely after the impregnation, drying and calcination stages in the manufacture of the catalyst. Under reaction conditions, or during pre-sulphiding, conversion of the Ni and Mo oxidic species present on the catalyst surface to sulphur compounds occur, and the latter constitutes the active form of the catalyst in the reactor. In this Chapter, a study of the sulphided state of selected catalysts (which showed different features in the oxidic state) is presented, and an attempt has been made to relate the characteristics of the sulphided state to the method of preparation and to the activity of the catalysts, largely by thermogravimetric and ESCA analysis.

7.2 EXTENT OF SULPHIDATION

The most direct indication of the nature of the sulphided species on the surface is given by the extent of sulphidation of the oxidic Ni and Mo precursors. A series of catalysts selected from those which showed different features in the oxidic state were sulphided in the microbalance reactor under the conditions described in 2.3.4, Chapter 2, i.e. under a flow of 188.2 $cm^3\ min^{-1}$ (STP) of a 10%v H_2S/H_2 mixture at 573K and at a pressure of 9.58 KPa.

Sulphiding of the oxidic catalyst always resulted in a net weight gain, due primarily to the difference between the S added and the O removed from the surface, and was carried out until no change in weight gain was observed (about 4 hours). More than 95% of the observed weight gain occurred during the first 40 minutes of the run, in agreement with the results of Massoth (1975). A complicating factor in these experiments is the fact that both H_2S and H_2O (formed during the sulphidation of the oxidic species) are also adsorbed on the surface. In order to eliminate the adsorbed H_2S and/or H_2O partially from the surface, the catalysts were purged for one hour with N_2 (after the sulphidation period) at the same temperature as the run, after which weight loss of about 2% was observed. The amount desorbed increased to about 20%w when the temperature of the purge treatment was increased to 773 K, suggesting that the amount of H_2S and/or H_2O adsorbed is significant. The amount desorbed could be expected to be similar for each catalyst after the purge treatment and since these experiments were designed to determine the differences in the extent of sulphidation in relation to the surface structure and the activity of the catalysts, no attempt was made to quantify exactly this amount. The results of thermogravimetric study, together with the catalytic activity of the catalysts (for thiophene HDS at 623 K and pre-sulphided under the same conditions as in the microbalance reactor) are given in Table 7.1.

In order to compare the extent of sulphidation of the various catalysts, it is convenient to define a parameter β for each catalyst as the ratio of the weight gain to the amount that would be observed if the Ni and Mo species (assuming they are present as NiO and MoO_3

TABLE 7.1

EXTENT OF SULPHIDATION (β)[a]

IN 10%v H_2S/H_2 MIXTURE AT 573 K

CATALYST[b]	Weight gain after 1 hr N_2 purge mg (g-cat)$^{-1}$	β[a]	Catalyst activity for thiophene HDS at 623 K g-mol (m^2-cat)$^{-1}$ hr^{-1} $\times 10^3$
Ni 773AW - Mo 773A	35.66	1.40	2.76
Ni 873AW - Mo 773A	36.11	1.42	2.61
Ni(B) - Mo(A)	34.18	1.35	2.25
Ni(A) - Mo(A)	32.90	1.30	2.04
Ni(B) - Mo(B)	24.76	0.97	1.82
Ni 673A - Mo 873A	25.15	0.99	1.77
Mo(A) - Ni(B)	22.76	0.90	1.68
Mo(A) - Ni(A)	23.76	0.94	1.54
Mo(B) - Ni(A)	20.71	0.82	1.53
AKZO-153S[c]	19.18	0.83	1.52

(a) defined as: $\beta = \dfrac{\text{weight gain}}{\Delta\ (MoO_3 + NiO \rightarrow MoS_2 + NiS)_{surface}}$

(b) 15%w MoO_3 and 4%w NiO

(c) 15%w MoO_3 and 3%w NiO

respectively) are completely sulphided to NiS and MoS_2, i.e.:

$$\beta = \frac{\text{weight gain}}{\Delta(MoO_3 + NiO \rightarrow MoS_2 + NiS)_{surface}}$$

Comparison of the extent of sulphidation with the activity of the catalysts (pre-sulphided) for thiophene HDS, Table 7.1, indicates that there is a good correlation between β and the activity of the catalysts, in agreement with the reults of de Beer et al (1976). Although it is not possible to establish an exact quantification of the stoichiometry of the sulphidation from these experiments (due to the interference of the adsorbed H_2S and/or H_2O), the high activity catalysts are clearly sulphided to a much greater extent, and the fact that the values of β are larger than 1.0 would indicate that, since the amount of adsorbed H_2S and H_2O is about 20 - 40%, they must be heavily sulphided. In fact, as indicated in the previous Chapter, the high activity catalysts are characterized by the presence of Mo in structures similar to that of Mo_8O_{23}, Mo_4O_{11}, etc., and these have a O/Mo ratio below that of MoO_3 (O/Mo = 3) and, therefore, the measured value of β as defined should be less than 1.0, neglecting the contribution of adsorbed H_2S or H_2O which would make the actual value somewhat greater than 1.0. Catalysts in which Mo is preferentially in tetrahedral sites and a lower degree of dispersion on the surface in the oxidic state are clearly sulphided to a much lesser extent (see, for example, catalyst Mo(B) - Ni(A), Table 7.1), well as catalysts in which a strong interaction between Mo and the support occurs (Ni 673A - Mo 873A). The influence of the structure of the oxidic state on the formation of the sulphided state will be discussed in more detail later.

7.3 ESCA CHARACTERIZATION OF THE SULPHIDED STATE OF THE CATALYSTS

In order to characterize further the surface of the sulphided state of the catalyst, similar series of catalysts were studied by ESCA. The catalysts were sulphided in the atmospheric pressure reactor described in 2.3, Chapter 2, for one hour at 573 K with a flow of 465.8 cm^3 min^{-1} (STP) of a 10%v H_2S/H_2 mixture, and then cooled to room temperature while still passing the sulphiding mixture, and kept in a sealed bottle before the analysis. The ESCA spectra for Mo_{3d} - S_{2s}, S_{2p} and $Ni_{2p^{3}/2}$ are shown in Figures 7.1, 7.2 and 7.3 respectively, and measured peak area ratios are given in Table 7.2 Peak area ratios from the ESCA spectra of the oxidic state of the same catalysts/samples as well as their activity for thiophene HDS at atmospheric pressure have been also indicated in Table 7.2 for comparison.

7.3.1 Molybdenum 3d Spectra

Figure 7.1 (a-g) shows the ESCA spectra in the region of binding energies (B.E.) from 220 - 240 eV (referred to C_{1S} = 284.3 or Al_{2p} = 74.5 eV), which is the region in which Mo_{3d} and S_{2s} signals appear. Typical values of 228.9 eV for Mo(IV), 231.0 eV for Mo(V) and 232.5 eV for Mo(VI) as well as 225.6 eV for S_{2s} (Stevens and Edmonds, 1975; 1978, Okamoto et al 1977; 1979, Gajardo 1978) have been indicated by vertical lines on the B.E. axis.

The catalyst spectra indicate the presence of two Mo species on the surface, namely Mo(IV) and Mo(VI), although the presence of traces of Mo(V) cannot be discounted, suggesting that Mo is not completely sulphided on the surface of the analysed samples. Since sulphided Ni(Co) - Mo surfaces can be partially re-oxidised

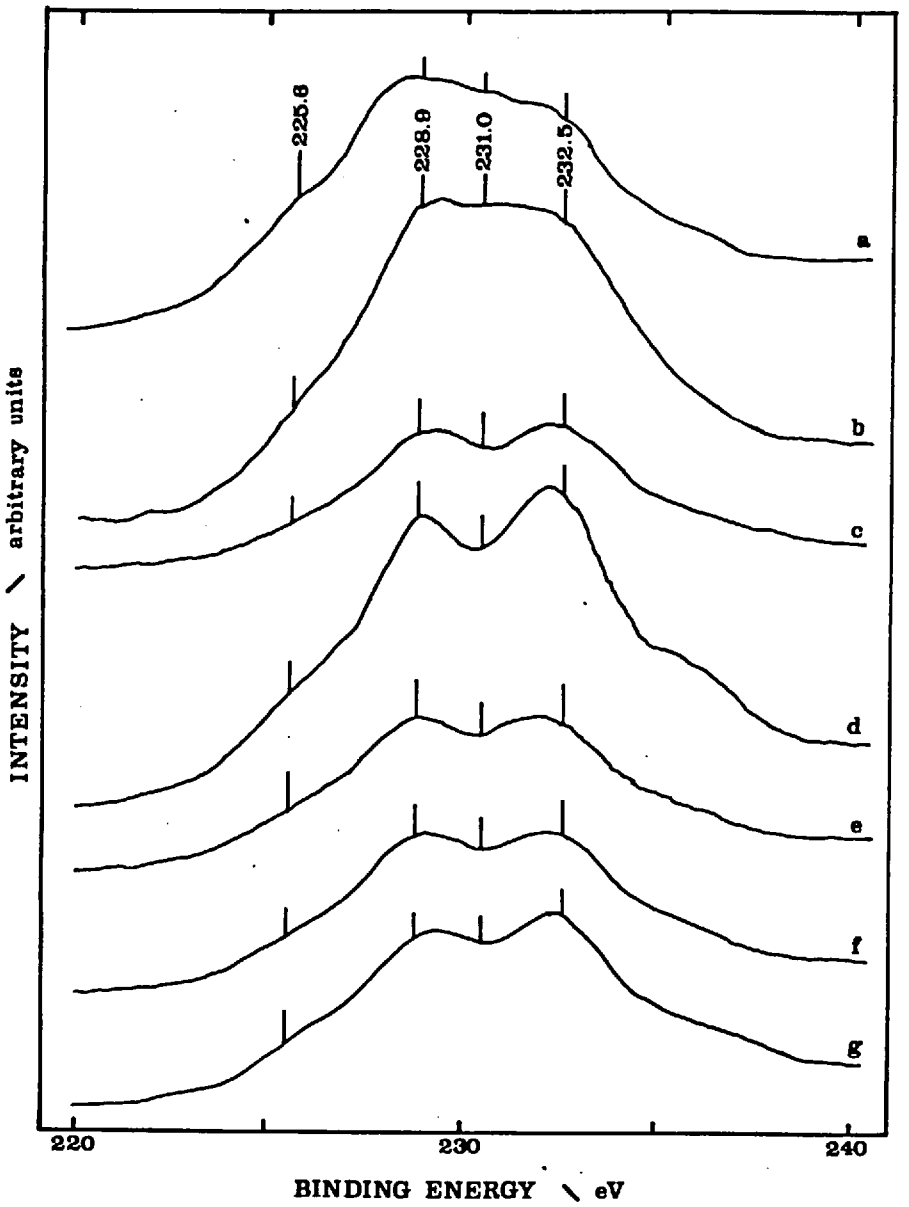

FIGURE 7.1. Mo(3d) ESCA SPECTRA OF CATALYSTS

(a) Ni 773AW - Mo 773A; (b) Ni 873A - Mo 773A;
(c) Ni(A) - Mo(B); (d) Ni 673A - Mo 873A;
(e) Mo(A) - Ni(B); (f) Mo(B) - Ni(A);
(g) Mo(A) (15%w MoO_3).

Typical literature values for S_{2s}, Mo(IV), Mo(V) and Mo(VI) have been indicated.

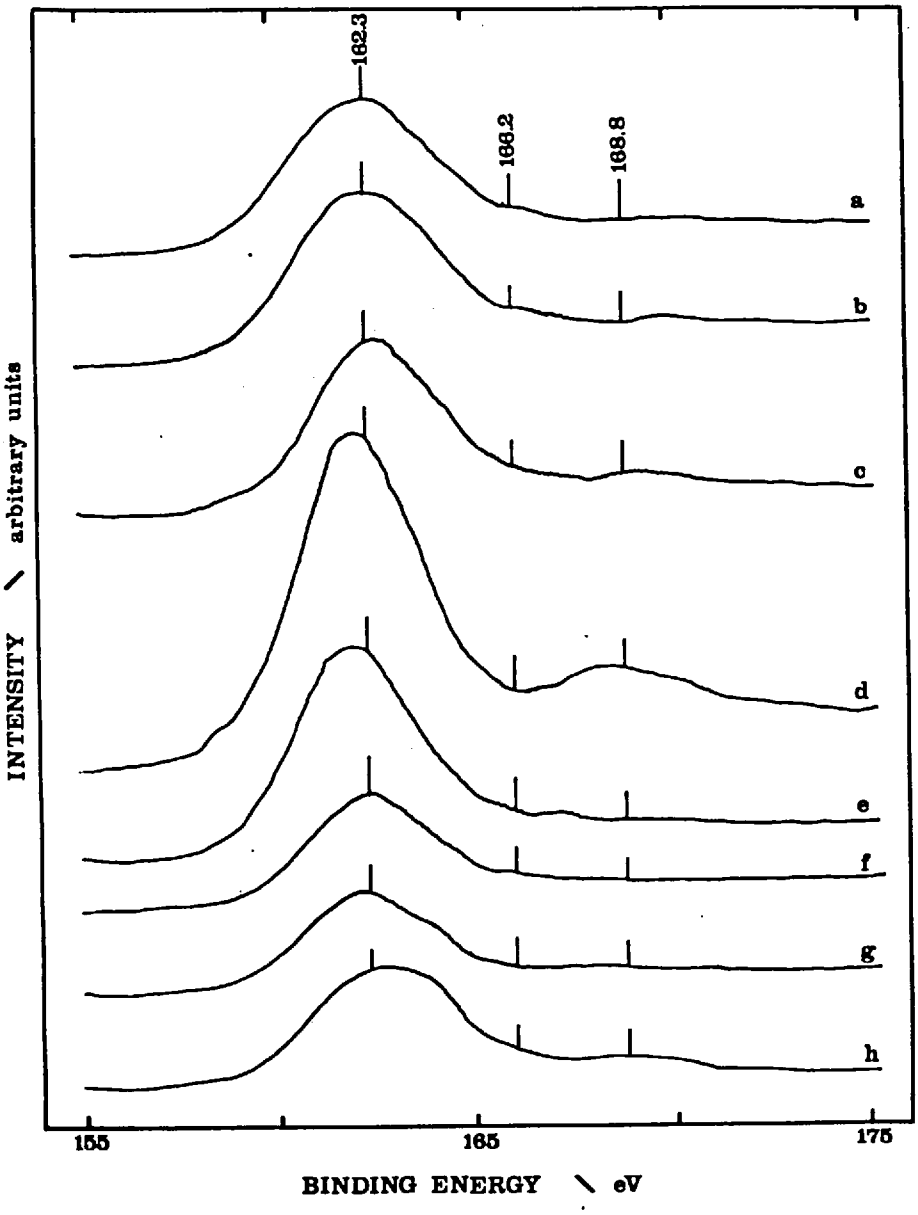

FIGURE 7.2. S(2p) ESCA SPECTRA OF CATALYSTS

(a) Ni 773AW - Mo 773A; (b) Ni 873A - Mo 773A;
(c) Ni(A) - Mo(B); (d) Ni 673A - Mo 873A;
(e) Mo(A) - Ni(B); (f) Mo(B) - Ni(A);
(g) Mo(A) (15%w MoO_3); (h) Ni(B) 773A (4% NiO)

Typical literature values for S_{2p} in metal sulphides, S-H and S-O groups have been indicated.

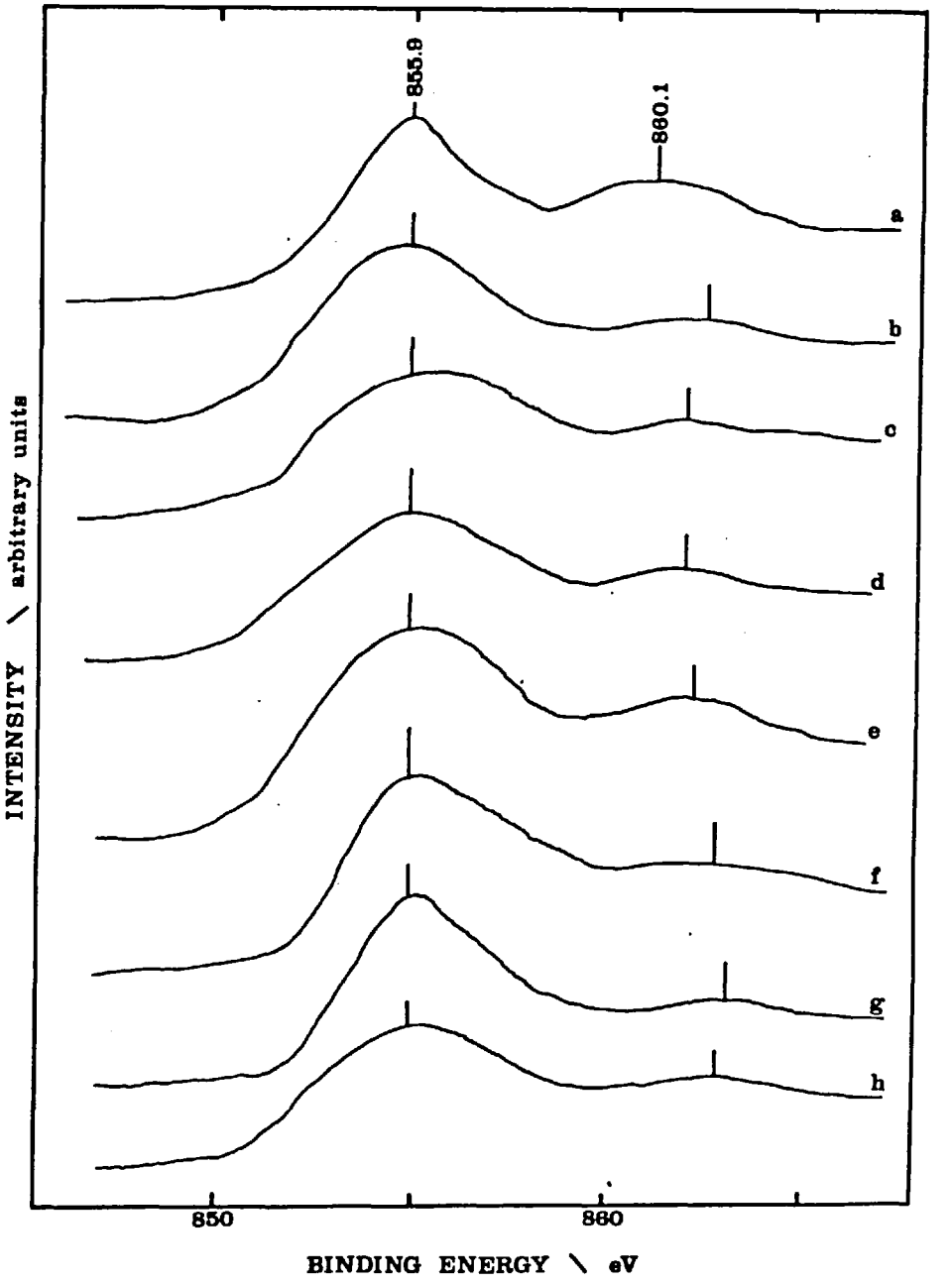

FIGURE 7.3. Ni(2p) ESCA SPECTRA OF CATALYSTS

(a) Ni 773AW - Mo 773A (oxidic state);
(b) Ni 773AW - Mo 773A (sulph. state);
(c) Ni 873A - Mo 773A; (d) Ni(A) - Mo(B);
(e) Ni 673A - Mo 873A; (f) Mo(A) - Ni(B);
(g) Mo(B) - Ni(A); (h) Ni(B) (4% NiO)

even at room temperature (de Beer et al 1976b), it is uncertain whether the presence of Mo(VI) species arises from the oxidation during the transfer of the sample to the spectrometer or whether they are actually present on the surface of the catalysts under reaction conditions. However, this partial re-oxidation phenomenon could not explain the big difference in the observed Mo(IV)/Mo(VI) ratios, Figure 7.1 (a-b). In fact, the most active catalysts, Figure 7.1 (a)(b), are clearly characterized by the presence of Mo preferentially in the lower oxidation state and the ratio Mo(IV)/Mo(VI) decreases as the activity of the catalysts decreases. Therefore, since the extent of sulphidation for the low active catalyst (β) measured in the microbalance reactor was below 1.0, this indicates that there are Mo(VI) oxidic species present on the surface of the low activity catalyst under reaction conditions. Since Mo(IV) must be present in sulphur surroundings such as MoS_2 or MoS_3 (Stevens and Edmonds 1975), these results indicate that the extent of sulphidation varies from catalyst to catalyst, in agreement with the results of the gravimetric studies presented in the previous sections. Moreover, they show the dependence of the extent of sulphidation on the preparation procedure of the catalyst, as will be discussed later.

7.3.2 Sulphur 2p Spectra

Figure 7.2 (a-h) shows the ESCA spectra in the region of B.E. 155 - 175 eV, where the signals of S_{2p} appear. Clearly, the signals of two different sulphur species can be seen, at 162.3 eV for metal sulphides (Stevens and Edmonds 1975) and 168.8 eV for sulphate groups (Chadwick and Hashemi 1979) although the presence of S-H groups (166.2 eV) cannot be completely ruled out. The presence of S-O groups is a confirmation that partial re-oxidation of the samples took place to some extent during the transfer of the sample from

the reactor to the chamber of the ESCA spectrometer. Sulphidation of samples containing only Ni or Mo also occurred, Figure 7.2(g)(h) and, since γ-Al_2O_3 does not sulphide (Gajardo 1978), this is a confirmation that Ni is sulphided on the surface.

7.3.3 Nickel 2p Spectra

Figure 7.3 (a-h) shows the ESCA spectra of the catalysts in the region of B.E. 840 - 860 eV which contains the Ni 2p signals. Comparison of the peak shapes of the spectra of the fully oxidic catalyst Ni 773AW - Mo 773A, Figure 7.3(a), with the corresponding sulphided catalyst, Figure 7.3(b), shows that in the latter case the peaks are broaded and the position of the Ni_{2p} "shake-up" satellite is 1.3 eV higher B.E. than that of the fully oxidic sample (Novakov and Prims 1972). The first effect would arise if differential charging of the surface is significant, but since this effect is not correlated in the Mo spectra of the same samples, this must be an indication of the coexistence of various Ni species in the surface. However, it is very difficult to establish the precise nature of this species, since the B.E. of $Ni_{2p\,3/2}$ is very insensitive to the surroundings of Ni (Gimzewski et al 1978).

7.3.4 Peak Area Ratios

The values of the peak area ratios of the Mo and Ni species on the surface in both the fully oxidic and sulphided states of the catalysts are given in Table 7.2. The most striking difference between the values of the oxidic and sulphided state is the fact that an increase in both Mo/Al and Ni/Al ratios is observed on sulphidation. This situation implies that either there is: (a) an increase

TABLE 7.2

PEAK AREA RATIOS FROM ESCA OF CATALYSTS IN OXIDIC AND SULPHIDED STATE

CATALYST	OXIDIC STATE			SULPHIDED STATE					Catalyst activity for thiophene HDS
	Mo_{3d}/Al_{2p}	$Ni_{2p^{3}/2}/Al_{2p}$	$Ni_{2p^{3}/2}/Mo_{3d}$	Mo_{3d}/Al_{2p}	$Ni_{2p^{3}/2}/Al_{2p}$	S_{2p}/Al_{2p}	$Ni_{2p^{3}/2}/Mo_{3d}$	$\frac{S_{2p}}{Ni_{2p}+Mo_{3d}}$	g-mol $(m^2\text{-cat})^{-1} \times hr^{-1} \times 10^3$
Ni(B)	-	1.00	-	-	1.10	0.16	-	1.07	-
Mo(A)	2.60	-	-	2.80	-	0.72	-	1.77	-
Ni 773AW - Mo 773A	2.02	1.16	0.57	3.21	1.51	1.27	0.47	1.88	2.76
Ni 873AW - Mo 773A	2.12	1.08	0.51	3.40	1.55	1.29	0.46	1.83	2.55
Ni(A) - Mo(B)	1.92	0.71	0.37	2.40	0.84	0.74	0.35	1.60	2.04
Ni 673A - Mo 873A	2.04	1.08	0.53	2.64	1.49	0.91	0.55	1.55	1.77
Mo(A) - Ni(B)	1.99	1.05	0.53	2.70	1.31	0.81	0.49	1.42	1.68
Mo(B) -Ni(A)	1.73	0.79	0.46	2.72	0.91	0.69	0.33	1.33	1.53
AKZO-153S	1.47	0.62	0.42	2.54	0.97	0.64	0.38	1.28	1.52

in the degree of dispersion of Ni and Mo on the surface, or (b) a migration of Ni and Mo to the outer surface of the catalyst particle since it is the external surface of the catalyst which is analysed by ESCA, or (c) a decrease in the $A\ell_{2p}$ signal by an expansion of the Ni/Mo phases at the surface. All these situations may simultaneously occur on the surface and it is interesting to compare also the Ni/Mo ratios in the oxidic and sulphided state.

The first situation (a) is unlikely to occur to any significant extent, at least in catalysts in which Mo was impregnated under acid conditions, since Mo is present already as a monolayer, or in small crystallites highly dispersed on the surface (see Chapter 5), and it is difficult to imagine that it can be further dispersed. Moreover, since MoS_2 is a layer structure (Brown et al 1977) in which the layers are bound only by van der Waal's forces, one would expect the dispersion of Mo to remain unchanged on sulphidation. The fact that both Ni/Aℓ and Mo/Aℓ in samples containing these compounds separately remain essentially constant (within the experimental error) indicates that the degree of dispersion of both Ni and Mo in both states of the surface, i.e. fully oxidic and sulphided, remains largely unchanged.

The migration of Ni and or Mo to the outer surface of the catalyst particle is a possibility. This has been observed by Okamoto et al (1977) on $Mo/\gamma\text{-}A\ell_2O_3$ catalysts in experiments in which the catalyst was sulphided in situ in a ESCA spectrophotometer under H_2S at 673 K and at 1.33 KPa, although this phenomenon was less significant when Co was also present on the surface. As was also suggested by these workers, this phenomenon would be greatly increased as the sulphiding pressure is increased. However, the nature of the interaction

between Ni and Mo with the support should be important in this case; the stronger the interaction (as in the case of the formation of $NiAl_2O_4$ spinel and $MoAl_2O_4$), the less likely this phenomenon is to occur. Comparison of the Ni/Mo ratio in the two states of the catalyst indicates that the ratio Ni/Mo for the catalyst Ni 673A - Ni 873A (strong interaction) remained constant when sulphiding, whereas for the most active catalyst (Ni 773AW - Mo 773A), the ratio varied from 0.57 to 0.46, suggesting that the net amount of Mo may have increased at the outer surface of the particle. This is consistent with the fact that the oxidic state is characterized by the presence of the $NiAl_2O_4$ spinel with Mo largely in octahedral surroundings, which must be relatively weakly bound to the surface.

The expansion of the outer surface would imply the diffusion of Ni from the spinel back to the surface. Evidence for the diffusion of Co(II) from bulk to the surface has been given (de Beer et al 1976b), and this is consistent with the present results, since $Ni/\gamma-Al_2O_3$ surfaces are found to be sulphided. Also, since ESCA signals come from the first 1 - 2 nm of the surface only (Carlson 1975), some decrease of the Al_{2p} signal is to be expected as the surface species are sulphided since they are thicker than the oxidic structures.

In order to gain some information concerning the stoichiometry of the sulphided surfaces, the ratio of S_{2p} to $Ni_{2p} + Mo_{3d}$ were calculated employing the values for the relative atomic sensitivity of the elements given by Wagner (1972). The sensitivity by peak area, referred to $F_{1S} = 1.00$, was: $Ni_{2p} = 3.68$, $Mo_{3d} = 2.04$ and $S_{2p} = 0.33$. Of course, the values calculated for the S/Ni + Mo ratios are only a rough approximation since they were derived assuming a total homogeneity of the surface. It can be seen that

there is a good agreement between the extent of sulphidation ($S_{2p}/Ni_{2p} + Mo_{3d}$ and β) and the activity of the catalyst, as shown in Figure 7.4(a)(b) consistent with the results of the gravimetric studies. Samples containing only Mo or only Ni showed an almost complete sulphidation to MoS_2 and NiS, and the fact that in the latter the observed value is larger than one indicates that Ni may be present in structures such as Ni_3S_4, although no definitive conclusion can be drawn as to the precise nature of the sulphided Ni species present from the ESCA data alone.

Assuming that the requirements for a good catalyst are the complete sulphidation of Ni and Mo on the surface to MoS_2 and Ni_3S_4, the final S/Ni + Mo ratio (for a loading of 15% MoO_3 and 4% NiO) should be 1.84. As observed in the thermogravimetric studies, catalyst Ni 773AW - Mo 773A (the most active one) showed the highest extent of sulphidation, and the S/Ni + Mo ratio calculated from the ESCA spectra is 1.88, which indicates that this may be the case. Therefore, the catalytic activity of Ni-Mo/γ-$A\ell_2O_3$ catalysts must be related to the formation of Ni and Mo sulphides on the surface.

Summarizing the findings from these studies of the sulphided state of the catalyst, the following features of the surface are required by an active catalyst:

(i) Mo must be completely sulphided on the surface

(ii) Ni must be also completely sulphided

(iii) a high dispersion of both Ni and Mo sulphides on the support,

and these conclusions are in agreement with the proposals of Stevens and Edmonds (1978).

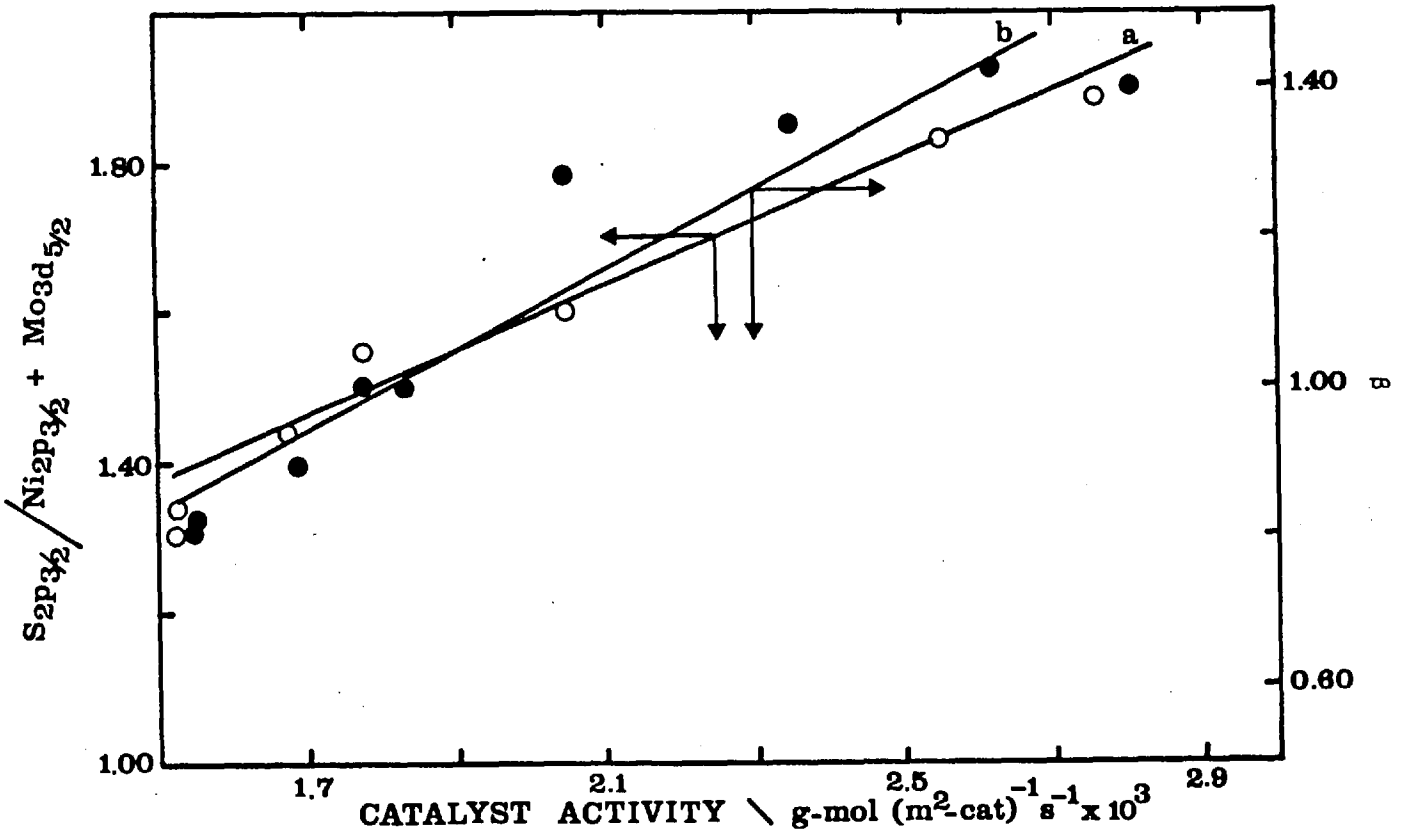

FIGURE 7.4. RELATIONSHIP BETWEEN DEGREE OF SULPHIDATION AND CATALYST ACTIVITY

(a) $S_{2p^3/2}/Ni_{2p^3/2} + Mo_{3d^5/2}$. from ESCA spectra

(b) Extent of sulphidation (β)

7.4 THE STRUCTURE OF SULPHIDED Ni-Mo/γ-Al_2O_3 CATALYST AND CORRELATION BETWEEN STRUCTURE AND CATALYTIC PROPERTIES

From a catalytic point of view, Ni-Mo/γ-Al_2O_3 catalysts are very complex systems, and several models for the active surface have been proposed (1.4, Chapter 1). When employed in coal hydrogenation processes they are able to promote hydrogenation, hydrocracking and hydrogenolysis reactions of S, N and O containing compounds, but the nature of the active site(s) remains largely unsolved. In addition, as shown in 4.4, Chapter 4, the support also plays an important role in the catalytic activity of Ni-Mo supported catalysts. Table 7.3 shows the results of activity tests of catalysts containing Ni, Mo and Mi-Mo on γ-Al_2O_3 carried out in the trickle-bed high pressure reactor, employing the model feedstock containing dibutylsulphide, quinoline, dibenzofuran and phenanthrene at the standard conditions (623 K, 6.89 MPa and WHSV = 2). Comparison of the results from catalysts containing Ni (4%w as NiO) or Mo (15%w as MoO_3) with the one containing Ni and Mo clearly illustrates the "synergetic" effect of Ni on the activity of the Mo compounds on the surface. In fact, although

TABLE 7.3

CATALYST ACTIVITIES FOR

HDN, HDO, HDS AND HYDROGENATION REACTIONS

CATALYST	Apparent kinetic constants g-mol $(g\text{-cat})^{-1}$ hr^{-1}				
	HDS	HDO	HDN	hydrogen.	hydrocrack.
Ni(B) (4%w NiO)	3.79	0	0	0.35	< 0.01
Mo(A) (15%w MoO_3)	6.64	.10	0.27	2.64	< 0.05
Ni(B) - Mo(A)	-	.46	1.64	4.05	0.88

$Ni/\gamma\text{-}Al_2O_3$ showed some catalytic activity for dibutylsulphide HDS and phenanthrene hydrogenation, this is very small in comparison with $Ni\text{-}Mo/\gamma\text{-}Al_2O_3$ catalysts. The fact that $Mo/\gamma\text{-}Al_2O_3$ catalysts are able to catalyse all the reaction considered suggests that the main sites must be associated with the presence of Mo on the surface. $\gamma\text{-}Al_2O_3$ by itself did not show any significant activity under the conditions of the test.

The promotional effect of Ni on the hydrogenolysis capability is much larger than on the hydrogenation function of the catalyst, Table 7.3, suggesting that there must be at least two kinds of active sites on the surface, one for hydrogenolysis and one for hydrogenation reactions, in agreement with the proposed models of the surface of $Co\text{-}Mo/\gamma\text{-}Al_2O_3$ catalysts (Massoth 1977, Stevens and Edmonds 1978, Hargreaves and Ross 1979). In the case of HDS, as indicated in Chapter 3, ring hydrogenation is not a pre-requisite to C-S bond scission and sulphur removal, whereas HDN, HDO and hydrocracking reactions do require a hydrogenation step prior to their occurrence. Therefore it is uncertain whether the same kind of site is involved in HDS, HDO and HDN reactions. In principle, S, O and N containing molecules may adsorb in the same kind of sites (since all have unpaired electrons in the heteroatom) but, since N containing molecules (strong bases) are known to be poisons for sulphided Ni(Co)-Mo catalysts (Cowley and Massoth 1978), the presence of more than one kind of hydrogenolysis site must be considered a strong possibility. As proposed by Satterfield *et al* (1975), one type of hydrogenolysis site may be very active for HDS but very sensitive to nitrogen bases and a second type, less active for HDS but less susceptible to poisoning, may be responsible for HDN and HDO in addition to HDS. The first type may allow the adsorption edge-on of the

S. N and O containing compound (N molecules being poisons of the sites and presumably O molecules) and a second allowing a two-point adsorption involving the π-electrons of the aromatic ring and the unpaired electrons of the heteroatoms. Once N and O containing molecules are adsorbed, hydrogenation of the ring should precede the C-N and C-O bond breaking (since this step decreases the energy of the heteroatom-carbon bond). It is unclear whether this second type of hydrogenolysis site is in fact a hydrogenation site nor is it clear whether C-N breaking occurs in the same site since intermediates (such as tetrahydroquinoline, o-propylaniline, etc.) Chapter 3, are observed among the products of HDN.

The surface of the catalyst under reaction conditions contains anion vacancies due to the reaction of sulphur ions from the surface with hydrogen atoms from the gas phase, and they are thought to form the active sites (Voorhoeve and Stuiver 1971, Schuit and Gates 1973, Massoth 1977). In the case of hydrogenolysis sites, the edge-on adsorption sites may be formed by single vacancies. If two-point adsorption sites exist they may be formed by adjacent vacancies or defects (Kilanowski et al 1978). As proposed by Stevens and Edmonds (1978), hydrogenation sites may also be formed on the edges of the MoS_2 crystallites on the surface, hydrogenolysis sites being located on the exposed basal planes of these structures. However, no definite conclusion can be drawn about the exact geometry of the active sites, and more work is needed in this field.

If anionic vacancies are responsible for the formation of the active sites, the presence of Ni(Co) must enhance the number of vacancies on the Mo sulphided phase. As shown in Chapter 6, the nature of the oxidic state of the surface depends strongly on the method of preparation and the results of the studies of the sulphided state of the

catalysts showed that there is a correlation between the characteristics of the two states and the activity of the catalyst. A model of the formation of the sulphided state from the various types of oxidic surfaces is represented in Figure 7.5(a-d).

Figure 7.5(a) represents a model of the surface of the high activity catalyst (catalyst Ni 773AW- Mo 773A), i.e. when Mo is adsorbed on a previously calcined Ni/γ-Al_2O_3 surface (impregnated under basic conditions) and calcined at temperatures such as to allow the formation of a Ni Al_2O_4 spinel and Mo octahedral structures on top of the surface. On sulphidation, Ni diffuses back to the surface, and as Mo species are heavily sulphided (if not all), leading to highly dispersed Ni and Mo sulphided phases with a high degree of contact between them. If the temperature of the calcination of the Mo species is high (catalyst Ni 673A - Mo 873A) a strong interaction, probably via the formation of Al_2MoO_4 surface compounds, Chapter 6, occurs and in this case, Figure 7.5(b), the extent of sulphidation is lower. If Mo is impregnated under basic conditions, Mo (tetrahedral) species are deposited on the surface with a low degree of dispersion (Chapter 5), and if the temperature of the calcination steps is low (catalyst Mo(B) - Ni(B)), there is a mixture of $NiAl_2O_4$ and NiO on the surface. On sulphiding, Figure 7.5(c), the Mo species are partially sulphided (either by the formation of MoO_xS_y compounds or by a sulphidation of the outer layers of the Mo (tetrahedra) oxidic species), leading to a low degree of sulphidation and a low degree of contact area between the sulphided species. The latter may also occur if either Ni is impregnated under acid conditions or calcined at low temperature (catalyst Ni(B) - Mo(A) or Ni(A) - Mo(A)), Figure 7.4(d), in which case the spreading of NiS species on the surface is low.

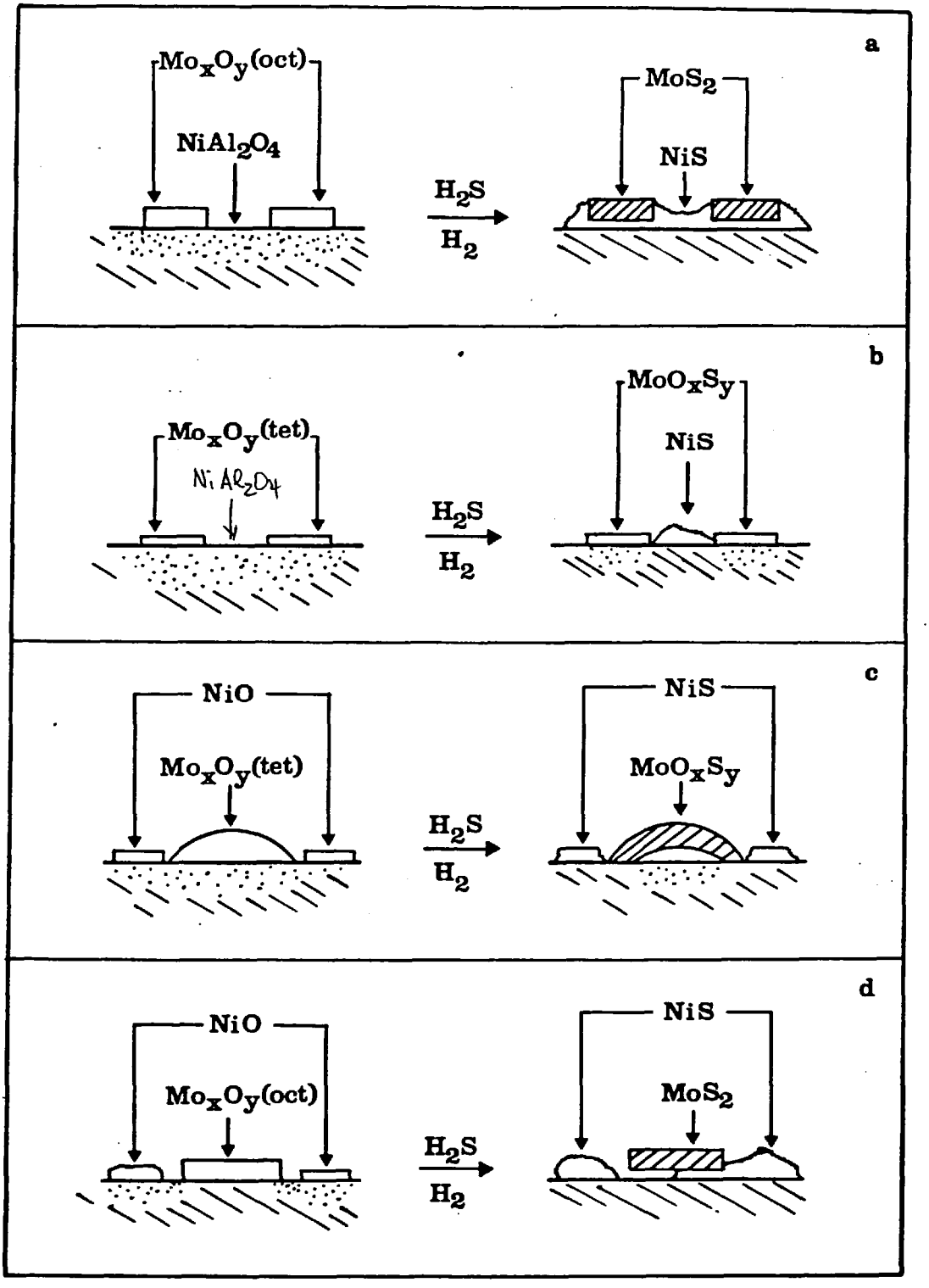

FIGURE 7.5, MODELS OF THE SURFACE OF Ni-Mo/γ-Al_2O_3 IN OXIDIC AND SULPHIDED STATE

Returning to the problem of the nature of the interaction between the Ni and Mo sulphides on the surface and the formation of the active sites, it is clear from the models presented before that the situation is very complex. The monolayer model (Schuit and Gates 1973) gives a good description of the surface of Ni-Mo/γAl_2O_3 catalyst in the oxidic state, i.e. the formation of a Ni Al_2O_4 spinel and the formation on top of the surface of a monolayer or at least highly dispersed Mo structures on the surface (covering about 60% of the surface, Chapter 5), with the exception that it pictures a strong interaction between Mo and the support. According to these authors, on sulphidation only the outmost O atoms on the Mo structures exchange with S atoms, to such an extent that the S/Mo ratio is 1.0. The present results show that the high activity catalysts are characterized by a S/Mo close to 2.0, and in fact, the extent of sulphidation depends on the conditions of the impregnation and calcination, which determines the interaction between Mo and the support. Perhaps the most striking difference between this model and the present findings is that it assumed that Ni(Co) is not present at the surface of the catalyst, and therefore does not sulphide. Evidence against this has been presented in this research and by many other workers (Voorhoeve 1971, de Beer et al 1976, van der Aalst and de Beer 1977, Gajardo 1978) and, therefore, this model can only give a partial explanation of the state of the surface, and it might apply only in the cases of the low active catalysts, such as those represented in Figure 7.5(b).

Since the activity of the catalyst correlates well the extent of sulphidation, the interaction between the Ni and Mo sulphided phases must be responsible for the enhancement of the catalytic activity. As discussed earlier, hydrogenolysis reactions (HDN, HDO) primarily involves the flat adsorption of molecules on the surface,

Therefore, these reactions should be favoured if MoS_2 is present on the surface with a maximum of basal plane area exposed, as suggested by Stevens and Edmonds (1978). Since the role of the promoter must be related to an increase in the amount of anionic vacancies, this may occur at the interface of NiS and MoS_2 phases on the surface or by an interaction between Ni and Mo over the whole surface of the MoS_2 monolayer, in which case MoS_2 must be on top of the NiS phase. These situations may coexist over the whole surface of the catalyst and therefore, the synergetic effect may occur by intercalation of Ni on the edges of MoS_2 (Farrager and Cosse 1971) in the former case and by contact between the NiS and MoS_2 phases in the latter (Hagenbach et al 1971).

Undoubtedly, more work is needed to determine the exact nature of the interaction between Ni and Mo sulphide species on the surface. The proposed models of the surface present a good explanation of the experimental results, and clearly illustrate the dependence between the surface structures present in the active state of the catalyst and the method of preparation.

CHAPTER EIGHT: CONCLUSIONS

This study was undertaken in order to elucidate the most important factors which affect the performance of Ni-Mo/γ-Al_2O_3 coal hydrogenation catalysts. The main conclusions which can be drawn from the present work can be summarized as follows.

1.- Hydroprocessing Reactions:

i) Under commercial conditions of operation (6.89 MPa), the relative ease of processing the various components of the model feedstock decreases in the sequence: dibutylsulphide HDS > dibenzothiophene HDS > phenanthrene hydrogenation > quinoline HDN > phenanthrene hydrocracking > dibenzofuran HDO.

ii) In the case of HDS, butane and diphenyl were the main products from dibutylsulphide and dibenzothiophene HDS. Sulphur was removed without need for ring saturation and, therefore, is a relatively straight-forward reaction.

iii) In the case of quinoline HDN, propylcyclohexane (at 673 K) and propylbenzene (at 753 K) were the main denitrogenized products. At 673 K, quinoline (Q) is rapidly converted, via tetrahydroquinoline (THQ), to o-propylaniline (OPA), whereas at 753 K, there is an equilibrium between Q and THQ and the conversion of THQ to OPA is relatively slower compared with 673 K. C-N breaking in OPA is the HDN rate limiting step.

iv) In the case of HDO, cyclohexylbenzene was the main product of the reaction. As in the case of HDN, at least one ring appears to require saturation prior to removal of the

heteroatom. This means that at least 7 molecules of hydrogen are required for each heteroatom removed and, since the oxygen content of coal-derived liquors can be high, this represents a significant use of hydrogen. The development of an efficient HDN and HDO catalyst is a key requirement for economic operation.

v) At 673 K, very little phenanthrene hydrocracking takes place and the main products of the reaction are a mixture of phenanthrene hydroderivatives. At 753 K, hydrocracking proceeds through a multistep mechanism involving hydrogenation, isomerization, cracking and hydrogenation. The main products are a complex mixture of di, monocyclic aromatics, naphthalenes and alkylaromatics. The presence of dicyclic products and benzene is significant amounts indicates that successive saturation and cracking of the phenanthrene central ring could be occurring. There is a need to seek a selective catalyst to promote central ring cracking as this is the most direct pathway to the production of alkyl-benzenes and benzene.

vi) The rate of carbon formation increases markedly, as the hydroprocessing temperature increases. This indicates that the choice of the reaction conditions for this type of process will require a careful balance if excessive saturation and carbon deposition are to be avoided.

2.- Support Characteristics: activity of the catalyst and performance of the reactor:

i) The catalyst particle size is critical for the performance of laboratory-scale trickle-bed reactors. It affects (a) the flow pattern in the reactor, and (b) the effectiveness

factor of the catalyst. Reactor diameter to catalyst particle diameter ratio of 20 - 40 are necessary to achieve a good performance of the catalyst in the reactor and to minimize internal mass transfer resistances.

ii) The pore size distribution of the catalyst is also critical for the performance. A bimodal pore size distribution (with a mean pore diameter above 10 nm) is desirable to ensure a sufficient amount of large pores for the larger molecules present in coal-derived liquids to react and to minimize internal mass transfer resistances.

iii) Increasing the surface acidity of the catalyst (given by the properties of the support) increases the rate of all the reactions studied, particularly the degree of hydrocracking relative to hydrogenation, but also increases the rate of carbon deposition. Therefore, high surface acidity catalysts, although possessing the highest initial activities, are unlikely to be successful commercial catalysts in fixed-bed reactors.

3.- Catalyst Preparation: relationship between surface structure and catalyst activity

i) The nature of the impregnation process of Ni and Mo (from solutions containing these ions) on γ-Al_2O_3 is pH dependent. Under acid conditions, Mo is adsorbed on the surface as polymolibdic ions (such as $Mo_7O_{24}^{6-}$) whereas Ni is deposited on the surface in clusters by crystallization of the cations contained in the solution filling the pore volume of the support during drying. Under basic conditions, the reverse

situation is observed, i.e. Ni is adsorbed on the support (as $Ni\ (H_2O)_6^{2+}$) and Mo is deposited on the surface in clusters having structures similar to that of $(NH_4)_2\ MoO_4.2H_2O$. Precise control of the pH is difficult due to the tendency of γ-Al_2O_3 to buffer the pH of the impregnating solution.

ii) Under co-impregnation conditions, Mo precipitates or adsorbs on the surface independently of the pH of the solution, whereas Ni behaves essentially as in solutions containing the cations separately.

iii) Higher initial activities are achieved when the support is impregnated with Ni first and calcined before impregnating Mo. Co-impregnation leads to catalysts with lower activities and successive impregnation in which Mo is impregnated first leads to low active catalysts.

iv) The pH at which the support is impregnated with Ni is not critical, although basic conditions do give an increase in activity whatever impregnation cycle is used, since a higher degree of dispersion of Ni on the surface is achieved. However, the temperature and atmosphere of the calcination of the Ni/γ-Al_2O_3 surface is important since there is a correlation between the relative pressure of NiO and Ni Al_2O_4 spinel on the surface and the activity of the catalyst. Higher initial activities are achieved when the temperature of the first calcination is above 673 K which favours the formation of Ni Al_2O_4, and best results are obtained when carried out at 773 K under air-saturated with water at 298 K.

v) Higher initial activities are achieved when Mo is impregnated under acid conditions (pH = 2 - 4) rather than basic conditions (pH = 7.5 - 8). Under acid conditions, the

surface of the catalyst in the oxidic state is characterized by the presence of Mo in a monolayer (on top of the Ni Al_2O_4 phase) or in structures highly dispersed on the surface with a small particle size which remains constant with loading, and in which Mo occupies preferentially octahedral sites. Under basic conditions, Mo is present is clusters of MoO_4 in which the Mo ion occupies the preferentially tetrahedral sites. Therefore, there is a correlation between both the degree of dispersion and the octahedral/tetrahedral Mo(VI) ratio of the Mo species on the surface and the activity of the catalyst. The temperature of the final calcination of the catalyst is critical, since temperature in excess of 773 K leads to the formation of Mo structures with a low octahedral/tetrahedral Mo(VI) ratio. The atmosphere of the final calcination is unimportant.

vi) On sulphidation, catalysts in which the oxidic state is characterized by the presence of Ni mainly as Ni Al_2O_4 and Mo preferentially in octahedral sites in the Mo oxidic structures are almost completely sulphided (if not all) to NiS and MoS_2,whereas catalysts in which Mo is present on clusters or in a monolayer in which Mo occupies preferentially tetrahedral sites are sulphided to a much lesser extent. The extent of sulphidation of Ni and Mo on the surface correlates well with the activity, suggesting that the catalytic activity of Ni-Mo/γ-Al_2O_3 catalyst is related to the formation of MoS_2 and NiS species on the surface.

vii) The high degree of dispersion of Ni and Mo in the fully oxidic state is retained in the sulphided state in the high activity catalysts. Therefore, in the active state of the catalyst the NiS and MoS_2 phases might be in intimate contact, and the interaction between the sulphided species may occur both at the edges and on the basal planes of the MoS_2 phases over the whole surface of the catalyst.

viii) From a catalytic point of view, the main active sites must be related to the MoS_2 phase, although NiS when present alone showed some HDS and hydrogenation activity. There might be two types of active sites involving anion vacancies and defects, and probably the sites involving single vacancies are responsible for HDS reactions, whereas those involving adjacent vacancies or surface defects are responsible for HDN, HDO and hydrogenation reactions. However, the present investigation does not allow definitive conclusions to be drawn about the exact nature of the active sites and about the role played by Ni as promoter for the reactions.

ix) Catalysts prepared following the "best" preparation procedure, on pellets rather than powders, i.e. impregnating the support first with Ni cations under basic conditions, dried and calcined at 773 K under air saturated in water at 298 K before impregnating Mo anions under acid conditions followed by calcination in air at 773 K, showed good activity in comparison with the commercial catalyst used as reference in this study, when employed in hydroprocessing a coal-derived liquor.

REFERENCES

van der Aalst, M. J. M. and de Beer, V. H. J., 1977, J. Catal., 49, 247.

Aboul-Gheit, A. K. and Abdou, J. K., 1973, J. Inst. Petrol. (London), 59, 188.

Aczel, T., 1972, Rev. Anal. Chem., 1, 226.

Ahmed, M. M. and Crynes, B. L., 1978, ACS Div. Petrol. Chem. Prepr., 23(4), 1376.

Akhtar, S. L., Sharkey, A. G., Shulz, J. L. and Yavorsky, P. M., 1974, ACS Div. Petrol. Chem. Prepr., 22(4), 74.

Ambrose, D. and Ambrose, B. A., 1971, "Gas Chromatography", George Newnes Ltd. London.

Amphett, C. B., 1974, "Inorganic Ion Exchangers", Elsevier, New York.

Anderson, J. R. 1975, "Structure of Metallic Catalysts", Academic Press, London.

Anderson, J. R. and Mainwaring, D. E., 1974, J. Catal., 35, 162.

Ashley, J. H. and Mitchell, P. C. H., 1968; 1969, J. Chem. Soc. (A), 2821; 2730.

Asmolov, G. N. and Krylov, O. V., 1970, Kinet. Katal., 11, 1028.

Bartsh, R. and Tanielan,C., 1974, J. Catal., 35, 353.

de Beer, V. H. J. and Schuit, G. C. A., 1976, in "Preparation of Catalysts" (B. Demon, P. A. Jacobs and G. Poncelet, Eds.) Elsevier, Amsterdam.

de Beer, V. H. J., Dahlmans, J. G. J. and Smeets, J. G. M., 1976, J. Catal., 42, 467.

de Beer, V. H. J., Bevelander, C., van Sint Fiet, T. H. M., Werter, P. G. A. and Amberg, C. H., 1976b, J. Catal., 43, 68.

van der Berg, G. H. and Rijnten, H. Th., 1978, 2nd Int. Symp. on Catalyst Preparation, Louvain-la-Neuve, paper C4.

Bernardo, C. A. A., 1977, Ph.D. Thesis, University of London.

Berrebi, G. and Bernusset, G., 1976, in "Preparation of Catalysts" (B. Delmon, P. A. Jacobs and G. Poncelet, Eds.) Elsevier, Amsterdam.

de Boer, J. H., Fortuin, J. M. H., Lippens, B. C. and Meijs, W. H., 1963, J. Catal., 2, 1.

British Petroleum, 1972, "Gas Making and Natural Gas", London.

Boudart, M., Consumano, J. A. and Levy, R. B., 1975, "New Materials for the Liquefaction of Coal", NTIS PB-247 618, US Dept. Comm.

Broekhoff, J. C. P., 1978, 2nd Int. Symp. on Catalyst Preparation, Louvain-la-Neuve, paper N2.

Brown, F. R., Makovsky, L. E. and Rhee, K. H., 1977, J. Catal., 50, 385.

Brunelle, J. P., 1978, 2nd Int. Symp. on Catalyst Preparation, Louvain-la-Neuve, paper C1.

Brunson, R. J., 1979, Fuel 58(3), 203.

Canesson, P., Delmon, B., Delvaux, G., Grange, P. and Zabala, J. M., 1976, 6th Int. Congr. on Catalysis, London, paper B32.

Carberry, J. J., 1976, "Chemical and Catalytic Reaction Engineering" McGraw-Hill, New York.

Carlson, T. A., 1975, "Photoelectron and Auger Spectroscopy", Pergamon Press, New York.

Cervello, J., Hermana, E., Jimenez, J. I. and Melo, F., 1976, in "Preparation of Catalysts" (B. Delmon, P. A. Jacobs and G. Poncelet, Eds.), Elsevier, Amsterdam.

Chadwick, D. and Hashemi, T., 1979, European Conf. Surf. Sci. Cambridge (in press).

Chiou, M. J. and Olson, J. H., 1978, ACS Div. Petrol. Chem. Prepr., 23(4), 1421.

Climax Molybdenum Co., 1973, "Aqueous Solutions of Molybdenum Compounds for Catalytic Applications", New York, Bulletin Cdb-16.

Climax Molybdenum Co., 1962, "Properties of Simple Molybdates", New York, Bulletin Cdb-4.

Consumano, J. A., Dalla Betta, R. A. and Levy, R. B., 1978, "Catalysts in Coal Conversion", Academic Press, New York.

Cotton, F. A. and Wilkinson, G., 1972, "Advanced Inorganic Chemistry", Interscience, New York.

Cowley, S. W. and Massoth, F. E., 1978, J. Catal., 51, 291.

Davies, G. O., 1978, Chem. Ind., Aug., 560.

Davies, G. O., Derbyshire, F. J. and Price, R., 1977, J. Inst. Fuel (London), L(404), 121.

Davis, J. C., 1976, Chem. Eng., 83(14), 77.

Day, G. V., 1972, Futures, Dec., 331.

Delmon, B. and Hualla, M., 1978, 2nd Int. Symp. on Catalyst Preparation, Louvain-la-Neuve, paper E1.

Donath, E. E., 1963, in "Chemistry of Coal Utilization, Supplementary Volume", (H. H. Lorry, Ed.), John Wiley & Son, New York.

Donath, E. E., 1956, Adv. Catal., 8, 239.

Dowden, D. A., 1972, Cat. Review, 5 1.

Dowden, D. A., Schnell, C. R. and Walker, G. T., 1968, 4th Int. Congr. on Catalysis, Moscou, paper 62.

Dowden, D. A., 1967, Chem. Engn. Progr. Symp. Ser., 63, 90.

Doyle, G., 1975, ACS Div. Petrol. Chem. Prepr., 2, 165.

Dupuis, T. and Duval, C., 1950, Anal. Chim. Act., 4, 173.

Ezra, D., 1978, Coal Science Lecture, London.

Farrager, A. L. and Cossee, P., 1971, in "Proc. 5th Int. Congr. on Catalysis", (J. H. Hightower, Ed.), North Holland. Amsterdam.

Fenelov, V. B., Neimark, A. V., Kheifets, L. I. and Samakhov, A. A., 1978, 2nd Int. Symp. on Satalyst Preparation, Louvain-la-Neuve, paper C2.

Fisher, P., Stadelhofer, J. W. and Zander, M., 1978, Fuel, 57(6), 345.

Fishlock, D., 1978, Financial Times (London), May 25th.

FMC Corp., 1975, "Char Oil Energy Development", Interim Rep. No. 4, USA.

Forni, L., 1974, Cat. Review, 8, 65.

Fransen, T., van Berge, P. C. and Mars, P., 1976, in "Preparation of Catalysts" (B. Delmon, P. A. Jacobs and G. Poncelet, Eds.), Elsevier, Amsterdam.

Frye, C. G., 1962, J. Chem. Eng. Data, 7, 592.

Frye, C. G., and Mosby, J. F., 1967, Chem. Engn. Progr., 63(9), 66.

Furimski, E. and Amberg, C. H., 1976, Can. J. Chem., 54(10), 1507.

Gajardo, P., 1978, Ph.D. Thesis, Université Catholique de Louvain.

Gardes, G. E. E., Nicoloan, G. A., Vicarini, M. A. and Tichner, S. J., 1976, J. Coll. Int. Sci., 5, 245.

George, Z. M., 1975, Ind. Engn. Chem. Prod. Res. Dev., 4, 298.

Geus, J. W., Dutch Pat. 6,705,259.

Gibson, J., 1978, J. Inst. Fuel (London), LI(407), 18.

Gimzewski, J. K., Padalia, B. D. and Affrossman, S., 1978, J. Catal., 55, 250.

Giordano, N., Bart, J. C. J., Vaghi, A., Castellan, A. and Martinotti, G., 1975, J. Catal., 36, 81.

Givens, E. N., and Venuto, P. B., 1970, ACS Div. Petrol. Chem. Prepr., 15, 183.

Gregg, S. J. and Sing, K. S., 1967, "Adsorption, Surface Area and Porosity", Academic Press, London.

Hagenbach, G., Courty, P. and Delmon, B., 1973, J. Catal., 31, 264.

Hagenbach, G., Courty, P. and Delmon, B., 1971, J. Catal., 23, 295.

Hargreaves, A. E. and Ross, J. R. H., 1979, J. Catal., 56, 363.

Hall, C. C. and Crawley, C. M., 1939, J. Soc. Chem. Ind., 58, 7.

Hall, W. C. and Lo Jacomo, M., 1976, 6th Int. Congr. on Catalysis, London, paper A16.

Hardin, A. H., Packwood, R. H. and Terman, M., 1978, ACS Div. Petrol. Chem. Prepr., 23(4), 1450.

Hillerbrand, L. J., Grotta, H. M., Felton, G. N., Harp, J. L., Alcorn, W. R. and Elliot, G. E., 1975, NTIS FE 232 117, US Dept. Comm.

Hualla, M., Nag., N. K., Sapre, A. V., Broderick, D. H. and Gates, B. C., 1978, AIChE J., 24(6), 1015.

Huang, C. S., Wang. K. C. and Haynes, H. W., 1977, in "Liquid Fuels from Coal" (R. T. Ellington, Ed.), Academic Press, New York.

Huisman, R., de Jonge, R., Haas, C. and Jellinek, F., 1971, J. Solid State Chem., 3, 56.

Ianibello, A., Marengo, S., Triffiro, F. and Villa, P. L., 1978, 2nd Int. Symp. on Catalyst Preparation, Louvain-la-Neuve, paper A5.

Ianibello, A. and Mitchell, P. C. H., 1978, 2nd Int. Symp. on Catalyst Preparation, Louvain-la-Neuve, paper E2.

Ianibello, A. and Triffiro, F., 1975, Z. Anorg. Allg. Chem., 413, 293.

Inogushi, M. et al, 1971, Bull. Japan Petrol. Inst., 13(2), 147.

Jackson, W. R., Larkins, F. P., Marshall, M., Rash, D. and White, N., 1979, Fuel, 58(4), 281.

Johnson, M. F. L., 1976, US Pat. 3,932,270.

Kang, C. C. and Gendler, J., 1976, ACS Div. Petrol. Chem. Prepr., 23(4), 1412.

Kilanowski, D. R., Teeuwenen, H., de Beer, V. H. J., Gates, B. C., Schuit, G. C. A. and Kwart, H., 1978, J. Catal., 55, 129.

Kovadi, S. M., Castle, L. J. and Brennett, J. V., 1978, Ind. Engn. Chem. Prod. Res. Dev., 17(1), 62.

Kruyt, H. R. (Ed.), 1952, "Colloid Science", Volume I, Elsevier, Amsterdam.

Laine, J., 1977, Ph.D. Thesis, University of London.

Landa, S., Kafka, Z., Galik, V. and Safar, M., 1969, Coll. Czech. Chem. Comm., 34, 3967.

Landa, S. and Monkova, A., 1966, Coll. Trav. Chim. Tech., 31, 2202.

Lee, H. C. and Butt, J. B., 1977, J. Catal., 49, 320.

Lipsch, J. M. J. G. and Schuit, G. C. A., 1969, J. Catal., 15, 163.

Lo Jacomo, M., Cimino, A. and Schuit, G. C. A., 1973, Gass. Chim. Ital., 103, 1281.

Lo Jacomo, M., Schiavello, M. and Cimino, A., 1971, J. Phys. Chem., 75(8), 1044.

Massoth, F. E., 1977, J. Catal., 47, 316.

Massoth, F. E., 1975, J. Cata., 36, 164.

McColgan, E. C. and Parsons, B. I., 1974, Mines Branch Research Report R273, Dept. Energy, Mines and Resources, Ottawa.

Mitchell, P. C. H., 1967, "The Chemistry of Some HDS Catalysts containing Molybdenum", Climax Molybdenum Co., London, Bulletin 3M 471 (C-29)

Mone, R. and Moscou, L., 1975, ACS Symp. Ser., 20, 151.

National Coal Board - Coal Research Establishment, 1976, private communication.

Neben, E. W., 1978, Chem. Engn. Progr., 74(8), 43.

Novakov, T. and Prims, R., 1972, in "Electron Spectroscopy". (D. A. Shirley, Ed.), North Holland, Amsterdam.

Ocampo, A., Schrodt, J. T. and Kovach, S. M., 1978, Ind. Engn. Chem. Prod. Res. Dev., 17(1), 56.

Ochoa, A., Galiasso, R. and Andreu, P., 1978, 2nd Int. Symp. on Catalyst Preparation, Louvain-la-Neuve, paper E4.

O'Hara, J. B., Klumpe, H. W., Bela, A. and Jentz, N. E., 1978, Chem. Eng. Progr., 74(8), 49.

Okamoto, Y., Shimokawa, T., Imanaka, T. and Teranishi, S., 1979, J. Catal., 57, 153.

Okamoto, Y., Nakano, H., Shiwokawa, T., Imanaka, T. and Teranishi, S., 1977, J. Catal., 50. 447.

Palmer, T. J. and Vahrman, M., 1972, Fuel 51(1), 14.

Parks, G. A., 1965, Chem. Reviews, 65, 177.

Pearson, M. J., Rigge, R. J. and Carniglia, S. C., 1977, US Pat. 4,001, 144.

Peri, J. B., 1965, J. Phys. Chem., 69(1), 220.

Peri, J. B. and Hannan, R. B., 1960, J. Phys. Chem., 64, 1526.

Perrin, D. D. and Dempsey, B., 1966, "Buffers for pH and Metal Ion Control", Chapman and Hall, London.

Pourbaix, M., 1966, "Atlas of Electrochemical Equilibria in Aqueous Solutions", Pergamon Press, London.

Qader, S. A. and McOmber, D. B., 1975, ACS Symp. Ser., 20, 82.

Qader, S. A., 1973, J. Inst. Petrol. (London), 59, 178.

Qader, S. A. and Hill, G. R., 1972, ACS Div. Fuel. Chem. Prepr., 16, 93.

Richardson, R. L. and Benson, S. W., 1957, J. Phys. Chem., 61, 405.

Rollman, D., 1977, J. Catal., 46, 243.

Satterfield, C. N., Modell, M., Hites, R. A. and Declerk, J., 1978, Ind. Engn. Chem. Proc. Res. Dev., 17(2), 141.

Satterfield, C. N., Modell, M. and Mayer, J. F., 1975, AIChE J., 21(6), 1100.

Satterfield, C. N., 1975, AIChE J., 21(2), 209.

Satterfield, C. N., Colton, C. K. and Pitcher, W. H., 1973, 19, 628.

Satterfield, C. N., 1970, "Mass Transfer in Heterogeneous Catalysis", MIT Press, Cambridge (USA).

Schiller, J. E. and Knudson, C. L., 1978, Fuel, 57(1), 36.

Schuit, G. C. A. and Gates, B. C., 1973, AIChE J., 19, 417.

Schuman, S. C. and Shalit, H., 1970, Cat. Review, 4, 245.

Shih, S. S., Katzer, J. R., Kwart, H. and Stiles, A. B., 1977, ACS Div. Petrol. Chem. Prepr., 22(3), 919.

Smith, H. A., 1957, in "Catalysis", Volume V, (P. H. Emmett Ed.), Reinhold, New York.

Smith, J. M., 1970, "Chemical Engineering Kinetics", McGraw-Hill, New York.

Solach, J., Hazlett, R. N., Hall, J. M. and Nowack, C. J., 1978, Fuel, 57(9), 521.

Sonnemans, J. and Mars, P., 1974, J. Catal., 34, 215.

Sonnemans, J. and Mars, P., 1973, J. Catal., 31, 209.

Sooter, M. C. and Crynes, B. L., 1975, ACS Div. Petrol. Chem. Prepr., 21(4), 720.

Spitz, P. H., 1977, Chem. Tech., 245.

Srinivasan, R., Liu, H. C. and Weller, S. W., 1979, J. Catal., 57, 87.

Stanulisis, J. J., Gates, B. C. and Olson, J. H., 1976, AIChE J., 22(3), 576.

Sternberg, H. W., Raymond, R. and Schweighart, F. K., 1976, ACS Div. Fuel Chem. Prepr., 21(7), 198.

Stevens, G. C. and Edmonds, T., 1978, 2nd Int. Symp. on Catalyst Preparation, Louvain-la-Neuve, paper E5.

Stevens, G. C. and Edmonds, T., 1975, J. Catal., 37, 544.

Sullivan, R. F., Egan, C. J. and Langlois, G. E., 1964, J. Catal., 3, 183.

Tanabe, K., 1970, "Solid Acid and Bases", Academic Press, New York.

Thomas, J. and Thomas, W., 1967, "Introduction to the Principles of Heterogeneous Catalysis", Academic Press, London.

Topsoe, H., Clausen, B. S., Burriesci, N., Candia, R. and Morup, S., 1978, 2nd Int. Sympt. on Catalyst Preparation, Louvain-la-Neuve, paper E3.

Trimm, D. L., 1978, 2nd Int. Sympt. on Catalyst Preparation, Louvain-la-Neuve, paper A1.

Trimm, D. L., 1973, Chem. and Ind., 21, 1012.

Tugrul, T. and Olcay, A., 1978, Fuel, 57(7), 415.

Voorhoeve, R. J. H., 1971, J. Catal., 23, 236.

Voorhoeve, R. J. H. and Stuiver, J. C. M., 1971, J. Catal., 23, 228.

Vorob'ev, L. N., Kalinevich, A. Yu. and Talipov, G. Sh., 1978, Kinet. Katal., 19(3), 582.

Wagner, C. D., 1976, Anal. Chem., 44(6), 1050.

Weisser, O. and Landa, S., 1973, "Sulphide Catalysts - Their Properties and Applications", Pergamon Press, London.

White, P. C. and Neuworth, M. B., 1976, "Coal Liquefaction", ERDA, US Dept. Comm.

Wu, W. L. and Haynes, H. W., 1975, ACS Symp. Ser., 20, 65.

Wu, W. R. and Storch, H. H., 1968, "Hydrogenation of Coal and Tar", Bureau of Mines, US Dept. of Interior.

Wyckoff, R. W. G., 1960, "Crystal Structures", Volume II, Interscience, New York.

Yamagata, N., Yutaka, O., Okazaki, J. and Tanabe, K., 1977, J. Catal., 47, 358.

Yavorsky, P. M., Akhtar, S. L., Weintrarb, M. and Reznick, A. A., 1975, Chem. Eng. Progr., 71, 79.

Yen, T. F., Erdman, J. G. and Pollaek, S. S., 1961, Anal. Chem., 33, 1587.

Zabala, J. M., Mainil, M., Grange, P. and Delmon, B., 1974, React. Kin. Catal. Lett., (2), 285.

APPENDICES

APPENDIX ONE

PROGRAM SURPOR

The calculation of surface area, pore size distribution and pore volume was carried out by means of the computer program SURPOR listed in the next pages, together with an example of the output. Subroutines POLYA, POLYB and POLYC were obtained directly from the Departmental Computer Library, and were used for interpolation of values from the experimentally measured desorption isotherm.

```
      PROGRAM SORPOR(INPUT,OUTPUT,TAPE5=INPUT,TAPE6=OUTPUT)
C*****************************************************************
C**                                                             **
C**   THIS PROGRAME CALCULATES SURFACE AREA AND PORE SIZE DISTRIBUTION **
C**   FROM GRAVIMETRIC DATA                                     **
C**                                                             **
C*****************************************************************
      DIMENSION NP(30),P(30),DW(30),DWCB(30),V(30),PR(30),BET(30),NAME(3
     *)
C*****************************************************************
C**                                                             **
C**   BUOYANCY CORRECTIONS                                      **
C**   ENTER NBC = N OF BUOYANCY CORRECTION DATA POINTS          **
C**   ENTER PRESSURE AND WEIGHT FOR EACH POINT, NBC POINTS IN TOTAL   **
C**                                                             **
C*****************************************************************
      READ,NBC
      PN=760.
      DO 100 I=1,NBC
  100 READ,P(I),DW(I)
      CALL LSQFT(NBC,DW,P,SLB,CIB,ER,ERS,ERI)
      WRITE(6,200)
      DO 101 I=1,NBC
      W=CIB+SLB*P(I)
  101 WRITE(6,201) I,P(I),DW(I),W
      WRITE(6,202) ER,CIB,ERI,SLB,ERS
C*****************************************************************
C**                                                             **
C**   ENTER ADSORPTION DATA                                     **
C**                          NPA= N OF ADSORPTION POINTS        **
C**                          WCAT= SAMPLE WEIGHT IN GRAMS       **
C**                          NAME= SAMPLE NAME                  **
C**                          P(I)= PRESSURE IN TOR              **
C**                          DW(I)= WEIGHT IN MG                **
C**                                                             **
C*****************************************************************
      READ(5,300)NPA,WCAT, (NAME(I),I=1,3)
  300 FORMAT(I2,1X,F5.4,1X,3A10)
      DO 102 I=1,NPA
      READ,NP(I),P(I),DW(I)
      DWCB(I)=DW(I)-(CIB+SLB*P(I))
      V(I)=DWCB(I)*799994.79*1.0E-06/WCAT
      PR(I)=P(I)/PN
  102 BET(I)=P(I)/(V(I)*(PN  -P(I)))
      N=0
      DO 103 I=1,NPA
      IF(PR(I).GT.0.3) GO TO 52
  103 N=N+1
   52 CALL LSQFT(N,BET,PR,SL,CI,ER,ERS,ERI)
      VM=1.0/(SL+CI)
      AR=4.36*VM
      WRITE(6,203) NPA,WCAT,N,(NAME(I),I=1,3)
      DO 104 I=1,NPA
  104 WRITE(6,204) NP(I),P(I),PR(I),DW(I),DWCB(I),V(I),BET(I)
      WRITE(6,205) VM,AR,SL,ERS,CI,ERI,ER
C*****************************************************************
C**                                                             **
C**   PORE SIZE DISTRIBUTION  ENTRE 0 IF NEEDED                 **
C**                                                             **
C*****************************************************************
      READ,J
      CALL POROSY(J,SLB,CIB,WCAT)
      STOP
  200 FORMAT(1H0///10X,"BUOYANCY DETERMINATION"///)
  201 FORMAT(1H0,I4,5X,F6.1,5X,2(F8.3,5X))
  202 FORMAT(1H0//5X,"ERROR=",E10.3,3X,"INTERCEPT=",F5.3,3X,E10.3,3X,
     *"SLOPE=",F7.4,3X,E10.3///)
  203 FORMAT(1H0,5X,"ADSORPTION ISOTHERM OF NITROGEN AT -198 C"// 5X,
     *"N OF POINTS=",I3,3X,"SAMPLE WEIGHT=",F7.4,1X,"GR"//5X,"BET POINTS
     *=",I3,5X,"CATALYST=",2A,3A10// 9X,"P",6X,"PR",7X,"DW",7X,"DWCB",5X,
     *"VADS",7X,"BET"/)
  204 FORMAT(1H0,I4,2X,F5.1,2X,F5.3,2X,2(F8.3,2X),F7.2,2X,E10.3)
  205 FORMAT(1H0///1X,"MONOLAYER=",F8.2,1X,"CC(STP)",3X,"SURFACE AREA=",
     *F7.2,1X,"M2/GM"//1X,"SLOPE=",2(E10.3,3X),"INTERCEPT=",2(E10.3,3X)/1X
     *,"ERROR=",E10.3///////)
      END
```

```
      SUBROUTINE POROSY (IN,SLB,CIB,WCAT)
C*****************************************************************
C**                                                             **
C**   SUBROUTINE TO CALCULATE PORE SIZE DISTRIBUTION            **
C**                                                             **
C*****************************************************************
      DIMENSION N(30),P(30),DW(30),V(30),PR(30),RK(30),RP(30),T(30),RPM(
     £30),F(30),DVP(30),PI(30),VI(30),FR(30),API(18),AVI(18)
      IF(IN.GT.0)GO TO 10
C*****************************************************************
C**                                                             **
C**   ENTER DATA OF DESORPTION POINTS                           **
C**                        NPD= N OF DESORPTION POINTS          **
C**                        P(I)= PRESSURE IN TOR                **
C**                        DW(I)= WEIGHT IN MG                  **
C**                                                             **
C**   ENTER 0 AFTER THIS DATA IF INTERPOLATION IS NEEDED        **
C**                                                             **
C*****************************************************************
      READ,NPD
      PN=760.
      DO 100 I=1,NPD
      READ,N(I),P(I),DW(I)
      DWCB=DW(I)-(CIB+SLB*P(I))
      V(I)=DWCB*799994.79*1.0E-06/WCAT
  100 PR(I)=P(I)/PN
      CALL CALPOR (NPD,PR,V,RP,RPM,F,DVP,SVP)
      WRITE(6,200) N(I),P(I),DW(I),PR(I),V(I),RP(I)
      S1=0.
      S2=0.
      S3=0.
      DO 101 I=2,NPD
      FR(I)=DVP(I)/SVP*100.
      S1=S1+RPM(I)*FR(I)
      S2=S2+(RPM(I)**2)*FR(I)
      S3=S3+FR(I)
  101 WRITE(6,201) N(I),P(I),DW(I),PR(I),V(I),RP(I),RPM(I),DVP(I),F(I),F
     £R(I),S3
      PV=SVP*0.00156
      RAPM=S1/100.
      VARD=S2/100.-RAPM**2
      RAPM=RAPM*2.
      VARD=SQRT(VARD)
      WRITE(6,202) PV,RAPM,VARD
      READ,NJ
      IF(NJ.GT.0)GO TO 10
      WRITE(6,206)
      CALL ADJ(PR,V,NPD,PI,VI)
      API(1)=PR(1)
      AVI(1)=V(1)
      DO 103 I=2,17
      API(I)=PI(I-1)
  103 AVI(I)=VI(I-1)
      API(18)=PR(NPD)
      AVI(18)=V(NPD)
      DO 106 I=2,18
      IF(AVI(I-1).GT.AVI(I)) GO TO 106
      AVI(I)=AVI(I-1)
  106 CONTINUE
      WRITE(6,207)
      DO 105 I=1,18
  105 WRITE(6,208) I,API(I),AVI(I)
      M=18
      CALL CALPOR(M,API,AVI,RP,RPM,F,DVP,SVP)
      WRITE(6,203)
      S1=0.
      S2=0.
      S3=0.
      DO 104 I=2,18
      FR(I)=DVP(I)/SVP*100.
      S1=S1+RPM(I)*FR(I)
      S2=S2+(RPM(I)**2)*FR(I)
      S3=S3+FR(I)
  104 WRITE(6,204) RP(I-1),RP(I),RPM(I),FR(I),S3
```

```
      PV=SVP*0.00156
      RAPM=S1/100.
      VARD=S2/100.-RAPM**2
      RAPM=RAPM*2.
      VARD=SQRT(VARD)
      WRITE(6,202) PV,RAPM,VARD
      WRITE(6,205)
   10 RETURN
  200 FORMAT(1H0,9X,"DESORPTION ISOTHERM / PORE SIZE DISTRIBUTION"//1H0
     &7X,"P",5X,"WEIGHT",3X,"PR",3X,"VADS",7X,"RP",6X,"RPM",5X,"DVP",4X,
     &"DVP/RPM",7X,"/",1X,3X,"/ACC"/1X
     &,I4,1X,F5.1,1X,F8.3,1X,F5.3,1X,F8.3,1X,F7.1,1X,F5.1)
  201 FORMAT(1H0,I4,1X,F5.1,1X,F8.3,1X,F5.3,1X,F8.3,1X,3(F7.1,1X),E12.5,
     &1X,F6.2,1X,F6.2)
  202 FORMAT(1H0/15X,"PORE VOLUME",7X,F7.3,1X,"CC/GR"/15X,"MEAN PORE DIA
     &METER",1X,F6.1,1X,"A"/15X,"VARIANCE",10X,F6.1///)
  203 FORMAT(1H0///5X,"PORE SIZE DISTRIBUTION"/6X,"(INTERPOLATED VALUES)
     &"//2X,"RANGE(A)",2X,"RPM",4X,"/ VOL",3X,"/ ACC"//)
  204 FORMAT(1X,F4.0,"-",F4.0,2X,F4.0,2X,2(F6.2,2X))
  205 FORMAT(1H0,/////"  "///)
  206 FORMAT(1H0,5X,"INTERPOLATED VALUES"//)
  207 FORMAT(1H0,5X,"FINAL INTERPOLATION"//)
  208 FORMAT(1X,I2,4X,F8.6,2X,F8.3)
      END

      SUBROUTINE LSQFT(N,Y,X,SL,CINT,ER,ERS,ERI)
      DIMENSION Y(N),X(N)
      R=N
      SX=0.
      SY=0.
      SX2=0.
      SXY=0.
      DO 100 I=1,N
      SX=SX+X(I)
      SY=SY+Y(I)
      SXY=SXY+X(I)*Y(I)
  100 SX2=SX2+X(I)*X(I)
      A=SXY-SX*SY/R
      B=SX2-SX*SX/R
      SL=A/B
      CINT=(SY-SL*SX)/R
      S=0.
      DO 101 I=1,N
      YA=CINT+SL*X(I)
  101 S=S+(YA-Y(I))**2
      VER=S/(R-1.)
      ER=SQRT(VER)
      ERS=ER*2.176/(SQRT(B)*SQRT(FLOAT(N)))
      ERI=ER*SQRT(1./R+(SX*SX/(R*R))/B)*2.776/SQRT(FLOAT(N))
      RETURN
      END

      SUBROUTINE CALPOR (N,PR,V,RP,RPM,F,DVP,SVP)
      DIMENSION PR(N),V(N),RP(N),RPM(N),F(N),DVP(N),T(30),RK(30)
      DO 100 I=1,N
      RK(I)=4.14*(1./ALOG10(1./PR(I)))
      T(I)=3.5*(5./ALOG(1./PR(I)))**(1./3.)
  100 RP(I)=RK(I)+T(I)
      SUSP=0.
      SVP=0.
      DO 101  I=2,N
      RPM(I)=(RP(I-1)+RP(I))/2.
      RKM=(RK(I-1)+RK(I))/2.
      DVM=(V(I-1)-V(I))
      DTM=T(I-1)-T(I)
      DVF=0.064*DTM*SUSP
      DVK=DVM-DVF
      DVP(I)=DVK*(RPM(1)/RKM)**2
      USP=31.2*DVP(I)/RPM(1)
      SUSP=SUSP+USP
      SVP=SVP+DVP(I)
  101 F(I)=DVP(I)/RPM(I)
      RETURN
      END
```

```
      SUBROUTINE ADJ(PR,V,NPD,P,VI)
      DIMENSION PR(NPD),V(NPD),X(4),VOL(4),VI(16),P(16)
      READ,(P(I),I=1,16)
      N=4
      K=NPD-2
      L=1
      DO 102 I=1,16
      IF(P(I).LT.PR(1)) GO TO 20
      L=I
      T=PR(1)*760.
      WRITE(6,200) T
  102 VI(I)= V(I)
   20 DO 100 I=2,K
      NI=I-1
      NC=NI-1
      DO 101 J=1,4
      X(J)=PR(NC+J)
  101 VOL(J)=V(NC+J)
      CALL POLY(X,VOL,N,P,VI,K,I,NPD,PR,V,L)
  100 CONTINUE
      RETURN
  200 FORMAT(1X,"INITIAL POINT BELOW 742 TOR,SAME VADS AS",F4.0,"TOR ASS
     EUMED")
      END

      SUBROUTINE POLY(PR,V,N,P,VI,NF,NI,JJ,AP,AV,L)
      DIMENSION PR(N),VI(16),V(N),COR(10,2),G(10),TAB(20,2),C(10),P(16),
     EAP(JJ),AV(JJ)
      M=3
      J1=M+1
      CALL POLYA(PR,V,N,XSCALE,XSHIFT,M,J1,TAB,COR,G)
      SHIFT1=0.
      SCALE=1.
      CALL POLYB(C,SHIFT1,SCALE,N,XSCALE,XSHIFT,M,J1,TAB,COR,G)
      DO 101 I=L,16
      IF(P(I).GT.PR(1)) GO TO 101
      IF(NI.EQ.0) GO TO 21
      IF(P(I).LT.PR(2)) GO TO 10
      XX=P(I)
      CALL POLYC(XX,YY,XSCALE,XSHIFT,M,J1,COR,G)
      VI(I)=YY
      PRINT,XX,YY
      GO TO 101
   21 IF(P(I).LT.PR(4)) GO TO 22
      XX=P(I)
      CALL POLYC(XX,YY,XSCALE,XSHIFT,M,J1,COR,G)
      VI(I)=YY
      PRINT,XX,YY
      GO TO 101
   22 T=PR(4)*760.
      WRITE(6,201) T
      VI(I)=V(4)
  101 CONTINUE
   10 RETURN
  201 FORMAT(1X,"FINAL POINT ABOVE 266 TOR,SAME VADS AS",F4.0,"TOR ASSUM
     ED")
      END
```

ADSORPTION ISOTHERM OF NITROGEN AT -198 C

OF POINTS= 10 SAMPLE WEIGHT= .0229 GR

BET POINTS= 6 CATALYST= NORTON SA-6175 40-50 MESH

	P	PR	DW	DWCO	VADS	BET
1	19.0	.025	1.260	1.216	42.27	.607E-03
2	47.0	.062	1.470	1.440	50.29	.151E-02
3	84.0	.111	1.590	1.586	55.39	.224E-02
4	128.0	.169	1.730	1.757	61.36	.330E-02
5	195.0	.257	1.910	1.964	69.50	.496E-02
6	216.0	.284	2.010	2.098	73.50	.542E-02
7	382.0	.503	2.540	2.745	95.89	.105E-01
8	532.0	.700	3.360	3.690	135.91	.172E-01
9	604.0	.795	4.710	5.071	177.15	.219E-01
10	730.0	.961	9.260	9.649	337.09	.722E-01

MONOLAYER= 83.18 CC(STP) SURFACE AREA= 362.93 M2/GR

SLOPE= .186E-01 .106E-03 INTERCEPT= .159E-03 .246E-04
ERROR= .284E-04

DESORPTION ISOTHERM / PORE SIZE DISTRIBUTION

	P	WEIGHT	PR	VADS	RP	RPM	DVP	DVP/RPM	%	%ACC
0	750.0	9.210	.987	337.935	745.0					
1	730.0	9.200	.961	337.095	254.2	499.6	.9	.18354E-02	.27	.27
2	710.0	9.180	.934	335.905	150.7	204.4	1.4	.67931E-02	.41	.67
3	690.0	8.900	.908	322.159	111.7	133.2	17.1	.12845E+00	5.01	5.68
4	670.0	8.500	.882	311.104	87.6	99.6	13.9	.13997E+00	4.06	9.74
5	650.0	7.500	.855	275.526	62.7	75.1	48.5	.64560E+00	14.19	23.93
6	598.0	6.620	.787	230.799	44.4	56.0	63.7	.11373E+01	18.65	42.61
7	561.0	4.900	.738	182.730	40.3	44.9	71.6	.15966E+01	20.96	63.57
8	515.0	3.000	.677	146.187	32.7	36.5	70.6	.19336E+01	20.60	84.25
9	470.0	2.200	.624	121.605	28.3	30.5	17.6	.58215E+00	5.20	89.45
10	441.0	2.050	.580	108.170	24.8	26.6	15.9	.59968E+00	4.66	94.04
11	585.0	2.030	.507	90.516	20.8	22.8	10.0	.43758E+00	2.92	97.01
12	369.0	2.030	.446	69.596	18.2	19.5	2.9	.14924E+00	.85	97.85
13	292.0	2.200	.384	61.507	16.0	17.1	6.4	.37576E+00	1.08	98.93
14	216.0	2.010	.284	73.304	13.1	14.6	.9	.59741E-01	.25	100.00

PORE VOLUME .553 CC/GR
MEAN PORE DIAMETER 110.0 A
VARIANCE 55.1

PORE SIZE DISTRIBUTION
(INTERPOLATED VALUES)

RANGE(A)	RPM	% VOL	% ACC
745.-400.	572.	.35	.35
400.-300.	350.	-.00	.35
300.-200.	250.	-.00	.35
200.-150.	175.	.81	1.16
150.-100.	125.	5.93	7.08
100.- 90.	95.	2.04	9.13
90.- 80.	85.	3.33	12.46
80.- 70.	75.	5.44	17.90
70.- 60.	65.	8.94	26.84
60.- 50.	55.	14.65	41.49
50.- 40.	45.	23.19	64.68
40.- 35.	37.	14.07	79.75
35.- 30.	32.	7.73	87.47
30.- 25.	27.	6.78	95.24
25.- 20.	22.	3.20	97.10
20.- 15.	17.	3.56	100.66
15.- 14.	14.	-.66	100.00

PORE VOLUME .532 CC/GR
MEAN PORE DIAMETER 110.0 A
VARIANCE 56.9

NOMENCLATURE

P	pressure (torr)
PR	relative pressure (P/760)
DW	observed weight gain (mg)
DWCB	weight gain corrected for buoyancy
VADS	adsorbed volume (cc (STP) $(g\text{-cat})^{-1}$)
BET	value of BET function (P/VADS (760-P))
RP	pore radius (A^{o})
RPM	mean pore radius in each step of desorption
DVP	volume of N_2 desorbed in each step
%	% of the total pore volume

APPENDIX TWO

COMPARISON OF THE ACTIVITY OF Ni 773AW - Mo 773A AND THE COMMERCIAL AKZO-153S Ni-Mo CATALYSTS EMPLOYING A COAL-DERIVED LIQUID

Catalyst Ni 773AW - Mo 773A (prepared on $\frac{1}{8}$" cylindrical pellets of the Norton SA-6175 γ-$A\ell_2O_3$ support) was submitted for testing for hydroprocessing of a coal-derived liquor to NCB-CRE. The test was carried out in a high-pressure trickle-bed reactor, and the results are shown in Table A, together with those of the commercial AKZO-153S Ni-Mo catalyst. The catalysts were pre-sulphided in situ, passing a mixture of a coal-derived liquid and CS_2 at 21.26 MPa and at 573 K.

From Table A it can be seen that the overall activity of catalyst Ni 773AW - Mo 773A (measured as the conversion of the components of the feed boiling above 420°C) is higher than that of the commercial AKZO-153S. The fact that the products from the Ni 773AW - Mo 773A catalyst are characterized by a higher boiling fraction below 355°C, and the presence of much lower amounts of coking precursors (measured by the Conradson carbon analysis), clearly illustrates the superior hydrocracking capabilities of this catalyst.

TABLE A

CATALYTIC TEST OF Ni 773AW - Mo 773A AND AKZO-153S CATALYSTS EMPLOYING A COAL-DERIVED LIQUOR

REACTOR CONDITIONS

Pressure	21.27 MPa
LHSV	0.5 hr^{-1}
Hydrogen feed rate	3.0 dm^3 min^{-1}
Catalyst volume	100 cm^3
Catalyst temperature	
top	723 K
middle	703 K
bottom	673 K

DISTILLATION RANGES	FRACTION (%w)		
	FEED	PRODUCT	
		AKZO-153S	Ni 773AW - Mo 773A
IBP - 170°C	0.2	1.4	4.4
170 - 250°C	2.4	11.3	10.8
250 - 300°C	8.3	28.9	29.4
300 - 255°C	35.1	33.8	33.6
355 - 420°C	24.6	18.0	16.3
> 420°C	29.4	6.6	5.5
CONRADSON CARBON %	9.0	0.4	0.15
CONVERSION OF PRODUCTS > 420°C		77.6	81.3

A study of nickel—molybdate coal-hydrogenation catalysts using model feedstocks

Ricardo Badilla-Ohlbaum, Kerry C. Pratt* and David L. Trimm†
Department of Chemical Engineering and Chemical Technology, Imperial College, London SW7 2BY, U.K.
(Received 7 August 1978)

A model feedstock consisting of dibenzothiophene, dibenzofuran, quinoline, and phenanthrene dissolved in heptane has been hydroprocessed in a flow reactor at 6.89 MPa and 400°C over a series of nickel—molybdate catalysts. Under simultaneous processing, the main product of dibenzothiophene hydrodesulphurization was diphenyl, the main product of quinoline hydrodenitrogenation was propylcyclohexane, and that of dibenzofuran hydrodeoxygenation was cyclohexyl benzene. Sulphur was removed without the need for saturation of the sulphur-containing ring. For both nitrogen and oxygen removal, the ring containing the heteroatom was saturated before scission of the C—N or C—O bond. The main products of the hydroprocessing of phenanthrene were hydroderivatives of varying degrees of saturation. Very little hydrocracking took place under our conditions, and this occurred predominantly by successive saturation and cracking of terminal rings. With increasing catalyst acidity, the rates of all reactions studied increased, as did the degree of hydrocracking relative to hydrogenation. Coke formation on the catalyst also increased markedly with acidity.

One result of the concern arising from the impending shortage of crude oil has been the revival of interest in the conversion of coal to useful chemicals[1,2]. Comparison of typical analyses (*Table 1*) shows that this conversion involves increasing the hydrogen content of coal, removing (inorganic) ash and removing heteroatoms which are chemically bound to the coal.

Although several processes have been developed over the years[1,2], the most direct route involves the hydrogenation of coal. In a typical process[3], coal is solvent-extracted to remove most of the ash and the resulting filtered liquid is subjected to catalytic hydrotreating. Most modern processes are based on catalysts containing molybdenum salts promoted by cobalt or nickel[1,4,5] and supported on alumina. Their mode of action is, however, subject to considerable doubt[6,7].

Part of the problem arises from the complexity of the reactions involved in the hydrotreating of coal. The major reactions involve the hydrocracking of multi-ring aromatics and the removal of the heteroatoms O, N and S as H_2O, NH_3 and H_2S. As a result, much work has been focused on coal[3] or on single feedstocks such as thiophene[8]. In the first case the complexity of the product spectra tends to obscure the underlying mechanisms while, in the second case, the absence of cross-interactions between various components of coal leaves the results open to question.

The present studies have been focused on the hydrogenation of a model feedstock containing compounds typical of those occurring in coal-derived liquids, but which give products that can be traced to individual reactions. The hydrogenation of this feedstock has been studied over a range of nickel-molybdate-based catalysts.

The elemental analysis of the model feedstock is given in *Table 1*. Coal-derived liquids contain large quantities of polynuclear aromatic hydrocarbons containing from 2 to 5 condensed aromatic rings. Anthracene and phenanthrene are the most common constituents[9] and the latter compound has been chosen as one constituent of the model feedstock.

Most organic sulphur exists in heterocyclic structures in coal, of which dibenzothiophene is most difficult to hydrogenolyse[10]: this compound was also used as a component of the feed. Nitrogen is thought to occur mainly

Table 1 Analysis of coal and oil

Component	Crude oil[1] (wt %)	Bituminous coal category III[1] (medium-rank bituminous) (wt %)	Model feed used in this study (wt %)
C	85.4	86.0	84.7
H	12.6	5.5	10
N	—	2.5	2.2
S	2.0		2.4
O	—	6.0	0.7
Atomic H/C ratio	1.7	0.76	1.42
Ash	10^{-2}	Up to ca. 15%	0

*Present address: CSIRO Division of Materials Science, Catalysis and Surface Science Laboratory, University of Melbourne, Parkville, Victoria, 3052, Australia
†Present address: Laboratory of Industrial Chemistry, The University of Trondheim, N-7034, Trondheim-NTH, Norway

0016—2361/79/040309—06$2.00

Table 2 Composition of the model feedstock

Component of coal	Model compound	Reactions expected	Composition (wt %)
Multi-ring aromatics	Phenanthrene	Hydrocracking Hydrogenation	10
Sulphur compounds	Dibenzothiophene	Hydrodesulphurization (HDS)	8
	Dibutylsulphide		5
Nitrogen compounds	Quinoline	Hydrodenitrogenation (HDN)	20
Oxygen compounds	Dibenzofuran	Hydrodeoxygenation (HDO)	7
	Heptane	–	50

Table 3 Catalyst characterization

	AKZO-153S	IC-124B	IC-124AS	IC-124A	IC-124SA
MoO_3 (wt %)	15	12	12	12	12
NiO (wt %)	3	4	4	4	4
Surface area ($m^2\ g^{-1}$)[a]	230	98	214	60	27
Pore volume ($cm^3\ g^{-1}$)[a]	0.48	0.25	0.33	0.15	0.05
Mean pore diameter (nm)	8	7	10	5	2
Surface acidity[b]	0.178	0.244	0.263	0.274	0.396
Support origin	–	BDH 100% Al_2O_3	Norton SA-6175	BDH 100% Al_2O_3	Norton SA-3232

[a] By nitrogen adsorption.
[b] As mg m^{-2} of chemisorbed pyridine

in five or six-membered heterocyclic rings[11]; the resistivity to denitrogenation decreases in the order: acridine > quinoline > pyridine > amines.

After some consideration, quinoline was chosen as a component of the model feedstock. Some 60% of the oxygen content of coal is present as phenolic hydroxyl groups[4], some of the rest is made up of aromatic ethers and (at very low ranks) carboxyl groups. Dibenzofuran is typical of the aromatic ethers and is resistant to hydrogenolysis[12]: this compound was also used as a component of the feedstock.

The concentrations of components in the feedstock were adjusted to approximate to these present in coal-derived liquids[5]. The composition of the feedstock, which was diluted (50 wt %) with heptane, is given in *Table 2*.

The active form of the catalyst is the sulphided state[4], maintained by the presence of hydrogen sulphide produced in the reaction. Dibutylsulphide, which is easily desulphurized, was added to the feed to provide an approximately constant distribution of sulphur through the catalyst bed.

EXPERIMENTAL

Catalyst preparation

On the basis of preliminary screening experiments, the nickel–molybdenum catalyst system was chosen for this study. For the initial experiments, the composition was fixed at 4% NiO, and 12% MoO_3 by weight. Four catalysts with the same nickel and molybdenum loadings on different alumina and silica–alumina supports were prepared. In addition, a commercial catalyst AKZO-153S was used for comparison. For each catalyst, preparation involved impregnation of the support with solutions of $Ni(NO_3)_2.6H_2O$ (BDH – Analar Grade), and $(NH_4)\ Mo_7O_{24}.4H_2O$ (BDH – Analar Grade). The catalysts were prepared by adding to the supports a solution containing the requisite amounts of nickel and molybdenum in a volume just sufficient to fill the pores; the excess of moisture was removed by evaporation.

Table 4 Experimental conditions

Weight of catalyst[a]	2 g
Liquid flow rate	20 $cm^3\ h^{-1}$
Hydrogen flow rate	500 $cm^3\ min^{-1}$ (STP)
Pressure	6.89 MPa
Temperature	400°C

[a] 74–100 B.S. mesh, diluted in a 1:1 ratio with ground silica glass

The characteristics of the catalyst used are shown in *Table 3*.

The reaction system

A continuous high-pressure trickle bed reactor was used, in which liquid feed, metered by a positive displacement pump, was mixed with hydrogen from cylinders, and passed downwards through the reactor. The reactor tube consisted of a 10 cm length of 8 mm i.d. stainless-steel tube containing approximately 2 g of catalyst mixed with ground silica glass. The catalyst was presulphided for a period of 12 h in a 10% H_2S/H_2 (v/v) mixture at 230°C, at a total pressure of 0.68 MPa. Conditions of operation for the experiments are given in *Table 4*.

Tests showed that no significant mass transfer limitations existed with the particle sizes and liquid rates employed.

Analyses

Liquid samples were collected at two-hourly intervals during each eight-hour run and analysed by GLC using a 2 m OV 101 column (Phase Separations Ltd). The column was maintained at 40°C for 7 min after injection of the sample and then temperature-programmed from 40 to 250°C at a rate of 4°C/min. A flame-ionization detection system was used. Product components were identified by the use of pure compounds where possible, and by mass

Table 5 Product compositions (wt % corrected to 100% mass balance using heptane as internal standard)

	Component		Catalyst				
			AKZO-153S	IC-124B	IC-124AS	IC-124A	IC-124SA
1	C_4H_{10}	Butane	2.49	2.62	2.64	2.94	3.56
2	C_6H_{12}	Benzene	0.01	Tr	Tr	Tr	Tr
3	C_6H_6	Cyclohexane	0.28	0.17	0.59	0.34	0.10
4	C_7H_{16}	Heptane	49.58	49.58	49.58	49.58	49.58
5	C_7H_{14}	Methyl cyclohexane	Tr	Tr	Tr	Tr	Tr
6	C_7H_8	Toluene	Tr	Tr	Tr	Tr	Tr
7	C_8H_{16}	Ethyl cyclohexane	0.05	0.08	0.01	0.09	0.10
8	C_8H_{10}	Ethyl benzene	Tr	Tr	Tr	Tr	Tr
9	C_9H_{18}	Propyl cyclohexane	9.95	6.58	10.53	6.02	3.43
10	C_9H_{12}	Propyl benzene	1.01	0.96	0.65	0.90	0.65
11		Alkyl cyclohex. A	0.09	0.49	0.04	0.58	0.57
12		Alkyl cyclohex. B	0.54	0.53	0.37	0.67	0.38
13		Alkyl cyclohex. C	0.01	Tr	0.01	0.01	Tr
14		Alkyl cyclohex. D	Tr	Tr	Tr	Tr	0.09
15	$C_8H_{18}S$	Dibutylsulphide	0	0	0	0	0
16	$C_{10}H_{12}$	Tetrahydro naphthalene	Tr	0.6	0.08	0.04	0.28
17	$C_{10}H_8$	Naphthalene	0.01	0.02	0.06	0.01	0.09
18	C_9H_7N	Quinoline	0	0	0	0	0
19	$C_9H_{13}N$	*o*-propylaniline	3.16	7.16	2.70	5.37	5.54
20	$C_{12}H_{22}$	Dicyclohexyl	0.18	0.12	0.08	0.21	0.10
21	$C_{12}H_{16}$	Cyclohexyl benzene	0.79	0.72	0.97	0.90	0.75
22	$C_{12}H_{10}$	Diphenyl	5.96	5.08	5.51	6.10	6.81
23	$C_{13}H_{16}$	Unknown	Tr	Tr	Tr	Tr	Tr
24	$C_{14}H_{24}$	Perhydrophenanthrene isomer	Tr	Tr	Tr	Tr	Tr
25	$C_{12}H_8O$	Dibenzofuran	5.53	6.01	5.31	5.99	6.18
26	$C_{14}H_{18}$	Octahydrophenanthrene isomer	0.61	0.16	0.80	0.24	0.09
27	$C_{14}H_{12}$	Dihydrophenanthrene	0.89	1.16	0.78	1.26	1.21
28	$C_{14}H_{18}$	Octahydrophenanthrene	1.97	0.68	1.85	0.65	0.14
29	$C_{14}H_{14}$	Tetrahydrophenanthrene	1.84	1.60	1.81	1.48	1.45
30	$C_{12}H_8S$	Dibenzothiophene	0	Tr	0	Tr	Tr
31	$C_{14}H_{10}$	Phenanthrene	2.94	4.74	2.23	3.90	5.35
32	$C_{14}H_{24}$	Perhydrophenanthrene isomer	0.73	0.42	0.51	0.47	0.19
33	$C_{18}H_{34}$	Dicyclohexylhexane isomer	Tr	Tr	Tr	Tr	Tr
34	$C_{18}H_{28}$	Unknown	Tr	Tr	Tr	Tr	Tr

Tr = trace

Table 6 Feed conversions

Conversions (%)	AKZO-153S	IC-124B	IC-124AS	IC-124A	IC-124SA
Dibutylsulphide	100.	100.	100.	100.	100.
Dibenzothiophene	100.	100.	100.	100.	100.
Quinoline (HDN)[a]	50.56	34.85	51.48	31.93	18.89
Phenanthrene total	64.44	49.04	76.00	58.10	42.73
Phenanthrene (hydrogenation)	61.31	41.14	58.65	41.86	32.09
Dibenzofuran	14.56	7.12	17.93	7.49	4.58

[a] Based on nitrogen removal from the organic ring

spectrometric analysis performed on some runs. No analysis of gaseous products was made.

RESULTS AND DISCUSSION

Steady-state performance of the catalyst was generally achieved after about 2 h. Product compositions in the steady state are given in *Table 5*. Overall conversions of feed components are shown in *Table 6*.

Desulphurization (HDS)

It is apparent from the complete conversion of dibenzothiophene and dibutylsulphide that HDS is the most facile reaction of all those considered. Most desulphurization studies reported in the literature have been carried out at atmospheric pressure[4,8,13,14]. Under these conditions, dibenzothiophene yields diphenyl as a product, although some ring saturation has been reported at higher pressures[15,16]. In principle, it is not possible to distinguish in our experiments between diphenyl, cyclohexyl benzene, and dicyclohexyl produced from either dibenzothiophene or dibenzofuran. However, a molar balance on the diphenyl produced showed that its production can be ascribed almost entirely to the converted dibenzothiophene. This suggests that there is no substantial further hydrogenation of the diphenyl produced. This might be expected since Hall and Cawley[12] found that, over MoS_2, hydrogenation of diphenyl to cyclohexyl benzene occurred only at pressures in excess of 20 MPa. Rollman[16] has reported cyclohexylbenzene formation from dibenzothiophene over Co–Mo catalysts at similar temperatures and lower pressures, and that diphenyl added to the feed was not hydrogenated to cyclohexylbenzene. This suggests that, on

Co–Mo, formation of cyclohexylbenzene from diphenyl occurs prior to desorption from the catalyst, and that this may not occur on Ni–Mo. If this were so, it indicates a considerable advantage of the Ni–Mo system in terms of reduced hydrogen consumption in desulphurization.

Thus, the general reaction path appears to be:

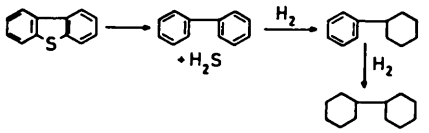

where, under the present conditions, there is no significant reaction beyond diphenyl.

If these observations are general for the commerical HDS of coal-derived materials, then it is apparent that, since sulphur can be removed without saturation of the ring structure, such reactions consume relatively little hydrogen, and there is no significant loss of aromaticity of the product as a result of desulphurization.

Denitrogenation (HDN)

Only traces of tetrahydroquinoline were detected among the products of reaction and, although quinoline and *o*-propylaniline are eluted almost simultaneously from the gas chromatograph, mass spectroscopy failed to detect any quinoline in the reaction products. Thus it appears that production of *o*-propylaniline is much faster than the subsequent breaking of the C–N bond, and that the latter is rate-determining in nitrogen removal.

This is in agreement with the proposal made by Rollman[16] for the reaction path of indole at higher temperatures, but seems, at first sight, to be contrary to the studies of Satterfield *et al.*[17]. Using a similar catalyst, the latter report that quinoline was hydrogenated to a near-equilibrium concentration of Py-tetrahydroquinoline and to Bz-tetrahydroquinoline (BzTHQ). They were, however, unable to distinguish BzTHQ from *o*-propylaniline and the present results show, in fact, that the latter compound was the major product. If this is so, then the studies are in good agreement.

A further molar balance shows that the total of the propyl benzene and propyl cyclohexane in the products corresponds closely to the conversion of *o*-propylaniline. These products could also arise from phenanthrene hydrocracking reactions, but the total hydrocracking conversion can be accounted for without reference to these compounds (see later). Thus, the results suggest the following reaction sequence for quinoline HDN:

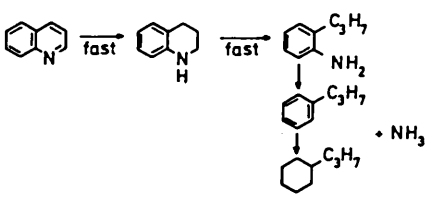

This finding would agree with the results of Landa[18] obtained with MoS_2 catalyst in batch experiments. It is apparent that, in contrast to sulphur removal, the nitrogen-containing ring must be saturated prior to removal of nitrogen. The extent of further saturation depends upon process conditions and the catalyst. In the present experiments, propyl cyclohexane was the major product.

Deoxygenation (HDO)

It has already been shown that diphenyl is unlikely to be a product of the deoxygenation of dibenzofuran, and it might be expected that the sequence for O removal would be analogous to that for N, i.e. via 2-cyclohexyl phenol:

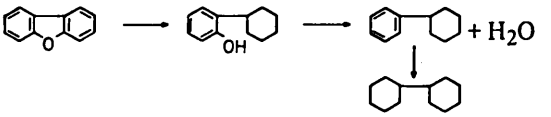

However, no 2-cyclohexyl phenol was detected, and the rate-determining step may be the production of the possible 2-cyclohexyl phenol intermediate. However, our data do not allow us to discriminate between the several reaction paths proposed by Weisser and Landa[4] for reaction over MoS_2.

Deoxygenation was the most difficult of the heteratom-removal reactions studied. The main product under our conditions was cyclohexyl benzene. The need for ring saturation prior to oxygen removal is seen again, and this reaction consumes much hydrogen. In view of the high oxygen content of coals, this is an extremely important area for study – the more so because of the paucity of existing data[4,12].

Hydrogenation and hydrocracking

Hydrocracking of phenanthrene on sulphide catalysts yields a complicated mixture of hydroderivatives of the initial substance saturated to differing degrees, of bicyclic and monocyclic aromatics, and of naphthalenes. Distribution of these species depends largely on the conditions used. Sullivan *et al.*[19] reported that the prevailing products from the hydrocracking of phenanthrene on a NiS/Al_2O_3 catalyst at 293°C are tetralin and methyl cyclohexane. However, Huang *et al.*[20], using a $Co–Mo/Al_2O_3$ catalyst reported that the main products of the reaction were perhydrophenanthrene isomers, indicating that cracking of phenanthrene occurs to a much lower extent than hydrogenation.

It is evident from studies carried out using sulphide catalyst that much higher temperatures (over 500°C) would be required to obtain substantial yields of cracked products. Catalyst deactivation as a result of carbon formation on the catalyst surface would most likely be a problem. Summarizing the available literature, it appears that the observed reaction paths could be represented by[21]:

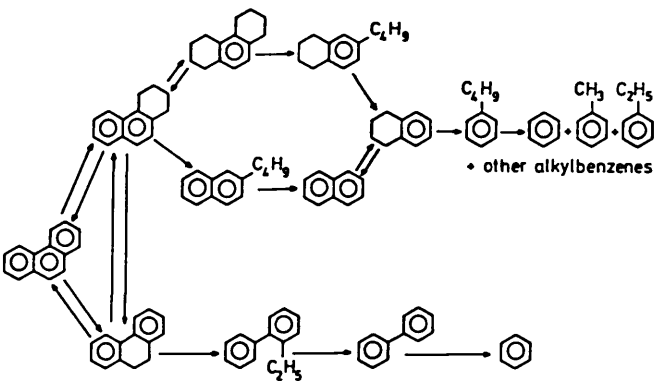

Under our conditions of operation (temperature), hydrogenation may be expected rather than hydrocracking. In agreement with this, the main products were a mixture of di-, tetra-, octa-, and perhydrophenanthrenes. It would

Table 7 Equilibrium and observed hydrogenation ratios for phenanthene

Reaction	AKZO-153S	IC-124	IC-124S	IC-124A	IC-124SA	Equilibrium
$C_{12}H_{16}/C_{12}H_{10}$	0.13	0.14	0.17	0.16	0.11	18.0
$C_{12}H_{22}/C_{12}H_{10}$	0.03	0.02	0.02	0.03	0.01	72.5
$C_{14}H_{12}/C_{14}H_{10}$	0.30	0.24	0.35	0.32	0.23	0.39
$C_{14}H_{14}/C_{14}H_{10}$	0.63	0.34	0.81	0.38	0.27	1.51
$C_{14}H_{18}/C_{14}H_{10}$	0.88	0.18	1.19	0.23	0.04	2.14
$C_{14}H_{24}/C_{14}H_{10}$	0.25	0.09	0.23	0.12	0.04	8.8

See Table 1 for reactant and product names

Table 8 Apparent kinetic rate constants per square metre of catalyst surface (gm^{-2} h^{-1} x 10^{-2})

Reaction	AKZO-153S	IC-124B	IC-124S	IC-124A	IC-124SA
HDN	3.06	4.37	3.38	6.42	7.74
HDO	0.68	0.76	0.93	1.30	1.74
Hydrogenation	5.01	6.87	6.67	14.50	20.62
Hydrocracking	0.81	3.29	2.02	9.83	19.56
Hydrocracking/hydrogenation ratio	0.16	0.47	0.30	0.67	0.94

appear that most of the pathways presented above are operating. Some hydrocracking was observed, and dicyclic derivatives account for most of the hydrocracking products.

A comparison of the equilibrium and the observed hydrogenation ratios is presented in *Table 7*. Equilibrium values were calculated using equations available in the literature[22], and observed conversions were obtained by subtraction of the yields of products from the total phenanthrene conversion.

The hydrogenation ratios are seen to be far from equilibrium, and only the dihydrophenanthrene/phenanthrene ratio is close to the equilibrium value. This is consistent with the observation that hydrogenation of the first aromatic ring proceeds quite rapidly[23]. The predominance of dicyclic products, and the trace quantities of diphenyl which could be ascribed to hydrocracking of phenanthrene (see discussion of HDS), suggests that successive saturation and cracking of the central ring of phenanthrene was not significant under the present conditions.

Catalyst comparison

In order to compare the catalyst performance, the apparent kinetic constants for the different reactions were evaluated from the conversion values, assuming a pseudo first-order reaction mechanism and a plug flow pattern in the reactor. For the hydrogenation and hydrocracking, the overall mechanism was simplified to:

Phenanthrene → hydrogenation → hydrocracking

and the results are shown in *Table 8*.

As the desulphurization reactions were complete on all catalysts no attempt was made to evaluate kinetic data.

It can be seen that the best catalyst per unit surface area is IC-124SA although IC-124AS was better if activities were expressed per gram of catalyst: in both cases the surface acidity was higher than the commercial catalyst. Generally speaking the apparent kinetic constants increase with surface acidity (from left to right in *Table 8*). However, while no significant deactivation was apparent over the 8 h run periods, the pressure drop over the reactor, as a result of interstitial build-up of coke, increased rapidly with surface acidity. Therefore, the high acidity catalysts, while possessing the best initial activity, are unlikely to be successful commercial catalysts in fixed-bed operation.

With the exception of the hydrogenation/hydrocracking selectivity, the acidity of the catalysts appears to have no significant influence on product distribution in the reactions considered.

CONCLUSIONS

Under commercial conditions of operation and in the presence of competing reactions of different types, the main product of dibenzothiophene desulphurization was diphenyl, the main product of the denitrogenation of quinoline was propyl cyclohexane, while that of the deoxygenation of dibenzofuran was cyclohexyl benzene. The main products of hydroprocessing of phenanthrene were hydroderivatives of varying degrees of saturation. Very little hydrocracking occurred at the present operating temperature (400°C).

Under these conditions, the relative ease of processing the various components of the model feedstock decreased in the sequence: dibenzothiophene HDS > phenanthrene hydrogenation > quinoline HDN > phenanthrene hydrocracking > dibenzofuran HDO.

In the case of HDS, sulphur was removed without the need for ring saturation, and is thus a relatively unimportant reaction. However, for oxygen and nitrogen removal, at least one ring appears to require saturation prior to removal of the heteroatom. This means that at least 7 molecules of hydrogen are required for each heteroatom removed, Since the oxygen content of coals can be high, this represents a significant use of hydrogen. Oxygen removal is difficult, and has been little studied in the past: thus it represents a current research priority.

Hydrocracking was not extensive at the temperature of the study. The predominance of di-cyclic derivatives indicated that cracking was occurring via successive processes of saturation and cracking of a terminal ring. This results in excessive gas production, a loss of aromaticity of the product and excessive hydrogen consumption. There is a

need to seek a selective catalyst to promote central ring cracking.

Increasing the acidity of the catalyst increased the rate of all the reactions studied and also the degree of hydrocracking relative to hydrogenation, but also increased the rate of carbon deposition. It is apparent that choice of catalyst and reaction conditions for this type of process will require a careful balance of all functions if excessive saturation and carbon deposition are to be avoided.

ACKNOWLEDGEMENTS

The authors are grateful to the National Coal Board for a substantial grant towards equipment and materials, and for performance of the mass spectrometric analyses. In addition, one of us (R.B.O.) is in recept of a grant for personal support from the National Coal Board. The views contained in this paper are those of the authors and not necessarily those of the Board.

REFERENCES

1 British Petroleum, *Gas Making and Natural Gas*, London, 1972
2 Spitz, P. H., *Chem. Tech.* 1977, 245
3 Frank, M. E. and Schmid, B. K. *Chem. Eng. Progress* 1973, 69 (3), 62
4 Weisser, O. and Landa, S., *Sulphide Catalysts – Their Properties and Applications*, Pergamon Press, New York, 1973
5 Yen, Y. K., Furlani, D. E. and Weller, S. W. *Ind. Eng. Chem.–Prod. Res. Dev.* 1976, 15 (1), 24
6 Schuit, G. C. A. and Gates, B. C. *AIChE J.* 1973, 19 (3), 417
7 Shuman, S. C. and Shalit, H. *Catalyst Review* 1971, 4, 245
8 Massoth, F. E. *J. Catal.* 1977, 47, 316
9 Sternberg, H. W., Raymond, R. and Schweighardt, F. K., *A.C.S. Div. Fuel Chem. Prepr.*, 1976, 21 (7), 198
10 Frye, C. G. and Moxby, J. F. *Chem. Eng. Progress* 1967, 63 (9), 66
11 Aboul-Gheit, A. K. and Abdov, J. K. *J. Inst. Petrol., Lond.* 1973, 59, 188
12 Hall, C. C. and Cawley, C. M. *J. Soc. Chem. Ind.* 1939, 58, 7
13 Bartsch, R. and Tanielian, C. *J. Catal.* 1974, 35, 353
14 Lee, H. C. and Butt, J. B. *J. Catal.* 1977, 49, 320
15 Landa, S. and Monkova, A. *Coll. Trav. Chim. Tech.* 1966, 31, 2202
16 Rollman, L. D. *J. Catal.* 1977, 46, 243
17 Satterfield, C. N., Modell, M., Hites, R. A. and Declerck, C. J. *Ind. Eng. Chem.–Process Design Dev.* 1978, 17, 141
18 Landa, S., Kafka, Z., Galik, V. and Safar, M. *Coll. Czech. Chem. Comm.* 1969, 34, 3967
19 Sullivan, R. F., Egan, C. J. and Langlois, G. E. *J. Catal.* 1964, 3, 183
20 Huang, C. S., Wang, K. C. and Haynes, H. W.; in *Liquid Fuels from Coal* (Ed. R. T. Ellington), Academic Press, New York, 1977, pp 63–78
21 Wu, W. L. and Haynes, H. W. *A.C.S. Symp. Series* 1975, 20, 65
22 Frye, C. G. *J. Chem. Eng. Data* 1962, 7, 592
23 Smith, H. A., in *Catalysis*, Vol 5 (Ed. P. H. Emmett), Reinhold Publ. Co., New York, 1957